The SEAL

A Thin Haul Transport and Air Taxi

Presented By:

TEAM η
Eta

Final Design Report

Team Members: Emil Broemmelsiek, Andrew Burke, Matthew Hogan,

Adam Maris, Nicholas Martin, Aakanksha Notey, Allen Wong

University of Illinois at Urbana-Champaign

Department of Aerospace Engineering

10 May 2019

Group Member Contributions

Name	Signature	Member Responsibilities	AIAA Number
Emil Broemmelsiek		Propulsion and Certification	983954
Andrew Burke		Structures and Interior	983471
Matthew Hogan		Stability and Control and Cost	984700
Adam Maris		Aerodynamics and Acoustics	983959
Nicholas Martin		Loads, Systems, and Landing Gear	738188
Aakanksha Notey		Performance and Avionics	981809
Allen Wong		Lead, Mass Properties, and Configuration	983958

Faculty Advisor	Signature	AIAA Number
Dr. Jason Merret		155270

Contents

List of Figures

List of Tables

Nomenclature

α	Angle of Attack
θ	Pitching Angle
λ	Taper Ratio
Λ	Sweep Angle
ρ	Density
σ	Stress
ϕ	Roll Angle
AIAA	American Institute of Aeronautics and Astronautics
AC	Air Conditioning
AR	Aspect Ratio
BFL	Balanced Field Length
C_D	Total Drag Coefficient
$C_{D_e}mp$	Empennage Drag Coefficient
C_{D_f}	Fuselage Drag Coefficient
$C_{D_f}lap$	Flap Drag Coefficient
$C_{D_g}ear$	Drag Coefficient due to Landing Gear
$C_{D_h}t$	Horizontal Tail Drag Coefficient
C_{D_i}	Induced Drag Coefficient
$C_{D_t}rim$	Drag Coefficient due to Trim
C_{D_w}	Wing Drag Coefficient
$C_{D_w}s$	Windshield Drag Coefficient
$C_{D_v}t$	Vertical Tail Drag Coefficient
C_{D_0}	Parasitic Drag Coefficient
C_l	Lift Coefficient (two-dimensional)
C_L	Lift Coefficient (three-dimensional)
dB	Decibel
CAD	Computer Aided Design
Calc	Calculated
CFD	Computational Fluid Dynamics
CFR	Code of Federal Regulations
CG	Center of Gravity
D_0	Total Skin Friction

Nomenclature continued

DRR	Design Rediness Report
Dry Weight	Weight excluding fluids such as oil, fuel, or lubricant
FAA	Federal Aviation Administration (United States of America)
FEA	Finite Element Analysis
ft	feet
fps	feet per second
GA	General Aviation
hp	Horsepower
in	inches
KEAS	Knots Equivalent Airspeed
KTAS	Knots True Airspeed
L	Lift
lb	Pounds
MAC	Mean aerodynamic chord
MTOW	Maximum Takeoff Weight
n	Load Factor
NACA	National Committee for Aeronautics
NTSB	National Safety and Transportation Board
p	Roll Rate
Pax	Passengers
psi	Pounds-force per Square Inch
q	Pitching Rate
r	Yaw Rate
Re	Reynolds Number
RFP	Request for Proposal
S	Wing Area
u	Forward Velocity
v	y-component of Velocity
V_A	Design Maneuvering Speed
V_C	Design Cruising Speed
V_D	Design Diving Speed
w	Downward Velocity
ZL	Zero Lift

Short Express
Air Liner

Executive Summary

This report presents the final design from Team Eta for the SEAL - a Thin Haul Transport and Air Taxi in response to the AIAA RFP for Undergraduate Groups 2018-2019. The team includes seven group members who are all undergraduate Aerospace Engineering students at the University of Illinois at Urbana-Champaign and this project is for the fulfilment of the course AE443 - Aircraft Systems Design (Senior Design) for Spring 2019.

In addition to the major airports in the United States which are serviced by frequent airline routes, there are thousands of smaller airports which show the potential for air service. In the past, due to limitations of small aircraft capable of operating at these airports, air service on these "Thin-Haul" routes has been low in frequency which makes the service inconvenient for passengers. Solutions to the low ridership of these flights include increasing flight frequency or providing on-demand service rather than scheduled service. The aim of the proposed aircraft is to create a design which is capable of operating more frequent flights to these airports while reducing cost for the operator with passenger comfort in mind, while also capable of performing on-demand missions as an air taxi. Current similar aircraft which can fill the role for these thin haul missions are the Cirrus SR22 and Piper PA-46.

The team's aircraft is designed with the following requirements as driving parameters: a takeoff distance of 2,500 ft, a range of 270 nmi (round-trip to a 135 nmi destination), a cruise altitude of 20,000 ft, cruise speed of 225 KTAS, typical payload of three passengers totalling 600 lb, a fuselage length of 372 in, and a fuselage maximum diameter of 73.2 in to accommodate three-abreast seating. These driving requirements were used as the major defining parameters in the team's design. Key parameters of the aircraft's design based on the requirements are an empty weight of 2,870 lb, 74 gal of fuel, a maximum takeoff weight of 4,550 lb, and a landing weight of 4,070 lb. The aircraft uses a Rolls-Royce M250 engine capable of producing 450 hp.

A major goal of the team is to deliver and aircraft with excellent passenger comfort in comparison to the other GA aircraft in this short-haul market segment. The selection of a high-wing design allows for more freedom of door location for easy ingress and egress without the need to step on the wing. In the interior, the aircraft offers 20 in. of legroom when passengers are sitting across from each other - enough room for them to stretch out their legs. An air conditioning system maintains a cabin temperature and active noise cancellation reduces propeller noise in the cabin.

For the design of this aircraft, the team used empirical formulas such as those found in the aircraft design textbooks by Raymer, Roskam, and Kroo as well as computational tools performing stability and aerodynamics validation in AVL, and structural analysis using finite element software.

I. Introduction

The goal of aircraft design is to fit the needs of the thin haul - low frequency - and on-demand flight operations serving primarily small airports and short routes. In comparison to General Aviation (GA) aircraft which have largely recreational roles, the proposed aircraft is designed with the passengers and regularly scheduled or on-demand service in mind. The platform will reduce operating costs to maximize profits for companies using these airplanes while providing better passenger comfort compared to similar thin-haul aircraft.

The target market for this aircraft is intended to fill the growing prospective need for air taxis - flights that will ferry passengers across cities or to nearby cities, requiring high flexibility and short range and runway operations. In addition to this market, an additional intended market for the SEAL also includes operations under the Essential Air Service which subsidizes the operation of flights to serve under served communities. The low cost of the aircraft and low number of seats, relative to regional aircraft, will allow operators to have a high frequency of flights for these marginalized areas, making the service more convenient for riders.

Planned certification for the aircraft is 2025 and is designed with currently deployed or demonstrated technology to achieve this deadline [1]. The maximum payload includes five passengers each weighing 180 lb with 20 lb of luggage and a single-pilot crew weighing 180 lb. The aircraft capable of operating a single mission of 250 nautical miles with the maximum payload.

II. Concept of Operations

A. Design Requirements

For this design, several of the driving requirements are taken from the AIAA RFP. Requirements from the RFP can be found in Table II.1 and were used by the team as major drivers in the during the design process. In addition to the design requirements outlined in the RFP, the group made a few modifications to be used in initial sizing. The range requirement was changed to 270 nmi with a 3 passenger payload to allow the aircraft to fly round-trip to a 135 nmi destination without refueling. This will decrease turnaround times and allow the operator to fly to and airports where the required fuel is not available. To provide increased quality of service and competitiveness compared to similar aircraft, the average cruise speed requirement was increased to 225 KTAS. Although these are the requirements set by the team, the SEAL may outperform in some of these categories based on the team's calculations.

Table II.1: Summary of requirements as specified by AIAA RFP with team goal deviations noted

Category	Requirement	Team Goal
Range	Capable of a total range of flight of 250 nmi and 45 minute reserve, including a climb to 3,000 ft. for a ferry mission	270
Speed	Average ground speed of 180 ktas	225 ktas
Takeoff Distance	Less than or equal to 2,500 ft over a 50 ft obstacle	–
Landing Distance	Less than or equal to 2,500 ft over a 50 ft obstacle	–
Payload	4-6 Passengers weighing 180 lb each and carrying 20 lb luggage each	5 Passengers
Crew	Single-pilot crew weighing 180 lb	–
Noise	Must be in compliance with single-engine noise limits per Part 36 Sec. G36.301(c)	–
Certification	Must be able to be certified under FAA 14 CFR Part 23, Level: 2, Performance: Low Speed	–
Technology	Existing or demonstrated technology ready for certification by the year 2025	–

B. Typical Mission Profile

The mission profile for which the aircraft is designed consists of 6 segments: taxi and takeoff, climb to cruise altitude, cruise for 135 nmi, descend for landing, climb to 3,000 ft and cruise for 45 minutes, and finally landing and taxi. A diagram of a typical single reference mission carrying 3 passengers can be found in Figure II.1. In addition to the typical mission profile presented in Figure II.1, the RFP also requires a long-range sizing mission with a 250 nmi requirement with a full payload.
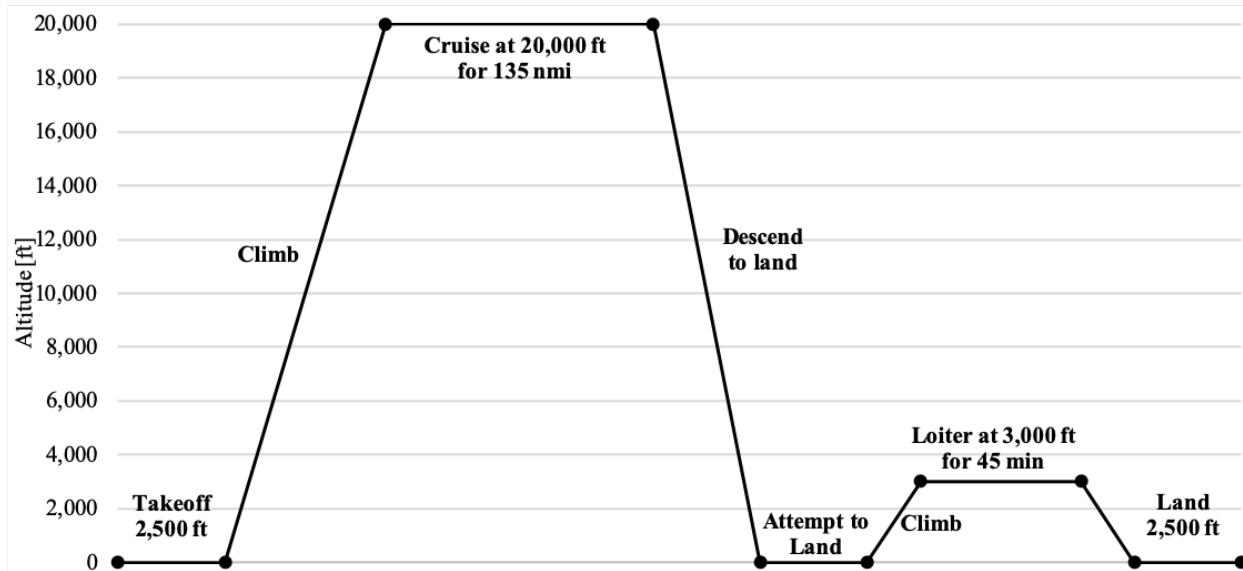
Figure II.1: Diagram of a Typical Single Mission Profile

III. Sizing Analysis

A. Initial Sizing

To perform the initial sizing analysis, key requirements were assembled using the RFP and studies of similar aircraft. Several aircraft of similar size and mission type were analyzed including the Piper PA-46, Cirrus SR22, Vulcanair V1.0, Pilatus PC-12, and Extra EA-500. Of these five aircraft, the Extra EA-500 was chosen to be the seed aircraft because of its similarity in payload of four passengers and its use of a turboprop engine. Key parameters that were used in the initial sizing are presented in Table III.1. Parameters from the seed Extra EA-500 aircraft were used with a change to the range to accommodate the short-haul missions, an increase in width to adjust for three-abreast seating, an increase in payload to six passengers, and landing and takeoff distances which meet the specifications set by the RFP.

Table III.1: Driving Parameters Used for Initial Sizing

Parameter	Value
Range	270 nmi
Payload	1,000 lb (5 passengers + baggage)
Takeoff Distance over 50 ft obstacle	2,500 ft
Cruise Speed	225 KTAS
Cruise Altitude	12,000 ft
Landing Distance over 50 ft obstacle	2,500 ft
Fuselage Length	386 in
Fuselage Maximum Diameter	70 in

The first initial sizing was used to confirm the validity of the design in achieving the requirements and select a set of parameters to build towards for detailed design. First order approximations using historical data and empirical methods were used including wetted area, drag approximations, and weight fractions from Raymer [2], performance equations from Roskam [3], and the wing weight equation from Kroo [4]. The team's initial sizing method began with a guess of the major weight components - empty, fuel, and payload weight - and used the aerodynamic equations from Raymer, performance equations from Roskam, and weight equations from Kroo to calculate the weights of the aircraft using the input weights and defined geometry of the aircraft to create a weight buildup. The weight buildup then leads to a new calculation of the original input weights. Since this method is recursive, several iterations are necessary to obtain a solution where the input weights are equal to those calculated.

B. Fuselage Diameter Trade Study

Similarity of the seed aircraft to the mission goal in terms of takeoff distance, range, and weight, meant that only minor changes were required in the initial sizing process. There were two major parameters which the team considered for trade studies - retractable vs fixed landing gear and the effects of an increase in fuselage diameter to increase the capacity from two-abreast to three-abreast seating. Due to limited resources available in the initial sizing process for the weight buildup of a retractable vs non-retractable landing gear, a trade study was not performed for initial sizing but is currently planned in the next iteration of preliminary design. All initial sizing assumed and accounted for the additional drag of fixed landing gear.

A trade study was performed for a change to the fuselage width to accommodate three-abreast seating in the cabin. This would allow for the placement of five passenger seats - three in the rear facing forward and two siting back-to-back with the pilot while facing rearward. The results of using an increased diameter can be found in Table III.2. This comparison was done with only a change in the diameter using weight equations from Raymer and Roskam. Both are sized to the same requirements of takeoff distance, range, speed, landing distance, and geometry (excluding fuselage diameter).

Table III.2: Comparison of key parameters for different fuselage widths

	Original 60 inch diameter	**New 70 inch diameter**
Empty Weight [lb]	3,030	3,075
Fuel Weight [lb]	350	355
Maximum Ramp Weight [lb]	4,180	4,230
Power Required [hp]	320	330
L/D	7.07	7.04

The results of the trade study for an increase in fuselage diameter show only small changes in the major parameters. The aircraft empty weight, fuel weight, and maximum ramp weight all increase by less than 1.5% while there is a slight reduction in the L/D. This small reduction in performance convinced the team to use this new diameter in the design of the aircraft to allow for an extra seat, bringing the maximum seating capacity to 5 passengers. The increased passenger seating provides operators with an increase profit per trip while maintaining similar operating costs.

C. Comparison to Similar Aircraft

Since the goal of this aircraft is to offer a competitive, cost-reducing alternative to the thin-haul market, it is important to compare it to aircraft of similar design. The aircraft solution obtained by the team in initial sizing is presented in Table III.3 and compared to similar aircraft based on mission and capability.

Table III.3: Key Parameters of Similar Aircraft

Aircraft	Pax Seats	Range [nmi]	BFL [ft]	Power [hp]	Cruise [KTAS]	Empty Weight [lb]	Fuel [gal]	Wingspan [ft]
Piper PA-46 [5]	4	1,343	2,090	350	213	3,165.5	120	43
Cirrus SR22 [6]	2	1,049	1,868	310	183	2,250	81	38.3
Vulcanair V1.0 [7]	2	575	1,310	180	128	1,627	50	32.83
Pilatus PC-12 [8]	6	1,845	2,602	1,845	285	5,468	402	53.3
Extra EA-500 [9]	4	1,600	2,050	450	226	3,131	172	38.3
SEAL	5	250	2,500	450	225	2,890	74	40.3

In comparison to different aircraft in the space, the SEAL is able to offer a competitive solution that cruises at a high speed while while operating at a weight typically seen with aircraft that carry less than five passengers.

IV. Configuration

A. Concept Considerations

Several configurations of aircraft were considered and OpenVSP models of each are presented in Figure IV.1. Two low-wing single-engine aircraft configurations were considered - one with a low horizontal stabilizer and another with a high "T-tail" stabilizer. Although the two low-wing configurations are valid designs, the team determined that a high-wing would be a design requirement to allow for the easy ingress and egress of the aircraft without having passengers step over the wing, a problem which may occur with a low-wing design.

Within high-wing configurations, a twin-engine option was considered, but this was set aside in favor of a single-engine turboprop. The motivating factor behind the choice of a single turboprop engine includes efficiency gains from only having a single engine, ease and cost of maintenance, and compliance to the noise requirement as detailed in Table II.1. The final configuration selected can be seen in the model presented in Figure IV.1d.

(a) Low wing, single engine configuration.

(b) Low wing, single engine, high tail configuration.

(c) High wing, twin engine, high tail configuration.

(d) High wing, single engine configuration.
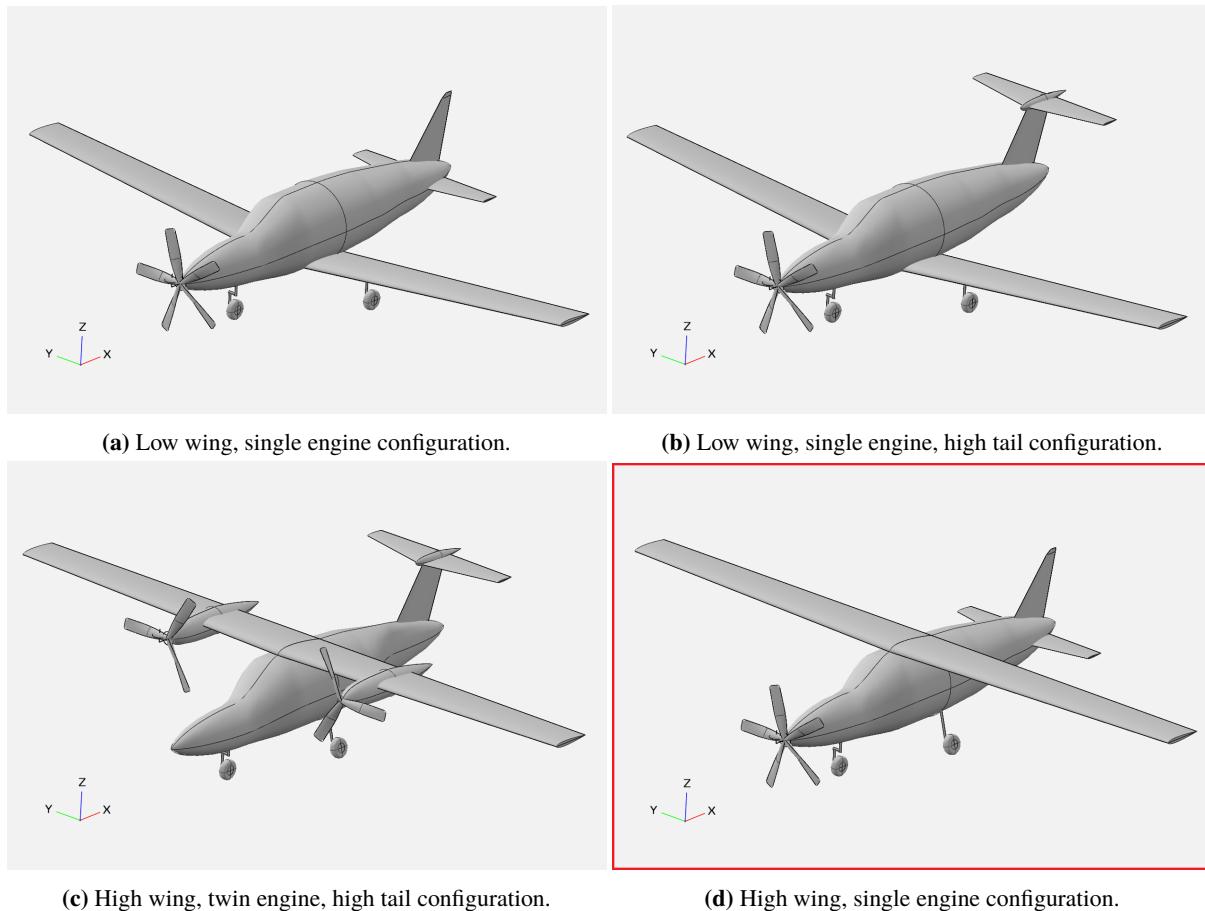
Figure IV.1: OpenVSP models of configurations considered.

B. Landing Gear Philosophy

The landing gear was chosen to be a three-wheel tricycle design fixed to the undercarriage of the aircraft with added wheel fairings to reduce the drag penalty and allow better fuel efficiency. Three wheel landing gear is very common for historical aircraft of a similar size because the three wheels provide enough stability during take off and landing without adding unnecessary weight or drag. The tricycle undercarriage was chosen over the taildragger configuration because it provides improved stability when landing. The key decision made regarding the landing gear was whether to design the aircraft with fixed or retractable landing gear. After comparing other aircraft designed for similar missions it was decided that fixed landing gear would provide a greater benefit than retractable landing gear. Although having retractable landing gear can often decrease drag significantly, and therefore improve fuel efficiency, its downsides far outweigh this benefit for this particular mission. In a low-speed and short haul mission, the effect of increased drag from the fixed landing gear is not large enough to justify spending extra money to design and maintain retractable landing gear or to add the extra weight of the retracting mechanisms. In a comparison done between two aircraft whose only difference is fixed vs. retractable landing gear, the retracting mechanisms of an aircraft of this size were estimated to be 120lbs [10]. Furthermore, it was found that the drag penalty of the fixed landing gear could be reduced when fairings are added on over the wheels, which is discussed further in the aerodynamics section of this report. Future work for the landing gear include a more detailed analysis of the drag contribution and the weight of the landing gear assembly. The tires will be sized, the braking and steering systems will be designed, the fairings will be sized and positioned, and the exact location and length of the landing gear will be decided.

C. Interior

The goal of this aircraft is to offer a cabin experience that is more comfortable than those in the GA market while increasing capacity and decreasing cost for the operator. The pilot and passengers of the SEAL experience luxurious comfort on their short trips. Space is in abundance, with fifteen inches of leg room for all passengers. The passengers need not worry about their knees being impeded by the rear of a seat when they fly on a SEAL. The seats are all 18.5 inches wide and 20 inches long. The 95th percentile of North American males ages 31-60 years old have a hip width of 15.5 inches [11]. This verifies that passengers will have plenty of excess room in their seats. The 5th percentile of female have hip widths of 12.12 inches [11]. This verifies that female passengers will not experience discomfort due to too much excess seat space. The major interior dimensions of the cabin and cargo area are shown in Figure IV.4. The position of the floor with respect to the seats is also visible. All dimensions shown are in inches. Additional optional features that an airline may consider to further improve passenger comfort are amenities such as active noise cancellation headphones and television screens for entertainment.
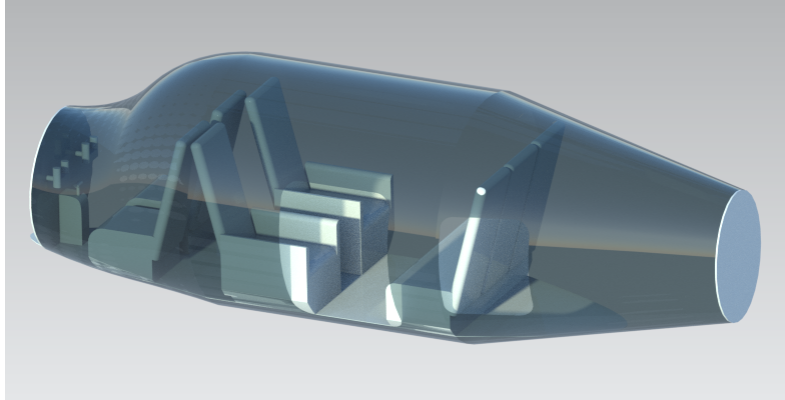
Figure IV.2: Interior Glass View of SEAL

The rendering of the aircraft cabin is shown in Figure IV.2. This view shows the seat configuration, cargo area, and door placements for the aircraft. The passenger door is 34 inches wide and 44.6 inches tall to allow for easy ingress and egress of the cabin. The cargo compartment is located behind the third row of seats. There is also a cargo door located on the side of the aircraft for easy stowing of luggage.
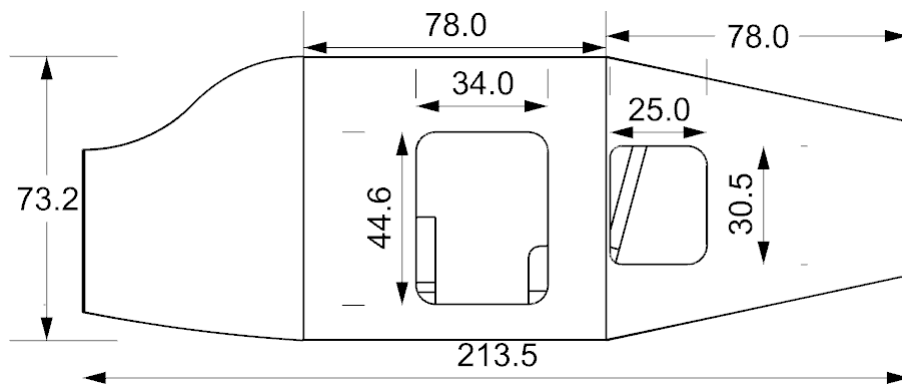
Figure IV.3: Door Dimensions of SEAL
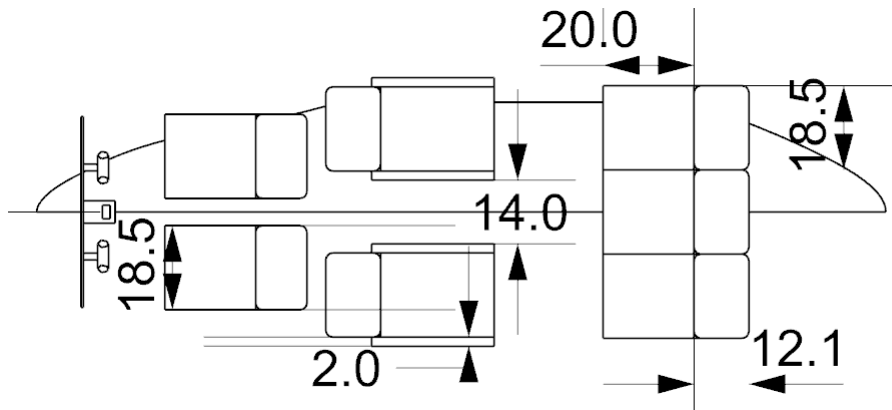
Figure IV.4: Interior Dimensions of SEAL

The comfortable experience of the SEAL does has its drawbacks, however. The aircraft provides comfort while sacrificing the inclusion of additional seats. An additional two person row of seats could be placed in between the existing rows. However, in order to implement this row, the seat dimensions would have to be diminished. This would result in a decrease in passenger satisfaction but an increase in passenger capacity. Since the objective of this aircraft is to provide a comfortable experience for the passengers, the implementation of an additional row was rejected.
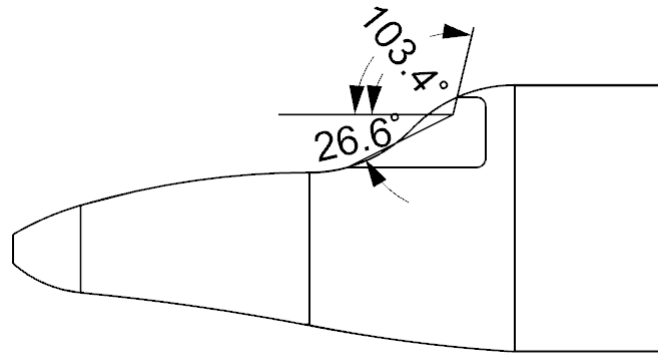
Figure IV.5: Pilot Horizontal Viewing Angles
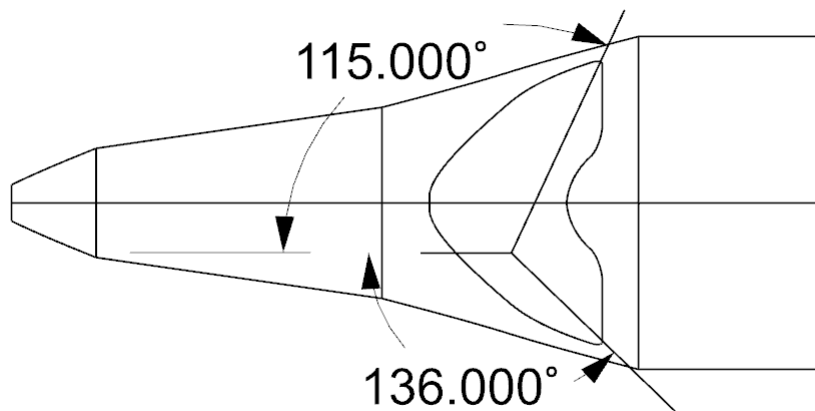
Figure IV.6: Pilot Vertical Viewing Angles

The pilot is seated in the port side seat. The pilot viewing angles are shown in Figure IV.5 and Figure IV.6. These angles satisfy Roskam's recommendations for both the horizontal and vertical viewing angles of 135°port, 30°starboard and 20°up, 15°down [3]. These angles also satisfy 14 CFR Part 23.773.

D. SEAL Design

A dimensioned three-view for the current model of the SEAL can be found in Figure IV.7.

Figure IV.7: Three-view of the SEAL with relevant dimensions.
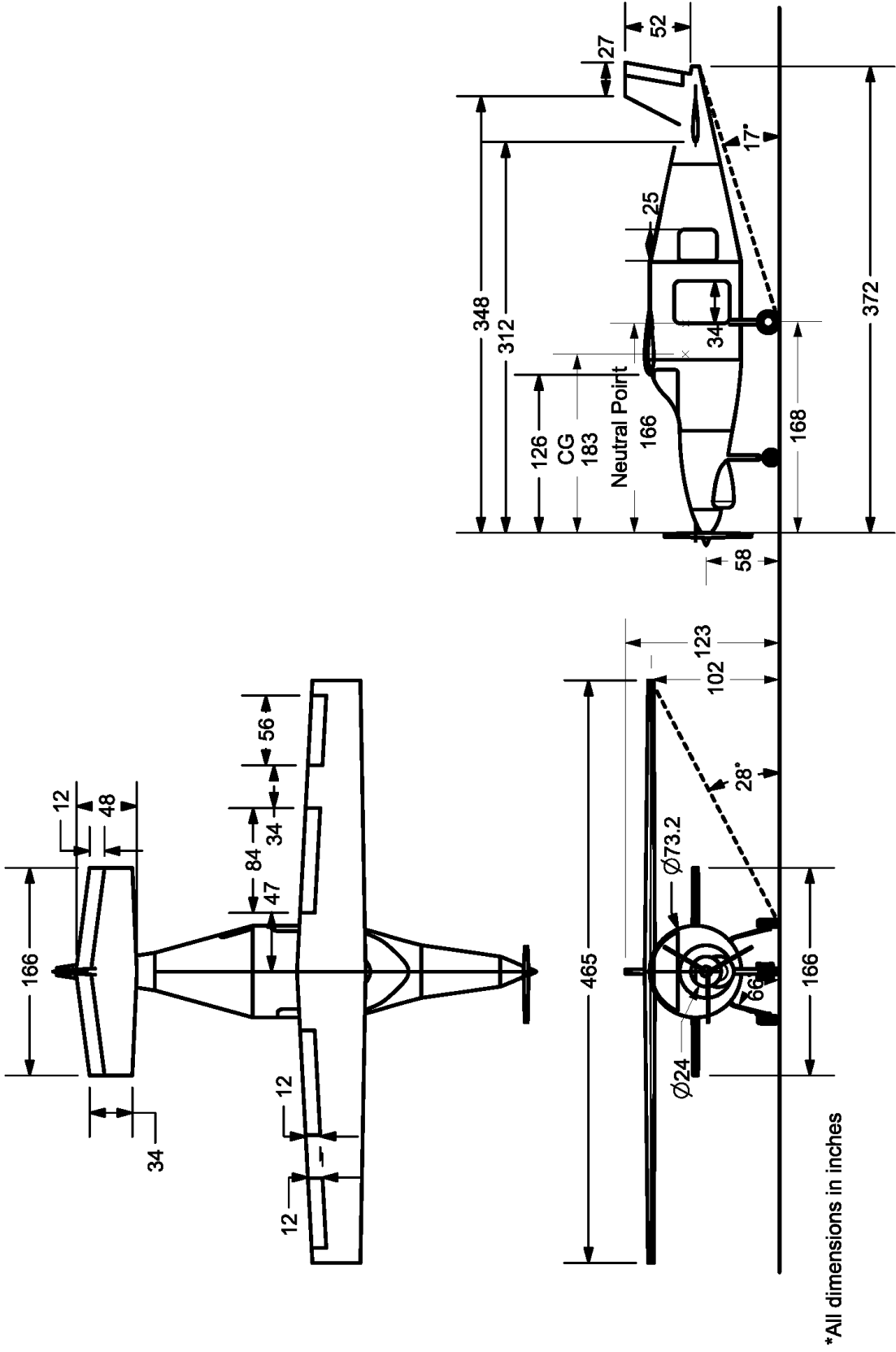
*All dimensions in inches

V. Propulsion

A. Engine Considerations and Selection

The given thin haul mission places any design in the realm of light aircraft with the range being only 250 nautical miles for the sizing mission. Initially, an electrically powered aircraft was considered but quickly ruled out because of the massive weight requirement of the battery. Using the maximum energy density specified in the RFP, a battery weight of 3,223 lbs was calculated as equal to the available power from 477 lbs of JetA fuel. This calculation included the estimated engine thermal efficiency of 14.5% and an assumed electric motor efficiency of 90%. Jet engines were ruled out on recommendation from Raymer [2] as the low range and weight requirements result in a low design Mach number of 0.4. The size of the payload places the power requirement in a sweet spot where either a reciprocating piston engine or a turboprop could be used, so data on appropriately sized engines of both types were gathered and compared.

Table V.1: Key Parameters of Plausible Engines

Engine	Power (shp)	Fuel Consumption (lb/hr/shp)	Dry Weight (lb)	Specific Power (hp/lb)	Type
Lycoming O-360	180	N/A	258	0.698	Four Cylinder, Horizontally Opposed
Lycoming O-540	300	N/A	438	0.685	Six Cylinder, Horizontally Opposed
Lycoming TIO-541-A1A	310	N/A	549	0.565	Turbocharged Six Cylinder, Horizontally Opposed
Continental IO-550-N	310	N/A	430	0.721	Six Cylinder, Horizontally Opposed
Pratt & Whitney PT6A-21	550	0.630	328	1.68	Turboprop
Lycoming LTP 101-600A-1A	615	0.544	325	1.89	Turboprop
Rolls Royce M250 TP	450	0.613	212	2.12	Turboprop

Table V.1 compares data at takeoff conditions for horizontally opposed, air cooled engine options with turboprops with powers on the low end of available turboprop engines. On top of the lighter weight of turboprops, the RFP requirement of a parachute with a reciprocating engine would add additional weight due to the parachute system and heavier structures to meet certification standards during parachute deployment. The similarity analysis in Section III found that a maximum of 330 hp would be required for our initial design, so no reciprocating engine would satisfy the design requirements alone. This motivated Team Eta to choose a turboprop engine type over a reciprocating engine.

B. Engine Requirements

The turboprop engines in Table V.1 were used on similar aircraft or in some cases alternate versions of the same plane as the reciprocating engines in Table V.1. Many turboprops' dimensions are designed as a power upgrade for common reciprocating engines [21]. Dry weight specific power was calculated for both reciprocating and turboprop engines, and the results show that turboprop engines can output significantly more power for the same weight. The trade-off is that turboprop engines generally burn fuel about 50% more quickly [2]. Choosing a single turboprop engine, however, simplifies the aircraft's design and reduces the maintenance required for the aircraft. The engine selected for the SEAL was Rolls Royce's turboprop engine M250 TP. Although this relatively small turboprop's maximum power output overshoots the power requirement significantly, it saves hundreds of pounds of dry weight when compared to reciprocating engines, is not subject to the RFP's requirement for a parachute with a single reciprocating engine, and allows the team to pursue a larger payload as well as mission flexibility. The M250 was first certified in 1988 but has been certified for use at least as recently as in 2014 for the EA-500.

C. Powerplant Performance

To validate choosing the M250 TP engine and to justify its applicability, more performance data must be acquired. Firstly, the M250 comes in many models of turboshaft and turboprop configurations so a submodel needs to be chosen before more specific data can be found. The chosen submodel is the 250-B17F/2 and is the newest model in the M250 series II of turboprop engines rated for a maximum power of 450 shp and comes furnished with a propeller reduction gearbox and a propeller speed governor. These accessories enable efficient flight at a wider range of velocities by allowing the propeller to spin faster for the same power and to automatically alter the pitch of the propeller's blades thereby keeping them at an efficient angle of attack. Unlike the 250-B17F/1, the 250-B17F/2 does not come with overspeed control and is intended for single engine, non-aerobatic applications. Power available as well as power-specific fuel consumption for turboprop engines are safely assumed constant through the relatively small range of Mach numbers experienced during normal operation [12]. These values do, however, change with density and therefore altitude. Their trends are shown in Figure V.2. Power available is estimated with the density change according to equation 1 from Dr. Danielle Soban's presentation on powerplant performance [12].

$$\frac{P_A}{P_{A,0}} = (\frac{\rho}{\rho_0})^n \tag{1}$$

The exponent n is a statistical value for turboprop engines the average value of which is 0.7. Since the n value is unknown for the Rolls Royce M250-B17F/2, the average of 0.7 was used to scale power with density for this estimation.
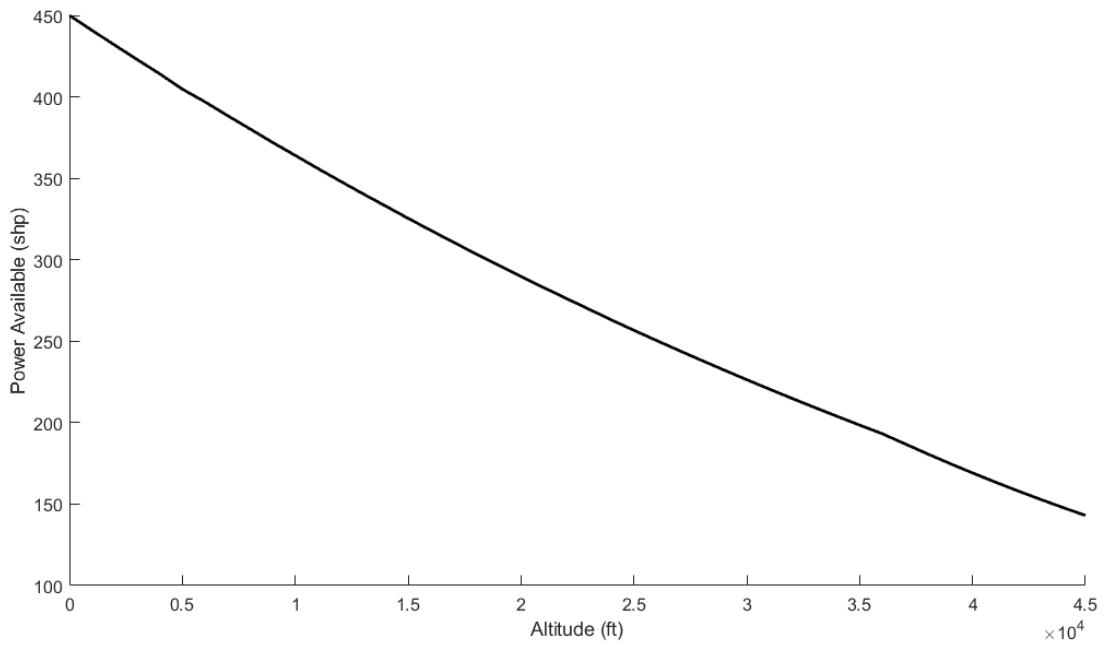
Figure V.1: Plot of available power against altitude
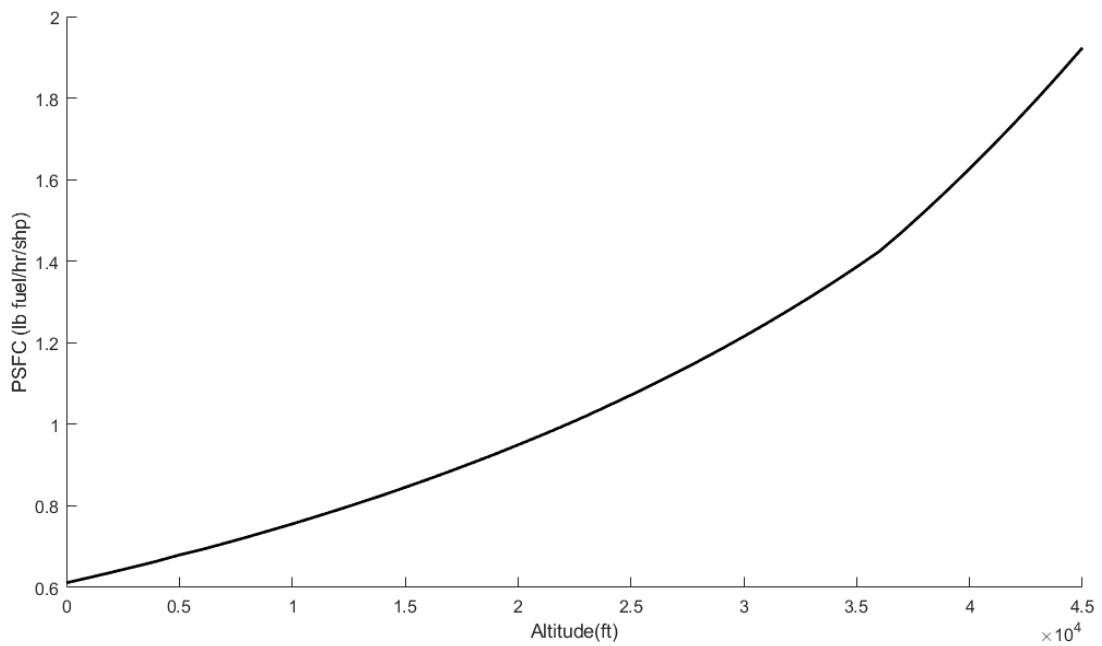
Figure V.2: Plot of power-specific fuel consumption against altitude

13

The power available shown in Figure V.2, while at a maximum of 450 shp at sea level, drops down to 289.7 shp at the cruise altitude of 20,000 ft. The power-specific fuel consumption (PSFC) was estimated using a constant fuel flow of 0.0764 lb/s and increases from 0.61 lb/hr/shp to 0.95 lb/hr/shp at cruise altitude, even though the specific fuel consumption remains about the same [12]. The efficiency of the powerplant was estimated to be 14.5% by comparing the available power at cruise and the total energy contained in the mass flow rate used for performance calculations. Further engine specification values are tabulated in Table V.2.

Table V.2: M250-B17F/2 Engine Specification

Parameter	B17F/2
Weight	212 lb
Power/ dry weight ratio	2.12:1 lb/shp
Airflow	3.82 lb/s
Pressure Ratio	7.9:1
Compatible Fuels	MIL-T-5624, JP-4, JP-5, JP-8, ASTM-1655, JetA*, JetA-1, JetB, MIL-T-83133
Oils	MIL-L-7808G, MIL-L-23699
FAA Type certificate number	E10CE
Maxiumum Rated Take-off power	450 shp
Length (overall)	44.924 in
Width	18.784 in
Height	22.596 in

D. Turbine Inlet and Integration

Given the cruise velocity and power available to the propeller, the inlet size requirement can be calculated. This comes with knowledge of the cruise altitude as well as the temperature, pressure, and density from the International Standard Atmosphere. Using NASA's general thrust equation and ignoring the jet thrust terms, the pressure change from atmospheric pressure caused by the propeller was estimated. This newfound pressure ratio was related to the air's density change through the isentropic flow relations. If the mass flow rate affected by the propeller all contributes to

---

*JetA was deemed the most available and ubiquitous fuel, with its energy density value of 26160 hp/lb used for all calculations.

the thrust (meaning no radial or azimuthal flow of air) then the mass flow rate across the propeller can be assumed constant. This equation can be manipulated to solve for the air's velocity change as proportional to the inverse of the air's density change. The new velocity behind the propeller can be converted to area with the required mass flow rate of air to the turbine and the air's density. The catch area of this engine inlet needed to maintain a fuel to air ratio of 0.02 at cruise altitude is 260 in^2. 225 in^2, 85% of this value was chosen to be the inlet size. This change increases the available fuel to air ratio for all altitudes, thereby improving takeoff performance but increasing the fuel to air ratio by only 0.035 at cruise. This increase is acceptable because JetA burns stoichiometrically at a fuel to air ratio of about 0.06.

The exhaust of the turbine exits near the bottom of the engine pointed down and away from the aircraft body, contributing nothing to thrust. This is away from the cockpit and any windows that could get smudged or have soot deposited on it.

E. Propeller Performance

Thrust provided by the engine comes from the propeller, so its design is vital to the performance of the aircraft. Thrust is generated by more propeller blades taking up a larger area. A convenient to compare propellers on different aircraft is by using the Advance Ratio, a non-dimensional parameter that includes the free stream velocity experienced by the propeller, the propeller diameter, and the rotational speed of the propeller. With the same planes that were used in the sizing analysis (III), a trade study was done on key propeller parameters with the results tabulated in Table V.3.

Table V.3: Key Parameters of Propellers on Similar Aircraft

Plane	Number of Blades	Propeller Diameter (in)	Cruise Speed (mph)	Propeller Rotational Speed (rpm)	Advance Ratio
Piper PA-46	3	80	245	2,500	1.29
Cirrus SR22	3	78	211	2,700	1.06
Vulcanair V1.0	2	74	150	2,700	0.793
Pilatus PC-12	4	105	328	1,700	1.94
Extra EA-500	5	82.7	67	2,030	0.422

Three propeller blades were chosen to maintain a higher efficiency instead of getting extra thrust from possible extra propellers. Based on the cruise velocity and the max rpms of the engine, the SEAL will have an advance ratio of 1.64. This lies safely near the range of light aircraft the were examined. Using this advance ratio, the propeller efficiency

can be estimated from the propeller efficiency chart in McCormick [22]. The propeller efficiency is estimated to be 85% using this method. As the propeller has variable pitch control, this efficiency will be maintained throughout the majority of the flight envelope.

Generally, the larger area that the propeller covers, the more efficient it is [2]. The diameter of the propeller is limited by the speed of the propeller tips, which can approach transonic speeds causing a large amount of drag. If a larger diameter means that the propeller is more efficient, then lower advance ratios mean slight increases in propeller efficiency. Therefore lower advance ratios would be ideal, except that doing so reduces the amount of thrust it's possible to create. A diameter near that of the low advance ratio of the Extra EA-500 was chosen to be 82 in.

The maximum rpm of the propeller is tied to the choice of engine, making the SEAL's propeller design very similar to the seed aircraft. Appropriately sized propellers made of lightweight composite material and a spinner selected from Hartzell Propeller Inc., who makes similar propellers for planes like the Piper PA-46 and the Pilatus PC-12. The model that will be used is the scimitar J3F00551STP from Hartzell, coming with a spinner.

F. Engine Auxiliary Systems

Rolls Royce's M250-B17F/2 is a light turboprop engine designed to operate efficiently at lower altitudes, and will be placed in the front of the aircraft in a conventional tractor propeller configuration. A physical firewall made of 0.015 in. thick stainless steel will be installed between the pilot and the engine at a forward bulkhead to keep the cabin safe in the case of an engine fire. This model of engine comes with a Bendix gas producer fuel control DP-P2 which controls the fuel flow rate and pressure as the fuel goes into the engine. Sitting toward the aft of the engine it also provides the electrical data that will read out these parameters to the pilot. A generator will also be placed behind the engine to take up to 9.3 hp or 150 amperes from the engine to charge a battery used for powering electrical devices onboard the SEAL. This battery will be the RG-380E/44LS valve regulated lead acid battery that weighs 91 lbs and holds 42 Ampere-Hours [33]. It is rated to start turbine engines multiple times after short flight duration and can be used to restart the engine in case of engine-out.

VI. Aerodynamics

A. Airfoil Selection

Airfoil selection an important driving factor in wing design, and several were selected for comparison. Many aircraft use different airfoils for the root and the tip of the wing, with a higher lift airfoil at the root and a more symmetric airfoil at the tip [14]. This change in airfoil geometry along the span of the wing introduces a natural twist in the wing and will move the stall towards the root of the wing inducing a safer stall. To begin the selection process, computer generated data from XFOIL was compared with experimental wind tunnel data to validate the computer models. Three airfoils were selected and their characteristics were compared and are shown in Table VI.1.

Table VI.1: XFOIL Comparison: Re=1,000,000

Airfoil	XFOIL Data				NACA Report Data [15]			
	$C_{l_{max}}$	Stall Angle	α_{ZL}	$C_{d\,ZL}$	$C_{l_{max}}$	Stall Angle	α_{ZL}	$C_{d\,ZL}$
NACA 23012	1.52	15.2°	−1.19°	.00620	1.75	16.5°	−1.5°	.0072
NACA 23018	1.51	17.0°	−1.17°	.00723	1.59	16.0°	−1.2°	.0072
NACA 0006	0.72	7.5°	0.00°	.00338	0.85	9.55°	0.00°	.0052

After comparing the data for those three airfoils, the team concluded that XFOIL is a software that will be able to validate the airfoils chosen in the selection process. Based upon the knowledge that many aircraft use two or more airfoils, the search for the airfoils had two parts. One part was for a cambered airfoil to use as the root airfoil, and the second part was for a symmetric airfoil to use as the tip airfoil. After examining many NACA airfoils, including the ones shown in VI.1, the airfoils chosen for the SEAL are listed in Table VI.2 with data from XFOIL.

Table VI.2: Airfoil Selections

Airfoil	$C_{l_{max}}$	Stall Angle	α_{ZL}	$C_{d\,ZL}$	$\frac{L}{D}$ max	$\frac{L}{D}$ max angle
NACA 23015	1.53	16.5°	−1.18°	.00723	90.5	9.25°
NACA 0012	1.38	15.2°	0.00°	.00542	75.6	7.50°

The airfoils selected for the SEAL are the NACA 23015 for the root airfoil and the NACA 0012 for the tip airfoil and are shown in Figure VI.1. The NACA 23015, which is used as the root airfoil for over 50 aircraft including the

(a) Drawing of the NACA23015 airfoil   (b) Drawing of the NACA0012 airfoil
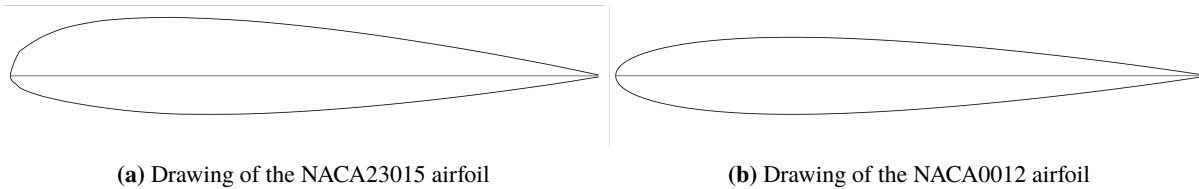
Figure VI.1: Drawings of airfoils used in the wing

Piper PA-46 [14], was chosen due to its high $C_{l_{max}}$ value, stall angle, and performance at lower Reynolds numbers. The NACA 0012 was chosen as the tip airfoil because of the relatively high stall angle among symmetric airfoils as well as a high $\frac{L}{D}$ max value. The lift curves and drag polars for both airfoils are shown in Figures VI.2 and VI.3.
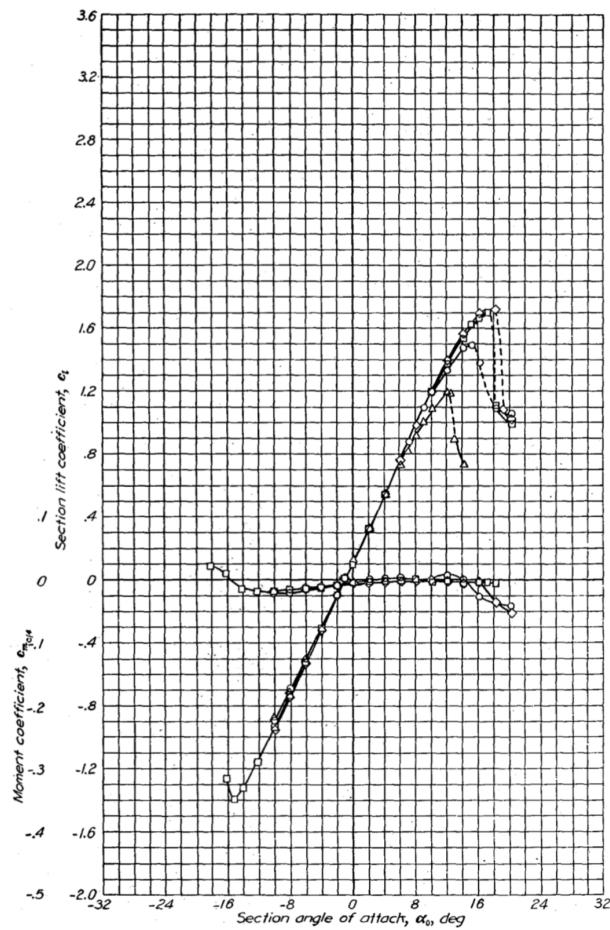
(a) NACA 23015 Lift Curve
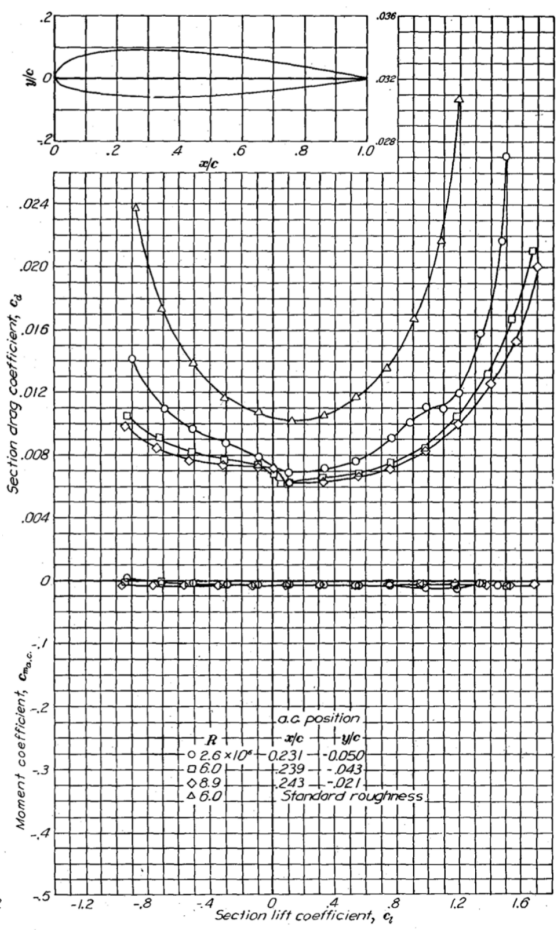
(b) NACA 23015 Drag Curve

Figure VI.2: NACA 23015 Experimental Performance Curves [15]
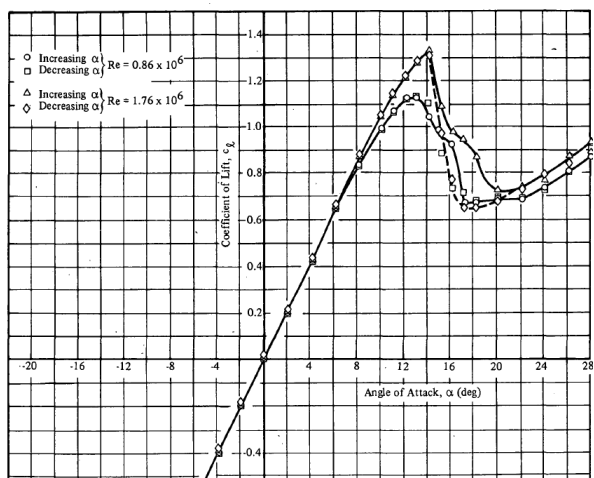
(a) NACA 0012 Lift Curve
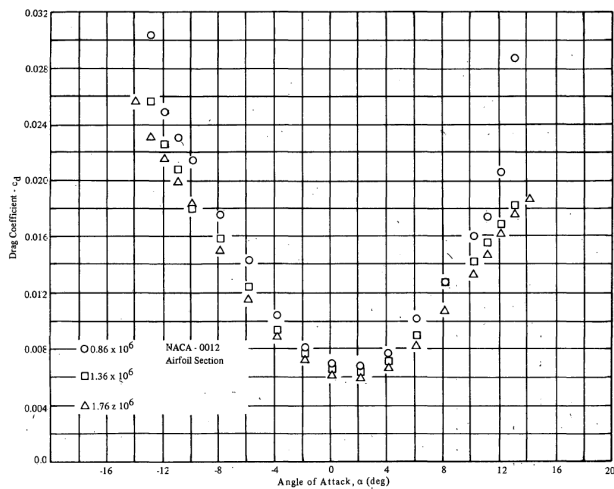
(b) NACA 0012 Drag Curve

Figure VI.3: NACA 0012 Experimental Performance Curves [16]

18

The graphs illustrate important characteristics of the airfoils. The lift curve in Figure VI.2 shows that the NACA 23015 has a positive lift coefficient at an angle of attack of $0°$. While the symmetric NACA 0012 airfoil produces no lift at an angle of attack of $0°$, it has a less steep reduction of lift once the airfoil stalls. The symmetric airfoil produces less drag especially at lower angles of attack. Combining these two airfoils will lead to high lift and low drag characteristics when applied to a wing.

It is important to note that there have been icing issues with aircraft that utilize the NACA 23015 airfoil in the past. One of the most notable accidents was Comair Flight 3272 in 1997. While the aircraft that unfortunately crashed used the NACA 23015, the NTSB put the probable cause and error on the FAA's lack of proper icing certification tests [17]. As a result of the investigation the FAA has stronger requirements on the use of deicing systems among other new policies about flight speed. With the deicing system installed on the SEAL and requiring the pilots to land the SEAL at greater speeds in probable icing conditions, the NACA 23015 will be a safe and functioning airfoil choice.

B. Wing Geometry

In addition to natural twist added with the use of different root and tip airfoils, five other wing geometry parameters, wing area, aspect ratio, taper ratio, quarter chord sweep, and dihedral angle, were explored as presented in Table VI.3. A taper ratio of 0.7 was chosen to increase the efficiency of the wing [18]. During the initial sizing process, it was determined that a higher aspect ratio correlated to increased aircraft performance and efficiency. This idea is illustrated in the contour plot shown below in Figure VI.4. This figure shows the trends between aspect ratio, wing area, and MTOW, which was tested between aspect ratios of 6 to 13 and wing areas of 140 to 180 ft^2.
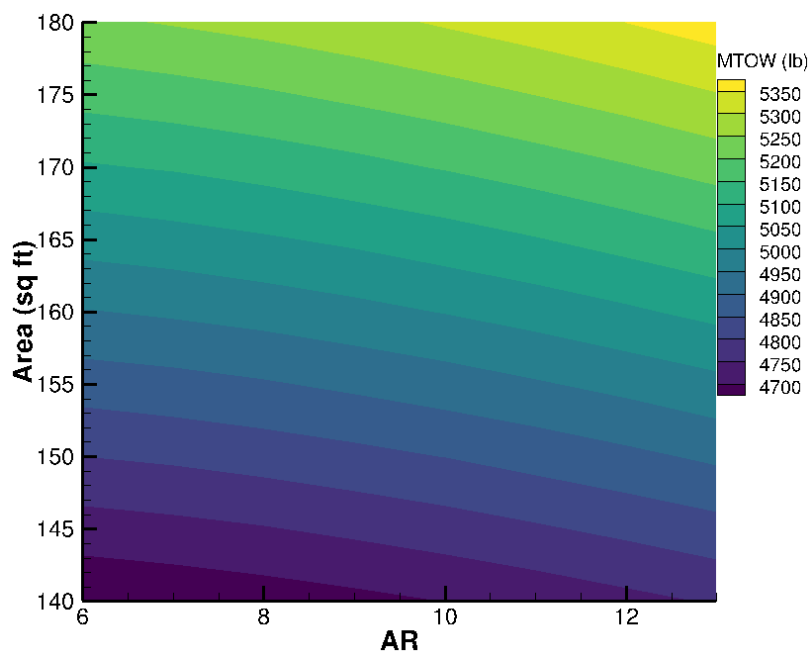
Figure VI.4: Contour Plot of Trade Study between AR and S

The values for aspect ratio and wing area were chosen to be similar to both the optimized values in Figure VI.4 and to the aircraft that were examined within the market space. A driving factor against using large and thin wings is the structural difficulty of having a large wing due to its greater weight. Another factor considered was the idea of adding dihedral angle, but was decided against due to the potential added difficulty of attaching the wing to the fuselage. Since the SEAL will not be flying close to the transonic region, wing sweep is not necessary and was not added to simplify manufacturing [2]. Table VI.3 outlines the defining parameters, followed by a three view of the wing in Figure VI.5.

Table VI.3: Major Wing Geometry Parameters

Parameter	Symbol	Value
Wing Area	S	150 ft^2
Aspect Ratio	AR	10
Wingspan	b	38.73 ft
Mean Aerodynamic Chord	MAC	3.91 ft
Taper Ratio	λ	0.7
Quarter Chord Sweep	$\Lambda_{c/4}$	0°
Dihedral Angle	Γ	0°
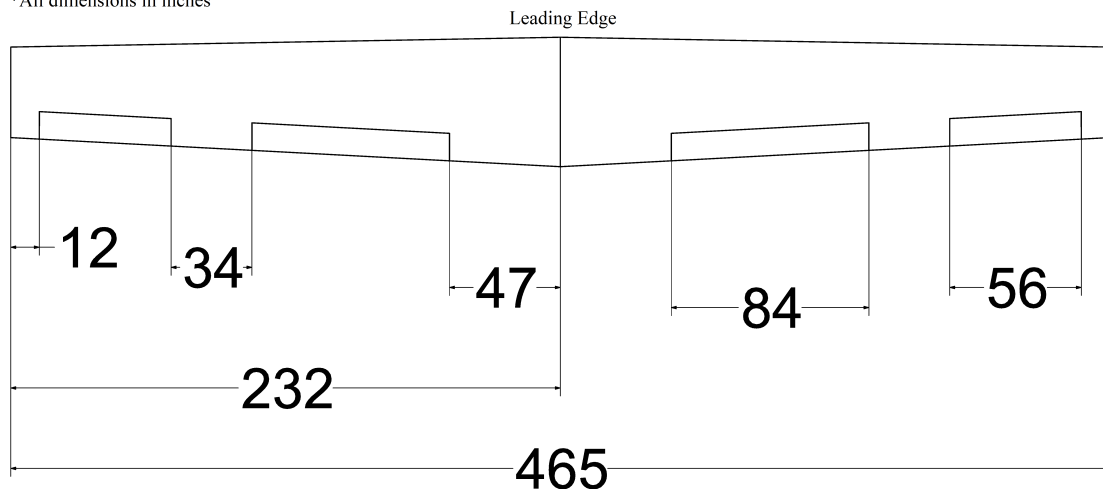
Figure VI.5: Top View of the Wing

C. Key Aerodynamic Values

Aerodynamic values are some of the most important factors in the design of aircraft. The team decided to obtain an estimate for the values of C_D, C_L, and $\frac{L}{D}$. To obtain an first order estimate for the zero-lift drag coefficient the wetted area of the aircraft was calculated. The values S_{wet}, friction coefficient, and C_{D_0} are displayed in Table VI.4.

Table VI.4: C_{D_0} First Order Estimate

Parameter	Value
S_{wet}	805.5 ft^2
C_f [2]	0.0055
C_{D_0}	0.0295

With this basic estimate for C_{D_0}, a more accurate estimate was required. Using the method outlined in the Roskam textbooks, the values used for a more robust estimate the drag are presented in Table VI.5 [3].

Table VI.5: Drag Buildup

Parameter	Takeoff (Flaps @ 15°)	Cruise	Landing (Flaps @ 30°)
$C_{D_{0_w}}$	0.0088	0.0086	0.0088
$C_{D_{i_w}}$	0.0612	0.0038	0.0420
$C_{D_{0_f}}$	0.0116	0.0106	0.0116
$C_{D_{i_f}}$	0.0025	0.0000	0.0011
$C_{D_{0_{ht}}}$	0.0012	0.0012	0.0012
$C_{D_{0_{vt}}}$	0.0007	0.0007	0.0007
$C_{D_{i_{emp}}}$	0.0357	0.0000	0.0185
$C_{D_{0_{flap}}}$	0.0077	0.0009	0.0309
$C_{D_{i_{flap}}}$	0.0277	0.0000	0.0992
$C_{D_{gear}}$	0.0039	0.0000	0.0039
$C_{D_{ws}}$	0.0019	0.0019	0.0019
$C_{D_{0_{trim}}}$	0.0002	0.0001	0.0002
$C_{D_{i_{trim}}}$	0.0016	0.0000	0.0019
C_{D_i}	0.1287	0.0038	0.1859
C_{D_0}	0.0360	0.0234	0.0360
$\mathbf{C_D}$	**0.1647**	**0.0278**	**0.2219**

The flaps are deployed for takeoff and landing at 15° and 30°, respectively, to generate more lift and decrease the required takeoff and landing speeds. As the flap deflection angle increases, the amount of lift, and therefore induced drag, increases as well. When the flaps are deflected to 30°, the largest increase in drag occurs. At cruise, the SEAL produces the lowest amount of drag by a significant margin. The drag produced at landing is considerably higher than at takeoff which will be beneficial when attempting to slow the aircraft during the landing process.

To obtain a more holistic view of the aerodynamic characteristics of the aircraft, the lift curves of the SEAL at takeoff, cruise, and landing were also examined. The lift values were taken XFLR5 and AVL. XFLR5 runs a panel method code and AVL runs a vortex lattice method code to analyze the aerodynamics of the aircraft. These programs allow for the calculation of the lift curve slope as well as the induced drag shown in Table VI.5. The lift curve, Figure

VI.6, and drag polar, Figure VI.7, for the wing at takeoff, cruise, and landing were generated from lift data from AVL and XFLR5 and drag values from the drag buildup.
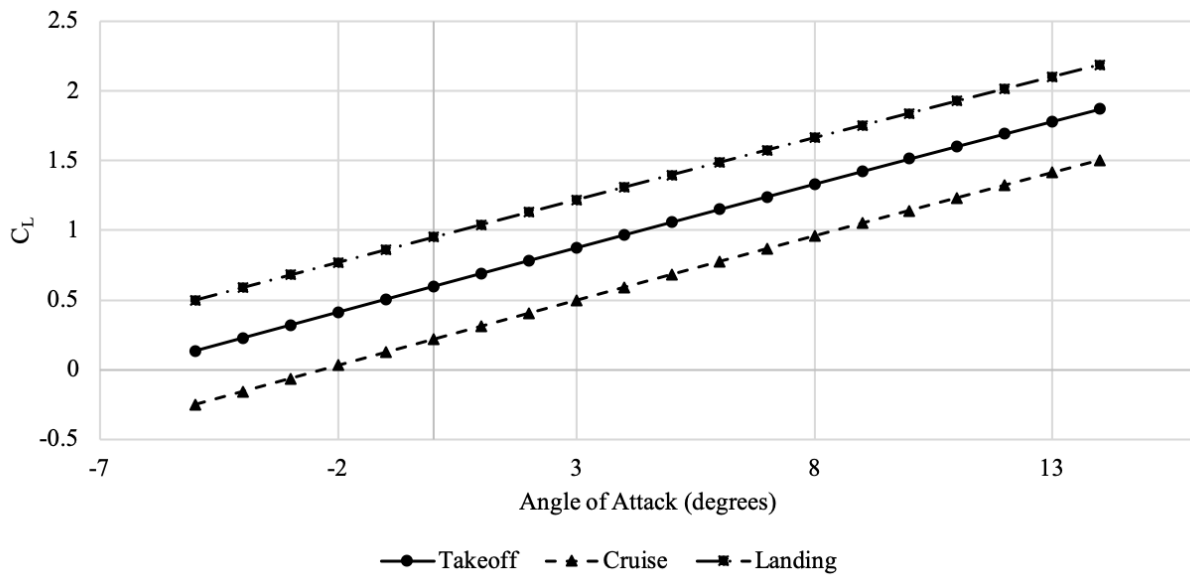
Figure VI.6: C_L vs Angle of Attack
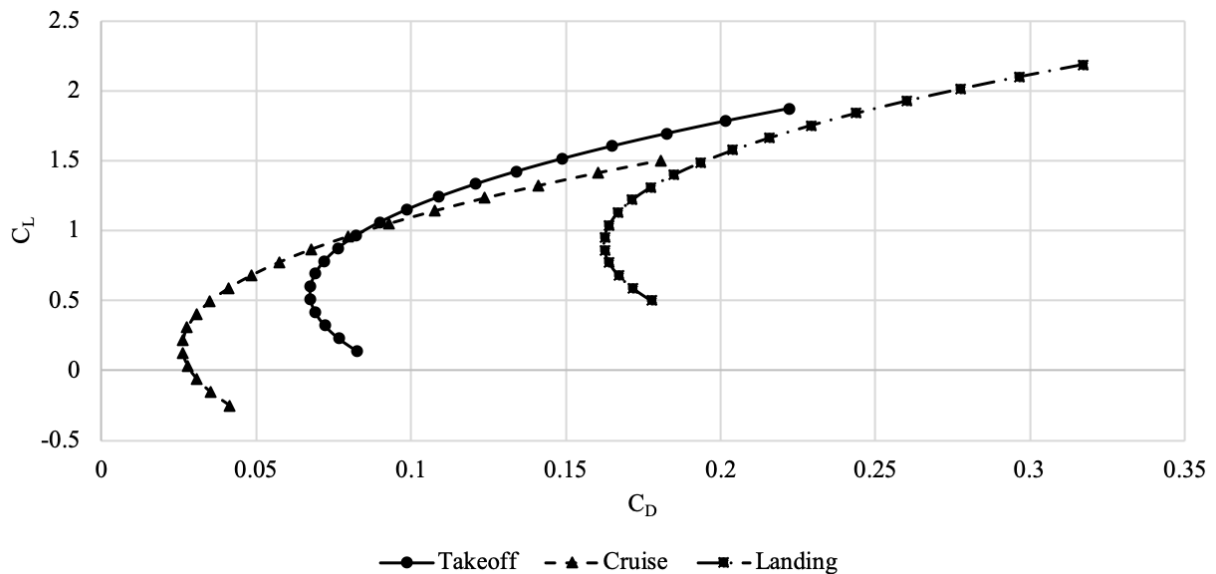
Figure VI.7: C_L vs C_D

As the flaps are deployed the lift curve is shifted higher, signifying a greater production of lift. The lift slope of each segment shown in Figure VI.6 decrease slightly with increasing flap deflection, but the increase in flap deflection increases the lift greatly as expected. The increase in lift also increases the induced drag, indicated by the difference in the shape of the drag polar shown Figure VI.7. At lower C_L values, the SEAL produces less drag than higher C_L

23

values in all three segments of flight.

The determination of the aerodynamic values at different points of flight are also important to analyze. These values are determined from the weight at the segment and the acquired data from AVL and XFLR5, and are shown in Table VI.6.

Table VI.6: Major Aircraft Aerodynamic Information

Parameter	Takeoff	Cruise Reference Mission	Cruise Sizing Mission	Landing
Weight (lbs)	4,550	4,500	4,500	4,090
Altitude (ft)	0	20,000	12,000	0
Velocity (KTAS)	80	225	225	70
Required C_L	1.61	0.33	0.25	1.64
Flap Deflection	15°	0°	0°	30°
Required α_{wing}	11.5	1.21	0.39	7.80
C_D	0.1647	0.0278	0.0278	0.2219
$\frac{L}{D}$	10.0	11.9	9.0	7.4

The values of weight in table are the MTOW, a weight at the beginning of cruise, and the landing weight. As shown in the table, the least efficient flight segment is during the landing process due to the high drag values. The most efficient flight will be during cruise during the reference mission. The difference in lift and $\frac{L}{D}$ values between the two missions during cruise is due to the different cruise altitudes. With the two required angle of attacks during cruise, it was chosen to mount the wing with $1°$ of incidence. This is to need minimal elevator deflection to pitch the SEAL to the proper angle of attack.

D. High-Lift Devices

To improve takeoff and landing performance, the proposed aircraft will be fitted with plain flaps. The sizing of these flaps will be determined as progress on the design continues. The decision to choose plain flaps over other high lift devices comes from the simplicity in manufacturing and design and low weight relative to other, more complex systems. There is also precedence for the usage of plain flaps in many applications similar to those called for in the proposal. These considerations, combined with the added production difficulties coming from the hinges or tracks required for higher lift solutions led to the final decision to use plain flaps.

As more specifications are finalized, analysis will be performed on takeoff and landing distance and changes will be made to the flap sizing in order to meet the requirements. Initial work on this includes the compilation of a spreadsheet with similar aircraft and their flap sizes tabulated to obtain a first order approximation for the size of flap required on the aircraft.

VII. Performance

A. Required Performance

The performance requirements for the thin-haul transport and air taxi reference mission include: an average ground speed greater than or equal to 180 ktas, total flight time less than or equal to 45 minutes, a minimum range of 135 nmi, a maximum take-off distance of 2500 ft, a maximum landing distance of 2500 ft, loiter for 45 mins and a maximum flight time of 45 mins. The reference mission must be completed at half payload weight equivalent to three passengers. The aircraft must also be able to complete a sizing mission with a few modifications to the reference mission which are: full payload, a minimum range of 250 nmi and no restrictions on speed or flight time.

B. Takeoff and Landing Performance

The RFP requirements for take-off are a maximum take-off distance and landing distance over a 50 ft obstacle of 2500 ft for both the reference and sizing mission. The take-off and landing analysis was done for different runway surfaces and at two airport elevations of sea level and 5,000 ft. The RFP specifies that missions are flown at sea level field elevation for takeoffs and landings at a standard day with zero wind conditions. The rotation speed for half payload is 127.88 ft/s and the lift-off speed is 133.7 ft/s. The rotation speed for full payload is 137.76 ft/s and the lift-off speed is 144.02 ft/s.

Table VII.1: Take-off performance at sea level

Surface	Ground roll (reference)	Take-off distance (reference)	Ground roll (sizing)	Take-off distance (sizing)
Dry concrete	1064 ft	1544 ft	1797 ft	2372 ft
Wet concrete	1085 ft	1565 ft	1842 ft	2417 ft
Icy concrete	1141 ft	1632 ft	1728 ft	2302 ft
Hard turf	1176 ft	1667 ft	1822 ft	2397 ft
Firm dirt	1163 ft	1654 ft	1789 ft	2363 ft
Soft turf	1203 ft	1694 ft	1896 ft	2470 ft
Wet grass	1123 ft	1603 ft	1926 ft	2500 ft

Table VII.2: Take-off performance at 5,000 ft elevation

Surface	Ground roll (reference)	Take-off distance (reference)	Ground roll (sizing)	Take-off distance (sizing)
Dry concrete	1705 ft	2276 ft	3055 ft	3783 ft
Wet concrete	1747 ft	2318 ft	3142 ft	3870 ft
Icy concrete	1840 ft	2400 ft	3020 ft	3748 ft
Hard Turf	1908 ft	2469 ft	3142 ft	3870 ft
Firm dirt	1883 ft	2444 ft	3096 ft	3824 ft
Soft turf	1964 ft	2525 ft	3256 ft	3984 ft
Wet grass	1825 ft	2395 ft	3325 ft	4052 ft

Table VII.3: Landing performance at sea level

Surface	Ground roll (reference)	Landing distance (reference)	Ground roll (Sizing)	Landing distance (sizing)
Dry concrete	686 ft	1714 ft	769 ft	1821 ft
Wet concrete	730 ft	1758 ft	821 ft	1861 ft
Icy concrete	2840 ft	3868 ft	3294 ft	4335 ft
Hard Turf	993 ft	2021 ft	1130 ft	2171 ft
Firm dirt	1198 ft	2227 ft	1371 ft	2411 ft
Soft Turf	1609 ft	2637 ft	1851 ft	2892 ft
Wet grass	1609 ft	2637 ft	1851 ft	2892 ft

Table VII.4: Landing performance at 5000 ft elevation

Surface	Ground roll (reference)	Landing distance (reference)	Ground roll (Sizing)	Landing distance (sizing)
Dry concrete	979 ft	2019 ft	1110 ft	2165 ft
Wet concrete	1550 ft	2590 ft	1780 ft	2835 ft
Icy concrete	3265 ft	4305 ft	3790 ft	4845 ft
Hard turf	1122 ft	2162 ft	1278 ft	2333 ft
Firm dirt	1360 ft	2400 ft	1557 ft	2612 ft
Soft turf	1836 ft	2876 ft	2115 ft	3170 ft
Wet grass	1836 ft	2876 ft	2115 ft	3170 ft

The take-off analysis was done using analytical method from Roskam [3]. The aircraft has a take-off distance over 50 ft obstacle higher than 2500 ft at 5,000 ft elevation with full payload. However, the aircraft meets the RFP requirements as the RFP specifies sea level take-offs and landings for both the reference and sizing missions. The landing performance was calculated by using analytical method equations from Roskam [3].SEAL satisfies the RFP requirement of a landing distance over a 50 ft obstacle of less than 2500 ft for dry and wet concrete runway surfaces, hard turf and firm dirt at sea level.

C. Mission Segment Performance

Fuel estimation - The fuel weight fraction estimate values for landing were taken from Raymer [2]. The fuel consumed during taxi and take-off was calculated using the SFC of engine during take-off from the engine data. A taxi time for 10 mins with 10 percent power at idle was assumed. The take-off times for the reference and sizing missions are 35 seconds and 51 seconds respectively. The fuel fraction for cruise was calculated depending on the range required for the two missions. Numerical integration method was used to determine fuel used in climb and descent. Fuel weight fraction for loiter was chosen by considering loiter time and velocity. A summary of fuel weight and fuel weight fractions for different mission segments are shown in Table VII.5 and Table VII.6.

Table VII.5: Fuel weight estimations for reference mission

Segment	Fuel used	Fuel fraction (percentage)
Taxi and take-off	7.52 lbs	0.18
Climb to 20,000 ft	56.83 lbs	1.5
Cruise	70 lbs	1.8
Descent and climb to 3000 ft	13.6 lbs	0.38
Loiter for 45 mins	82 lbs	2.3
Land	18 lbs	0.5
Total Fuel Consumed	247.95 lbs	

Table VII.6: Fuel weight estimations for sizing mission

Segment	Fuel used	Fuel fraction (percentage)
Taxi and take-off	8.5 lbs	0.187
Climb to 12,000 ft	31.73 lbs	0.72
Cruise	180 lbs	3.5
Descent and climb to 3,000 ft	12 lbs	0.29
Loiter for 45 mins	95 lbs	2.3
Final descent and landing	20.96 lbs	0.5
Total Fuel Consumed	348.19 lbs	

Drag estimation per mission segment - Drag for every mission segment was calculated by combining parasite drag and lift-induced drag.Drag values are shown in Table VII.7.

Optimal velocity for maximum aerodynamic efficiency was calculated to minimize drag during cruise. This value is given by the velocity at which C_L/C_D is maximum which is around 150 ft/s for both reference and sizing mission. However, cruise velocities were chosen to be 380 ft/s (225 KTAS) for reference mission and 350 ft/s (207.37 KTAS) for sizing mission in order to meet the flight time requirement of 45 minutes and minimum speed of 185 KTAS.Moreover, a velocity of 150 ft/s is below stall velocity at cruising altitudes of 20,000 ft for reference mission and 12,000 ft for sizing mission.The estimated drag during landing is the highest because of aerodynamic brakes and low flaps.

Table VII.7: Drag per mission segment

	Reference mission	Sizing mission
Take-off	590 lbs	695 lbs
Climb	540 lbs	560 lbs
Cruise	240 lbs	252 lbs
Loiter	329 lbs	378 lbs
Landing	1080 lbs	1153 lbs
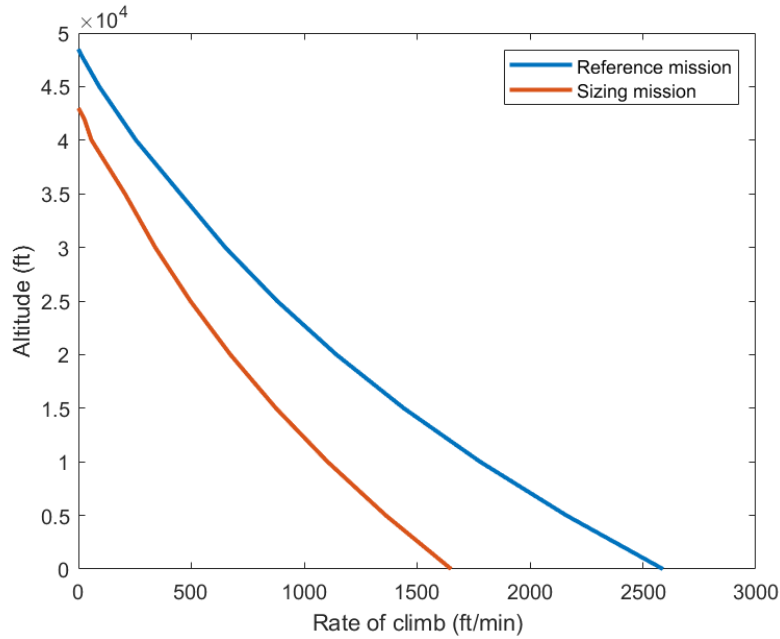
Figure VII.1: Variation of rate of climb with altitude

Climb Performance- The reference mission with half payload has a maximum take-off rate of climb of 2638.6 ft/min at a velocity of 135.42 ft/s and a flight path angle of 5.5 degrees. The sizing mission with full payload has a maximum take-off rate of climb of 1650.86 ft/min at a velocity of 156.42 ft/s and a flight path angle of 7 degrees. The climb performance was calculated using equations in Anderson [20]. These equations make use of difference in thrust required and thrust available at various altitudes to calculate the rate of climb. The performance based service ceiling was determined by finding the altitude at which ROC reaches 100 ft/min. The absolute ceiling is determined by the altitude at which ROC becomes 0 ft/min. Figure VII.1 shows the variation of rate of climb for the reference and sizing missions with altitude. The absolute ceilings for reference and sizing mission were found to be 48,500 ft and 42,000 ft respectively. The service ceilings for reference and sizing missions were determined to be 45,000 ft and 37,000 ft respectively.

The service ceiling was not a limiting factor in choosing the best cruise altitude as an altitude lower than 20,000 ft was calculated to give a better aerodynamic efficiency and range. The high thrust available from the engine supports a higher ceiling.

Cruise Performance- As per the RFP requirements, the design aircraft must achieve a minimum range of 135 nmi for the reference mission and 250 nmi for sizing mission. SEAL satisfies these requirements by achieving a maximum range of 337 nmi at a cruise altitude of 20,000 ft and a cruise velocity of 380 ft/s (225 KTAS) for reference mission and a maximum range of 382 nmi at a cruise altitude of 12,000 ft and a cruise velocity of 350 ft/s (207.37 KTAS) for the sizing mission.This is shown in the payload-range diagram later in the section.

Loiter Performance- The RFP requires an optimal loiter velocity for 45 mins of loiter time. This velocity can be found by determining the velocity at which $C_L^{3/2}/C_D$ becomes maximum. The variation of $C_L^{3/2}/C_D$ with velocity is plotted in figure VII.2. The graph shows an optimal velocity of 102 ft/s (60.4 KTAS) for both reference mission and sizing mission at a loiter altitude of 3,000 ft. A velocity of 102 ft/s is below the stall velocity at 3,000 ft. Therefore, higher loiter velocities of 280 ft/s and 300 ft/s were chosen for reference and sizing mission respectively, keeping in mind the safety margins.
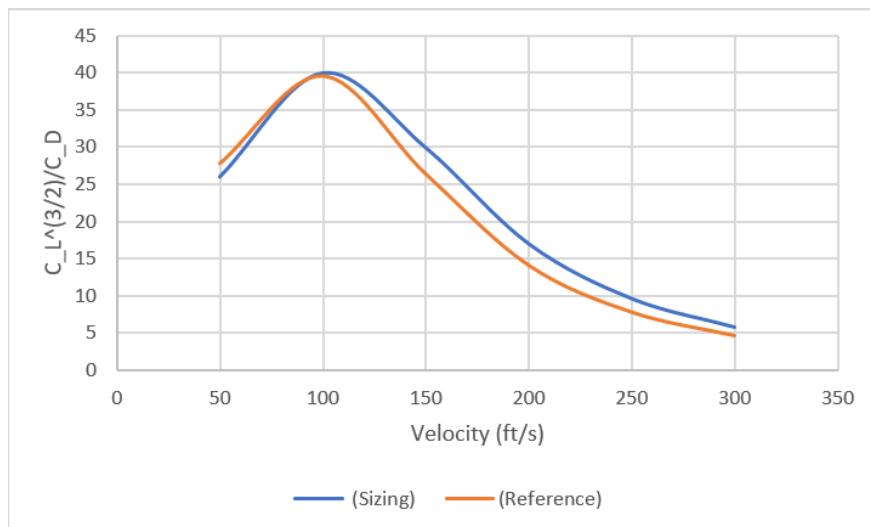
Figure VII.2: Variation of $C_L^{3/2}/C_D$ with velocity at 3000 ft for reference and sizing mission

Other Aircraft Performance Coefficients- Two other important performance coefficients are C_L/C_D and $C_L^{1/2}/C_D$. The variation of these coefficients with velocity at an altitude of 20,000 ft for reference mission and 12,000 ft for sizing mission are shown in Figures VII.3 and VII.4. C_L/C_D is a measure of aerodynamic efficiency. The flight is the most efficient in terms of thrust required at maximum C_L/C_D.The maximum range of an aircraft corresponds to the maximum value of $C_L^{1/2}/C_D$.
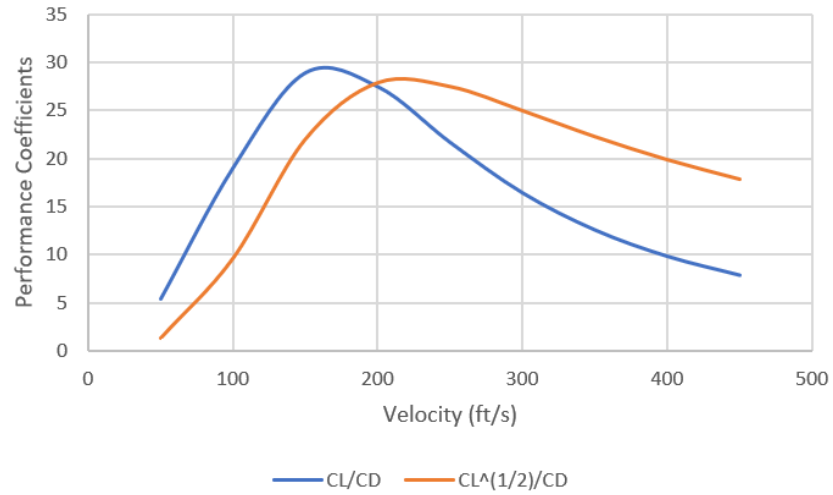
Figure VII.3: Reference mission
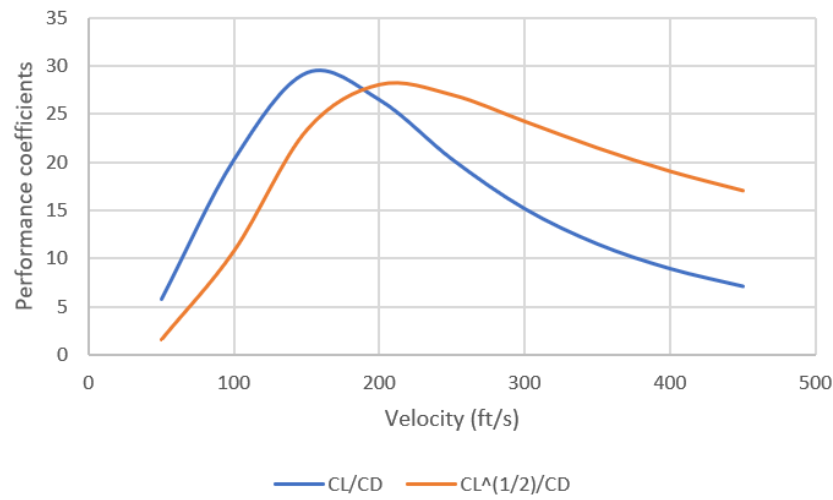
Figure VII.4: Sizing mission

Payload-Range diagram- The payload range diagram is a graph which shows the effect of trading payload for fuel in a mission. The payload-range diagram is comprised of three fundamental limits: maximum payload, maximum take-off weight and maximum fuel carrying capacity. The payload-range diagrams for SEAL are as shown in Figure VII.5 and VII.6 .
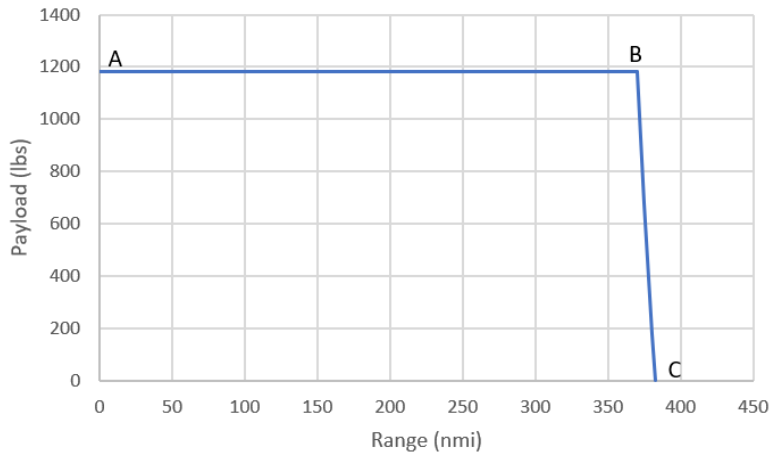
Figure VII.5: Payload Range diagram for SEAL at 12,000 ft at a cruise velocity of 207.37 KTAS
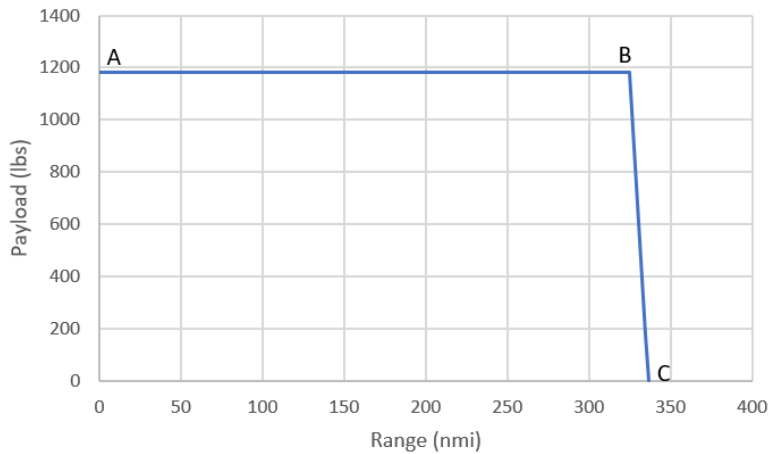
Figure VII.6: Payload Range diagram for SEAL at 20,000 ft at a cruise velocity of 225 KTAS

The payload range diagram illustrates the trade-off relationship between payload and range. Once the aircraft is loaded with maximum payload, fuel can be added to get a desired range while keeping the total weight under the maximum take-off weight. In Figure VII.5 and VII.6,line AB is calculated by taking maximum payload carrying capacity of the aircraft and the fuel can be added to reach any range.Line BC represents the fuel volume limit. The aircraft tanks are full and range is further increased by reducing the payload.

Flight envelope- An aircraft's flight envelope is the region on an altitude vs. velocity plot in which the aircraft is capable of operating. The airplane is limited by lower stall speed and higher maximum velocity. This maximum velocity corresponds to the maximum velocity that is achievable at an altitude at which thrust required is lower than thrust available. The flight envelope for reference and sizing mission of SEAL are shown in Figures VII.7a and VII.7b.
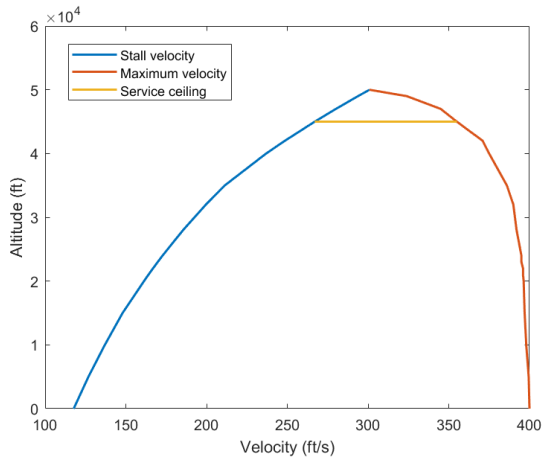
(a) Flight envelope for reference mission
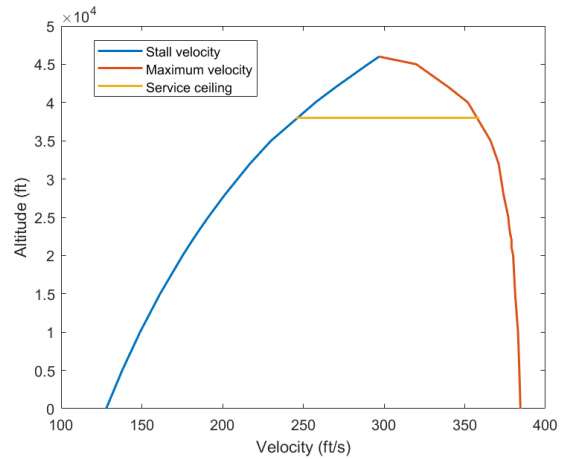
(b) Flight envelope for sizing mission

Figure VII.7: Flight envelope for different missions

Specific excess power- Specific excess power is mapped over full range of velocity and altitude to determine the climb capability of the aircraft. This creates specific excess power contours of constant specific excess power for a range of velocities and altitudes.
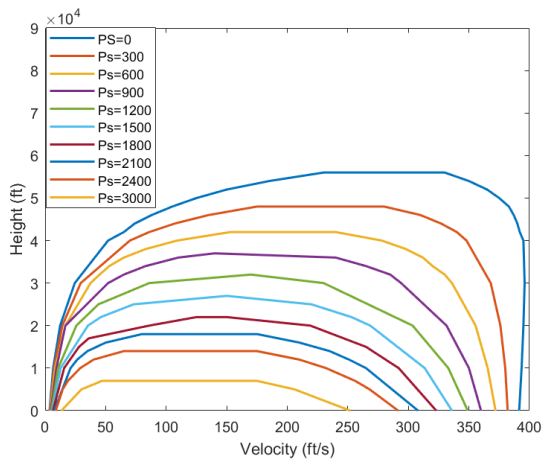
(a) Specific excess power for reference mission (ft/min)
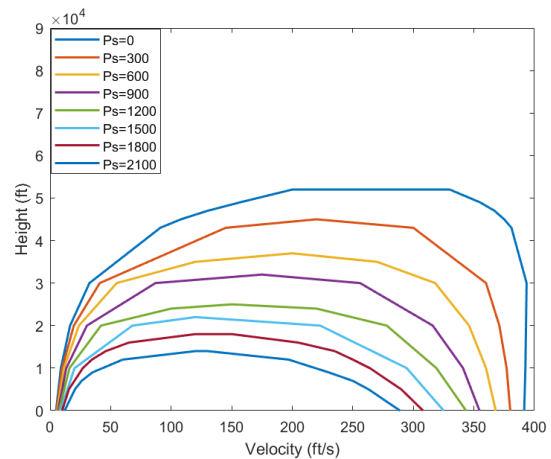
(b) Specific excess power for sizing mission (ft/min)

Figure VII.8: Specific excess power for different missions

Conclusion- SEAL meets all the RFP requirements of take-off and landing distance less than or equal to 2500 ft over a 50 ft obstacle at sea level for both the reference and sizing mission except for the landing distance on icy concrete, soft turf and wet grass. The average ground speed in climb-out to descent segments is also greater than 185 KTAS for the reference mission. The average ground speed for reference mission is 204.5 KTAS. The reference mission is completed in 44 mins with 11 minutes of climb, 16 minutes of cruise and 17 minutes of descent.

Trade Study 1: Cruise velocity After a cruising altitude was decided depending on pressurization system constraints and duration of total flight, a trade study was carried out to determine the optimal velocity for maximum range. The plot of cruise velocity vs. range for reference mission is shown Figure VII.11.
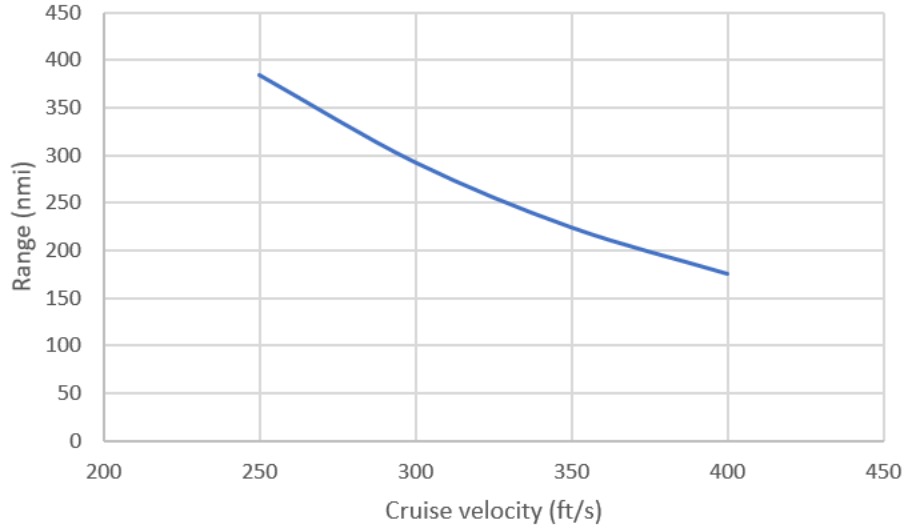
Figure VII.9: Variation of range with cruise velocity at 20,000 ft for reference mission with maximum fuel

Figure VII.11 shows that a lower cruise velocity provides a higher range. However, due to RFP requirements of a minimum average ground speed of 185 KTAS , a cruise velocity of 380 ft/s (225 KTAS) was selected with a maximum cruise range of nearly 336.7 nmi with maximum fuel.

Trade Study 2: Landing Gear Our initial design included a fixed landing gear instead of a retractable one. The main reason behind this choice was a reduction in weight and complexity. However, after performance calculations, it was discovered that the landing gear introduces too much drag, especially at high speeds for reference mission. This increase in drag leads to the aircraft not meeting both the RFP requirements of cruise velocity and range at the same time. The calculation results are shown in Table VII.8.

Table VII.8: Range with non-retractable landing gear

Cruise velocity at 20,000 ft	Range	Cruise altitude at 340 ft/s	Range
245 ft/s	136 nmi	10,000 ft	54 nmi
280 ft/s	107 nmi	15,000 ft	63 nmi
300 ft/s	94 nmi	20,000 ft	74 nmi
320 ft/s	83 nmi	25,000 ft	87 nmi

VIII. Mass Properties

Weights are an area of high importance in the design of aircraft as they are often the driving factors for several other design parameters such as propulsion and lift. In addition, the center of gravity of the aircraft and its components are critical to the stability and controllability of the aircraft. The proceeding mass properties section will discuss the component weight buildup of the aircraft as well as the center of gravity as well as the CG travel during different phases of flight.

A. Initial Aircraft Weights

The aircraft weights were first estimated during initial sizing with the calculation of primary structural weights such as the wing, fuselage, and tail sections. An empty weight and fuel weight were guessed and used in the calculations of the structural wing weight formula obtained from Kroo and by using weight trades for differences compared to the seed aircraft [4]. An initial weight buildup of the important aircraft weights was obtained and are tabulated in Table VIII.1. These aircraft weights were used as a reference point of design until more detailed weight calculations could be performed.

Table VIII.1: Important aircraft weights obtained from initial sizing

Parameter	Weight (lb)
Empty Weight	3,075
Maximum Takeoff Weight	4,230
Maximum Zero Fuel Weight	4,275
Fuel Weight	355
Wing Weight (Stuffed)	1,240
Landing Weight	4,100

The weights described in Table VIII.1 were used for the preliminary design portion and have been refined to reflect values which are more accurate for the exact design. Better weight estimation tools were used such as CAD and manufacturer data from real components. Throughout the entire design process, the empty and maximum takeoff weight remain very close and do not deviate over ten percent of the values found in initial sizing.

B. Component and Structural Weights

For the preliminary weight estimation, the aircraft structural and component weights were done using an iterative method with empirical equations dependent on the takeoff or landing weights. Several methods of weight estimation were used including the statistical weights methods described in Raymer and the Cessna and USAF GA Class II weight

estimation methods described in Roskam [2] [3]. The Class II methods in Roskam define a bottom-up weight buildup method as opposed to iterative guessing. This was then further refined by using structural weights obtained by CAD models and exact component weights sized from similar aircraft. Engine weight was based on the dry weight provided by the manufacturer - Rolls Royce [21]. Weights obtained from the structural CAD also included a ten percent margin to account for skin and rivets as well as modifications to the design. Other equipment sized from similar aircraft used exact weights taken from manufacturer data or known aircraft Weight and Balance and an additional five to ten percent factor to account for wiring and other miscellaneous items. The greater ten percent is applied when an exact component could not be used and was the size difference from the SEAL had to be accounted for. The payload includes five 180 lb passengers carrying 20 lb of luggage each as well as a 180 lb pilot. A tabulated summary of the aircraft weights can be found on Table VIII.2.

The estimated empty weight of the aircraft is 2,890 lb which is comparable to similar aircraft such as the Extra EA-500 and Piper PA-46 as presented in III.3. These similar aircraft have four passengers in comparison to the SEAL's five, providing the SEAL with a competitive advantage. Lower fuel weight due to the shorter required mission range also gives the SEAL a low takeoff weight of 4,550 lb.

C. Components and Structures CG

In addition to the weight of the aircraft structures and components, their centers of gravity are also essential to maintaining the stability of the aircraft. The CG of components along the longitudinal axis of aircraft with the datum at the tip of the fuselage is tabulated with the weights in Table VIII.2. The CG location of structural components are based on CAD estimates and the component CGs are based on their placement within the aircraft as determined by the auxiliary systems. For the x-direction lateral CG, locations are taken from a datum 100 inches in front of the nose of the aircraft to allow for future changes to the aircraft length. Y-direction moment arms are taken from the centerline and z-direction arms are taken from the height from the ground when the aircraft is one the ground.

Table VIII.2: Weight and balance summary of major aircraft structures and components

Item	Weight [lb]	Source	X Loc [in]	X Mom [in lb]	Y Loc [in]	Y Mom [in lb]	Z Loc [in]	Z Mom [in lb]
Structures	**1590**		**282**	**448,600**	**0**	**0**	**74.5**	**118,170**
Wing	450	CAD	253	113,888	0	0	105	47,304
Horiz. Tail	67	Roskam	443	29,695	0	0	71	4,728
Vert. Tail	20	Roskam	433	8,733	0	0	0	0
Fuselage	865	CAD	283	244,484	0	0	71	61,035
Gear System	185	Roskam	280	51,800	0	0	0	0
Propulsion	**410**		**148**	**60,553**	**0**	**0**	**0**	**62,714**
Engine (Installed)	275	Manuf.	143	39,420	0	0	62	16,929
Prop+Spinner	85	Manuf.	96	8,153	0	0	62	5,233
Fuel Sys + Tanks	50	Roskam	260	12,962	0	0	105	5,256
Systems	**847**		**250**	**211,181**	**0**	**0**	**28**	**23,980**
Flight Controls	205	Roskam	259	53,095	0	0	55	11,316
Instruments/Navi	20	Roskam	259	5,180	0	0	105	2,102
Hydraulics	42	Roskam	355	14,910	0	0	84	3,528
Batteries	84	Manuf.	262	21,998	0	0	57	4,788
Elec. + Alternator	36	Manuf.	232	8,352	0	0	62	2,246
Avionics	80	Manuf.	262	20,950	0	0	62	4,992
Furnishings	185	Roskam	272	50,401	0	0	62	11,544
AC + Press.	190	Roskam	182	34,504	0	0	57	10,830
Load & Handling	5	Roskam	358	1,790	0	0	71	353
Misc	25	Roskam	232	5,800	0	0	0	0
Payload	**1,680**		**275**	**432,630**	**74.5**	**118,170**	**75.5**	**126,990**
Pilot	180	RFP	236	42,516	18	3,240	62	11,232
2nd Row	360	RFP	251	90,432	0	0	62	22,464
3rd Row	540	RFP	311	168,048	0	0	62	33,696
Luggage	100	RFP	358	35,800	0	0	62	6,240
Fuel (Full)	500	Calc	252	125,834	0	0	105	39,375
Fuel (Landing)	20	Calc	252	5,033	0	0	105	2,100
Ballast	225	Calc	358	80,550	0	0	71	15,975

Figure VIII.1 shows the CG at several aircraft payload weights that are of most interest - dry, operating, and maximum payload. Additionally, the 'x' markers show the loading when there is full fuel for each payload conditions. A CG location of 258 in required for the aircraft to be stable as defined by Stability and Control. As Figure VIII.1 conveys, the aircraft CG falls forward of this limit when dry and with only operating items. To counteract this, a ballast may be required during training or repositioning mission when there would only be a pilot in the front row. This ballast would weigh 225 lb and be placed in the luggage compartment in the rear. The reduce the need for the ballast, operators can consider operating with cargo during repositioning flights which can also assist in cost recovery during these non-revenue flights.
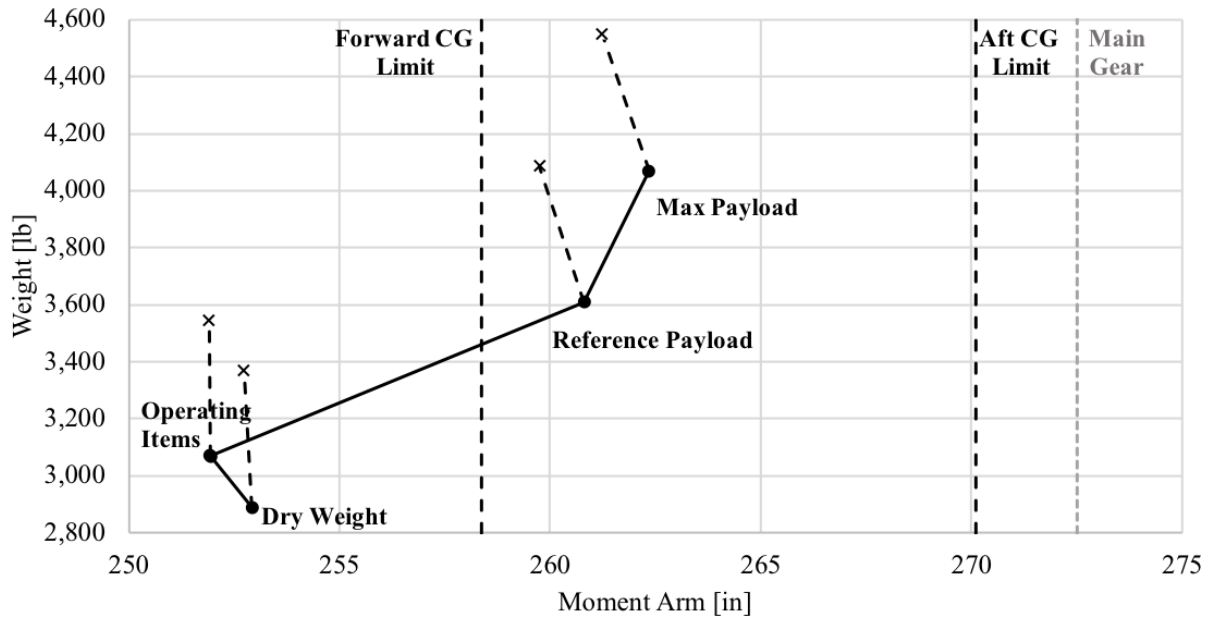
Figure VIII.1: CG at different payload conditions. x indicates full fuel positions.

In addition to the CG location of components on the aircraft, the CG during different loading conditions are ana-lyzed. A case where the luggage is loaded onto the rear of the aircraft first before the passengers and fuel will create a the greatest CG shift. Figure VIII.2 shows the CG movement when an empty aircraft with no fuel is loaded from the rear first in the order of: the luggage, the third row occupants (three passengers), the second row occupants (two passengers), and the pilot.
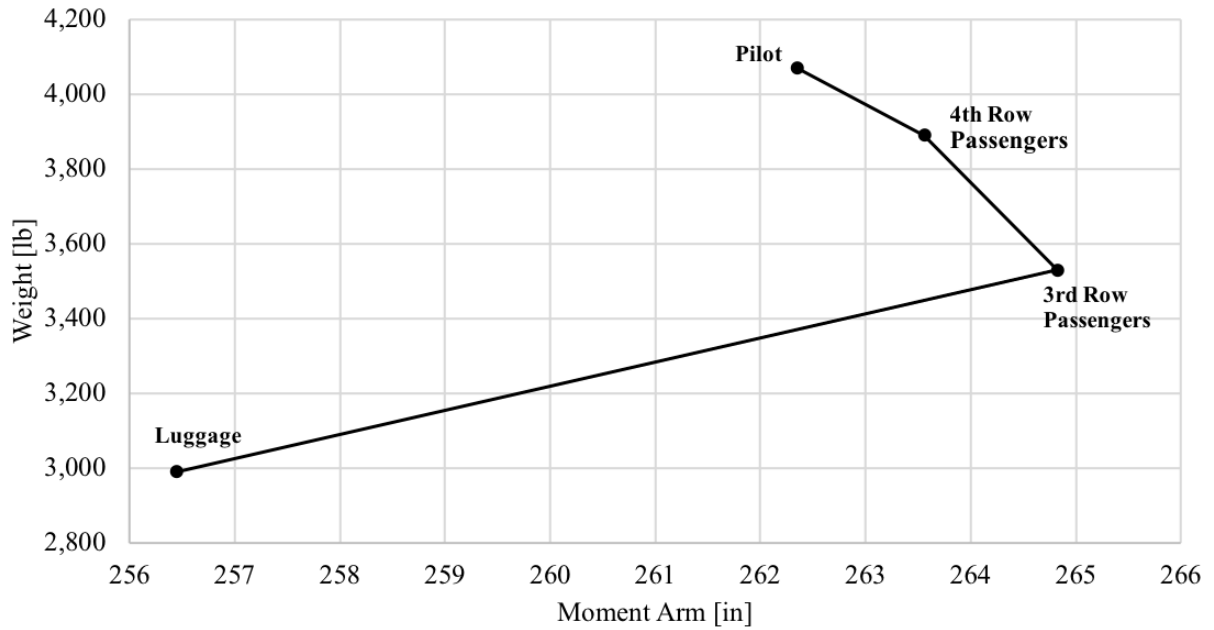
Figure VIII.2: CG movement during extreme passenger loading order

The adverse loading diagram in Figure VIII.2 shows the movement of the CG when the plane is loaded from rear to front with no fuel. Even with the rear of the plane loaded first, the CG does not move behind the location of the main gear which is at 273 in from the datum, indicating that there is no danger of tip over.

Figure VIII.3 shows the CG movement during regular reference mission flight with 3 passengers and full fuel at takeoff as well as the CG during landing, at which there will be approximately 20 lb of fuel remaining. At a full load, the CG is fully within the acceptable stability range for the aircraft and shifts only an inch in total. This is because the CG location of the fuel tanks is close to the CG of the aircraft, so fuel burn does not significantly contribute to a change in CG.

Figure VIII.4 shows the CG movement during a sizing mission flight with 5 passengers and full fuel and the CG during landing, at which there will be approximately 20 lb of fuel remaining. Similar to the reference mission, there is also minimal change to the CG.
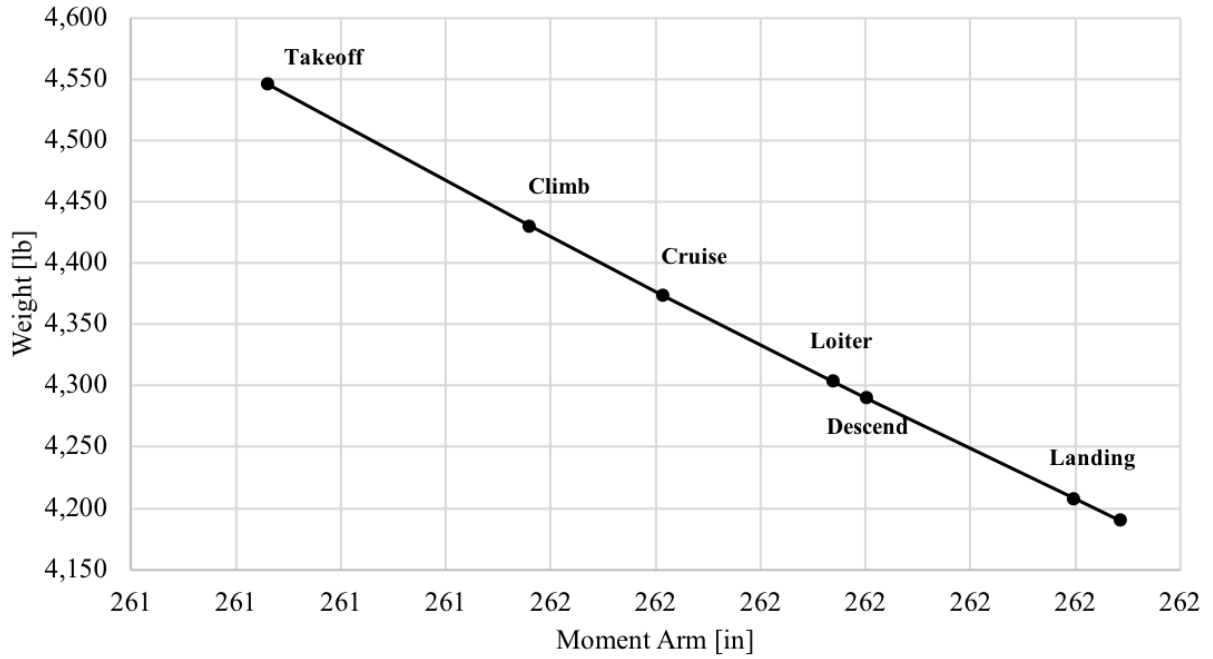
Figure VIII.3: CG movement during a reference mission with 3 passengers
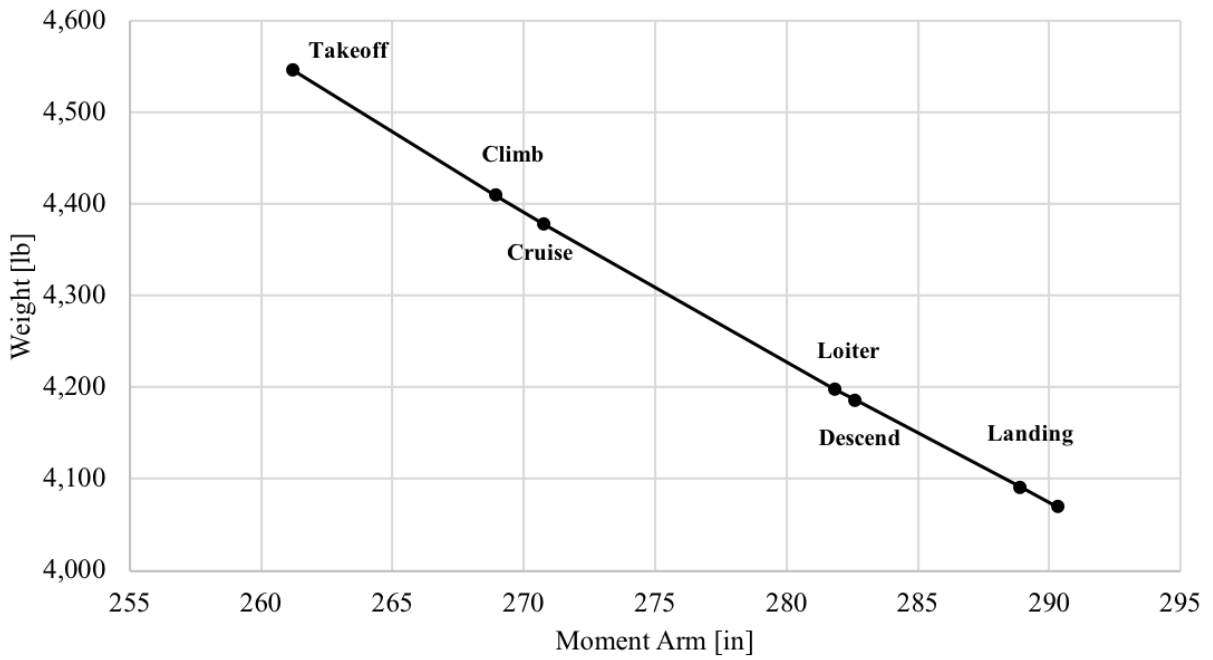
Figure VIII.4: CG movement during a sizing mission with 5 passengers

D. Weight Trade Analysis

Several component changes and the weight differences associated with them were studied to analyze the effects of changing components on the aircraft. The weight differences are presented in Table VIII.3.

Table VIII.3: Weight Changes for Different Component Changes

Item	Weight Difference [lb]
Pressurization Equipment	+80 to +100
Composite Wing	-73.13
Retractable Landing Gear	+60.62

The weight addition of pressurization equipment was difficult to estimate as Raymer, Roskam, and Kroo do not provide equations for the weight of equipment used for pressurization for GA aircraft. They are either not provided, or are included with another system such as the AC and Pressurization from Raymer and as seen in the Weight Summary Foldout Table. The Pressurization equipment weight was estimated using the AC + Pressurization presented by Roskam USAF GA equations and compared to the weight of AC systems presented by Kroo and the Cessna method in Roskam. The study estimates that the pressurization equipment for the SEAL will be between 20 and 80 lb. This is a significant range, but is within 100 lb and was a driving factor in the consideration of pressurization for higher cruise altitudes.

Although the team is satisfied with the structural weight of the aircraft, additional explorations into weight savings were conducted. As composites have gained prevalence in several new GA aircraft such as the Cirrus SR20 and SR22 and Diamond DA40 and DA60, composites have been proven to be applicable to the GA market. The team explored the weight savings provided by using a composite wing which was found to be a 73 lb reduction. This was calculated by applying a 0.9 factor of weight reduction based on Raymer [2]. A 73 lb weight savings is significant and is analogous to the weight required to add pressurization, retractable landing gear, or interior furnishings such as inflight entertainment. Despite the weight savings, the team have decided to forgo the application of composites due to the other challenges associated the use of composites including the difficulty of attaching composites to a metal frame, the limited resources of performing structural analysis of composites, and the difficulty of repair if damaged. Due to the focus on low cost in both manufacturing and operating of this aircraft, composites were not considered to be viable.

Retractable landing gear were also explored for the possible drag reduction during flight. Retractable landing gear adds weight due to the additional mechanical equipment and storage compartment required. By comparison of the Cessna retractable landing gear equation in Raymer, the weight addition compared to a fixed landing gear is 60.6 lb. This weight addition may be countered by the drag reduction provided by retractable landing gear and was used as a driving factor in the selection of retractable landing gear.

IX. Structures and Loads
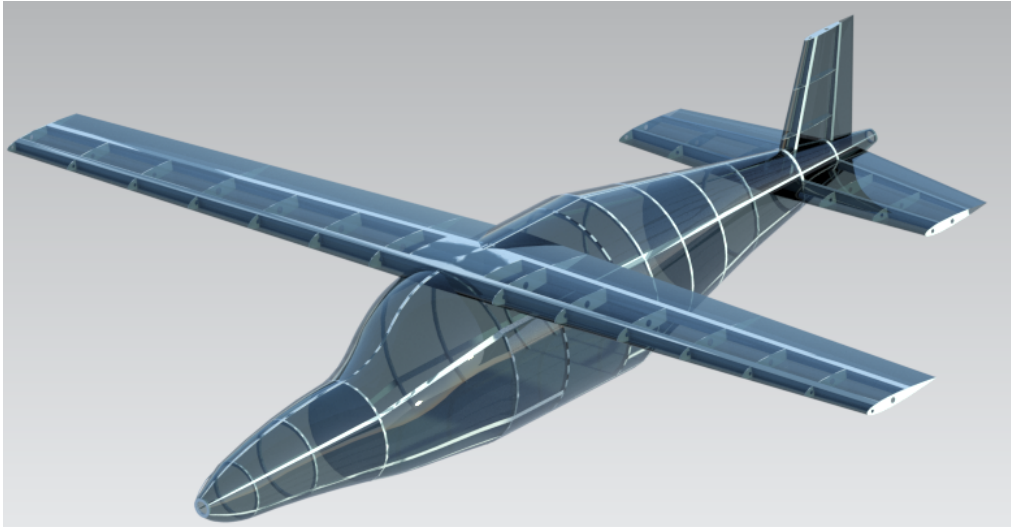
Figure IX.1: Structural Layout of the SEAL

A. V-N Diagram, Load Cases, and Load Paths

The V-N diagram is a useful plot that illustrates the structural limits of the aircraft. Within the diagram, the aircraft can safely fly. The diagram utilizes wing loading as well as performance velocities and limit load factors necessary to formulate the diagram. The limit load factors are determined in accordance with 14 CFR Part 23.337. The positive limit load factor is 3.78, and the negative limit load factor is -1.51. The values for V_A, V_C, and V_D were determined to be 148.5, 202.5, and 253.1, respectively. These values are representative of the maneuvering speed, cruise speed, and dive speed. The V_C gust lines used were 50 feet per second. The V_D gust lines used were 25 feet per second. For the SEAL, the positive gust lines do not increase the structural envelope while the negative gust lines slightly extend the structural envelope. Take note that the V-N diagram displays velocity as KEAS not KTAS. The V-N diagram was determined using sea level conditions where the aerodynamic forces on the aircraft are the greatest.
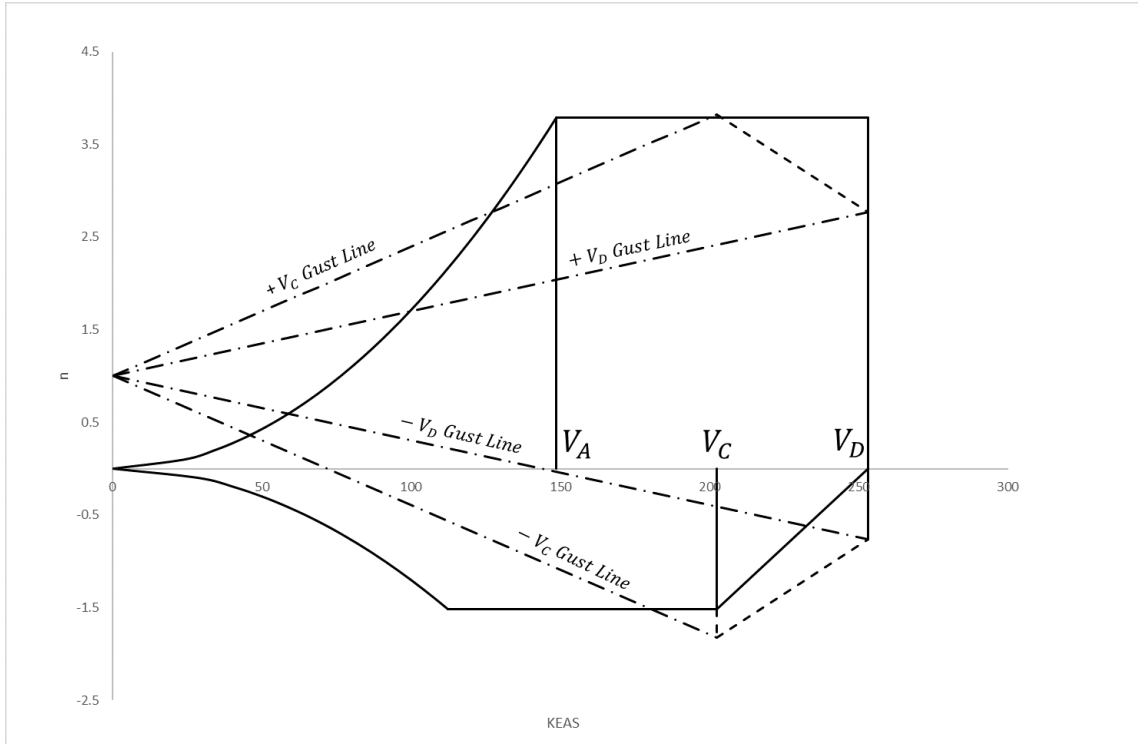
Figure IX.2: V-N Diagram

Schrenk's distribution was used to determine the spanwise lift distribution along the wing [25]. For this calculation, a factor of safety of 1.5 was assumed and the limit load factor of 3.78 was used. With the distribution determined, the shear and moment distributions were determined. This distribution was used in performing the wing box analysis to size the spars of the wing.
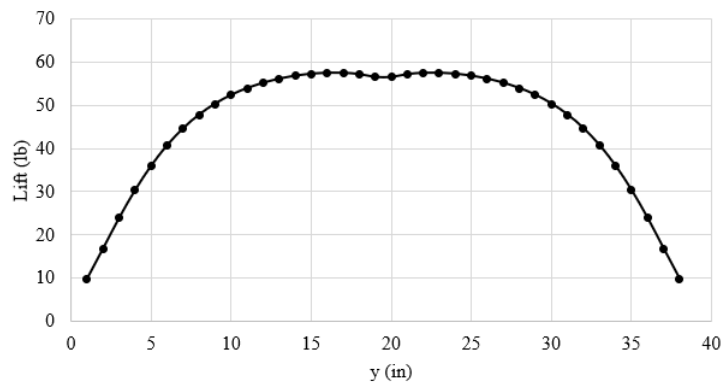
Figure IX.3: Lift Distribution

The wing shear force distribution is shown in Figure IX.4. The plot varies from centerline of the wing to the wingtip. The loading is symmetric for the other half of the wing. Notice that the shear force is zero at the wingtip. The ultimate shear load, about -10,000 lb, is located outboard of the centerline where the wing and fuselage are attached.

This ultimate shear load is necessary to calculate the shear flow within the wing box. This results in an estimate for rib thickness in the wing structure.
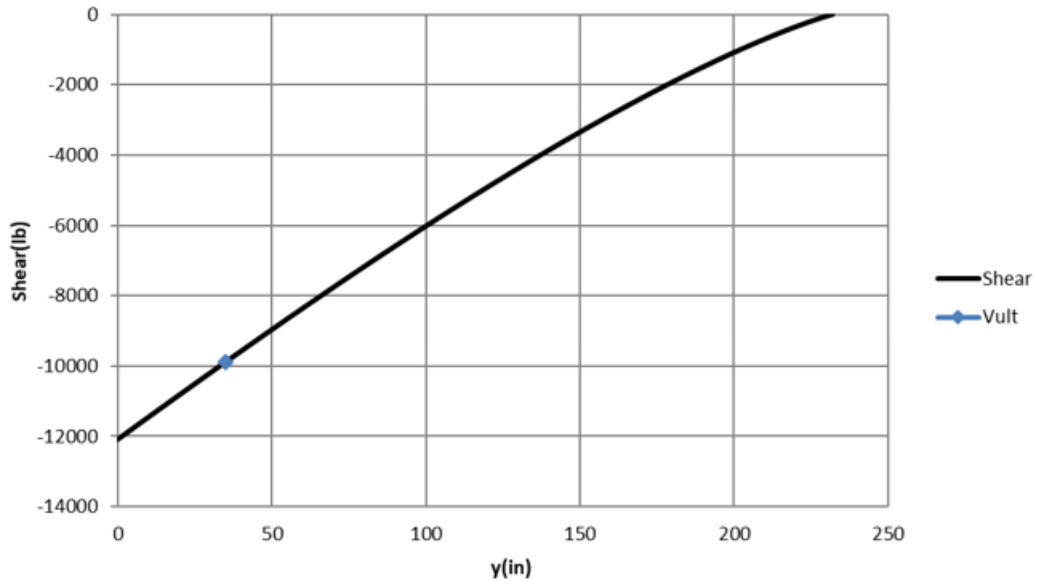
Figure IX.4: Wing Shear Distribution

The wing bending moment distribution is shown in Figure IX.5. The plot also varies from centerline to the wingtip. The loading is symmetric for the other half of the wing. Notice that the bending moment is zero at the wingtip. The ultimate bending moment, about 900,000 in-lb, is located outboard of the centerline where the wing and fuselage are attached. The ultimate bending moment is necessary to calculate the stress experienced by the spars within the wingbox. This results in an estimate for dimensions of the spars.
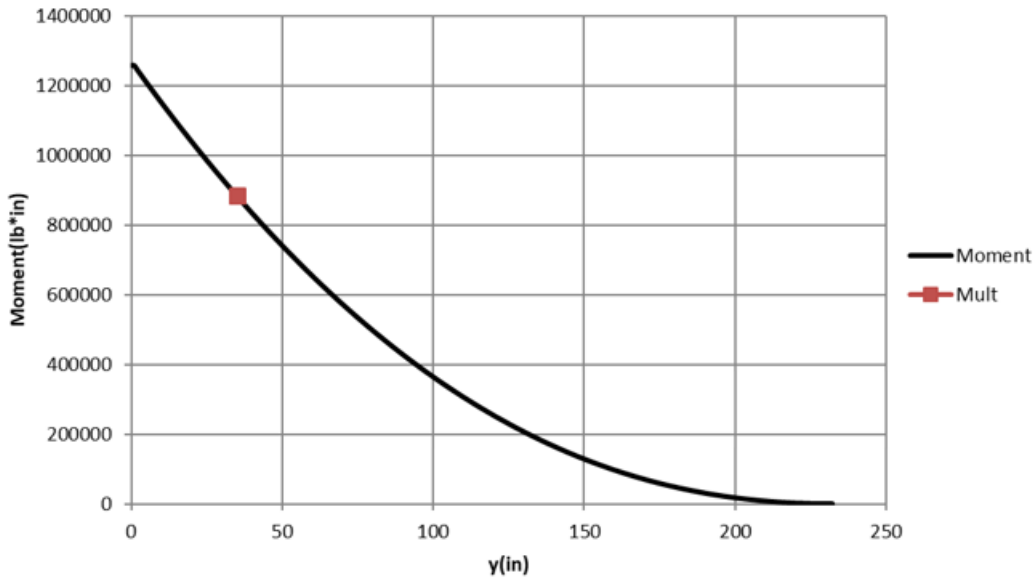
Figure IX.5: Wing Moment Distribution

B. Material Selection

Aluminum has historically played a significant role in the structures of aircraft. Relative to other metals, it is a light material that has the strength to support aircraft structures efficiently. Three different aluminum alloys, shown in Table IX.1, were considered for the structure of the main load bearing components of the SEAL. These three alloys have very similar densities, however, they differ significantly with their maximum yield stresses. The ratios of maximum yield stress and density favor Al 7075-T6 over Al 2024-T351 and Al 6061-T6. For this reason, Al 7075-T6 was chosen to be the alloy for the main structural components of the aircraft. The Steel 300M alloy is used for the landing gear to ensure that failure does not occur upon landing. The aircraft needs to land safely and using steel rather than aluminum for the struts provides an additional factor of safety. Steel is significantly more dense, but the increase in weight is necessary to ensure that failure does not occur due to the high stress on impact during landing.

Table IX.1: Material Properties

Metal Alloy	σ **yield**	σ **ultimate**	ρ
Al 6061-T6	35,000 psi	42,000 psi	0.09754 lb/in^3
Al 2024-T351	41,000 psi	68,000 psi	0.1004 lb/in^3
Al 7075-T6	63,000 psi	74,000 psi	0.1015 lb/in^3
Steel 300M	230,000 psi	280,000 psi	0.2380 lb/in^3

Challenges arise when a composite is considered for the aircraft structure. A qualitative analysis of metals and composites ensues. First, metals are isotropic, meaning they have the same material properties in every direction. Many composites are anisotropic, meaning they only exhibit their high strength properties in one direction. This can cause issues in aircraft structures since many structural components will undergo multidirectional loads during flight. An option is to use a quasi-isotropic composite which exhibits behavior similar to isotropic materials. Manufacturing of composites require an autoclave to set and must remain as a single piece to exhibit the intended properties. Since this is the case, rivets cannot be used to assemble the components, but rather they must be glued together. Additionally, the leading edge of wings on composite aircraft typically are reinforced with aluminum in the event of a bird strike. An accurate FEA model with composite materials is either difficult to create or just impossible depending on the program that is used. When used correctly, composites can be extremely beneficial for weight savings that increase efficiency of the aircraft; however, the cost of manufacturing composites is significantly greater than that of metals [23]. Although, this difference is decreasing with every year as composites become more commonly used. Composites also reduce maintenance costs by eliminating corrosion and metal fatigue. Ultimately, the chosen material was Al 7075-T6 for the SEAL.

The spar dimensions for the wing are sized such that the maximum yield stress of the alloy is not exceeded while the maximum bending moment is applied. Shown in IX.2, the three aluminum alloys that were considered for the internal structure of the aircraft are sized appropriately to their maximum yield stress. This spar sizing constitutes the cross section where the wing attaches to the fuselage.

Table IX.2: Spar Sizing Trade Study

Metal Alloy	Cap Width	Cap Depth	Web Width	Web Depth	Max Bending Stress	Area
Al 6061-T6	3.2 in	0.25 in	0.25 in	7.5 in	34,197 psi	3.475 in^2
Al 2024-T351	2.6 in	0.25 in	0.25 in	7.5 in	40,475 psi	3.175 in^2
Al 7075-T6	2 in	0.2 in	0.2 in	7.5 in	61,335 psi	2.3 in^2

A conclusion can be made that the choice of Al 7075-T6 results in a significant reduction in weight compared to the usage of Al 6061-T6 or Al 2024-T351. This is due to its greater ultimate yield stress. It is more capable and efficient and as a result the cross-sectional area is significantly smaller than that of both Al 6061-T6 and Al 2024-T351. Al 7075-T6 is a more expensive alloy in terms of cost, but the reduction in material helps alleviate this discrepancy. The trade study helps to reaffirm the decision of using Al 7075-T6 as the structural material.

C. Wing Structure

The structure of the SEAL must be able to withstand the aerodynamic forces necessary for flight while also being lightweight. With Al 7075-T6 chosen, the properties of this metal limit what loads the wing can withstand. A wing box analysis as well as a shear flow analysis was used to size the spars and ribs [24]. The lift distribution, ultimate shear load, ultimate bending moment, and limit load factor discussed in Section IX.A, were used for these analyses. These loads are found at the intersection furthest from the centerline of the wing and fuselage. The load factor of 3.78 and an additional factor of safety of 1.5 were applied to these max loads. For the spars, an I-beam shape was assumed. The I-beam shape is ideal for wing structure since the spar caps carry the bending loads and the spar webs carry the shear loads. Roskam recommends the front spar to be located at 15-30% chord and the aft spar to be located at 65-75% chord [3]. The front and aft spar locations were chosen to be 15% and 60% of chord, respectively. They are located at these locations because there needs to be sufficient space for the control surfaces such as the aileron or flap. The resulting spar dimensions were determined with the spar cap width as 3 in, and the spar cap depth as 0.25 in. The spar web width is 0.2 in, and the spar web depth is 7.5 in at the wing root. The height of the spars are that of the height of the airfoil sections spanwise along the wing. Roskam's recommendation for rib spacing is 36 in [3]. There are 14 ribs for the entire wing with an average spacing of 33.2 in. Figure IX.6 shows the internal structure of one half of the wing. The thickness for each rib is 0.2 in and they conform to the shape of their respective airfoil cross-section. The ribs maintain the shape of the wing by supporting the spars and skin. The ribs have holes applied in them, which allows fuel transfer between fuel tanks in the wing as well as pathways for wiring and systems for the control surfaces. The majority of the ribs have the trailing edge portion removed to allow the control surfaces to be placed. The wing is attached to the fuselage via a carry through spar which is then bolted to the front two fuselage frames of the cabin. This ensures loads are transferred from the wing into the fuselage structure. The leading edge of the wing structure has additional skin thickness to maintain structural integrity in the event of a bird strike.
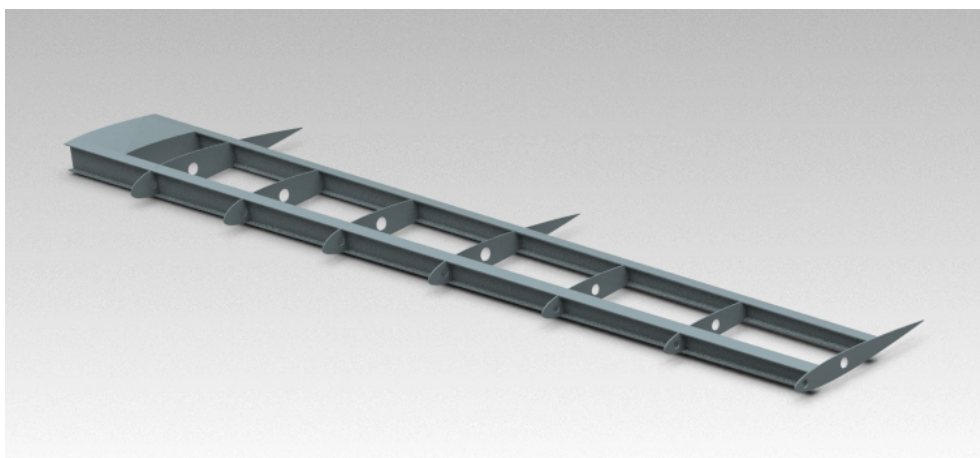
Figure IX.6: Internal Wing Structure

A finite element analysis was conducted in NX to analyze the stresses and displacement of the wing. An elliptical load distribution was applied spanwise along the wing. This elliptical load distribution assumed the maximum load factor of 3.78 and was increased by ten percent to 4.16 as an additional factor of safety. The von Mises yield criterion was used for this model. This FEA model included the skin, spars, and ribs and is shown in Figures IX.7 and IX.8. The darker blue colors indicate low values for displacement and stress whereas yellow and red indicate higher values.
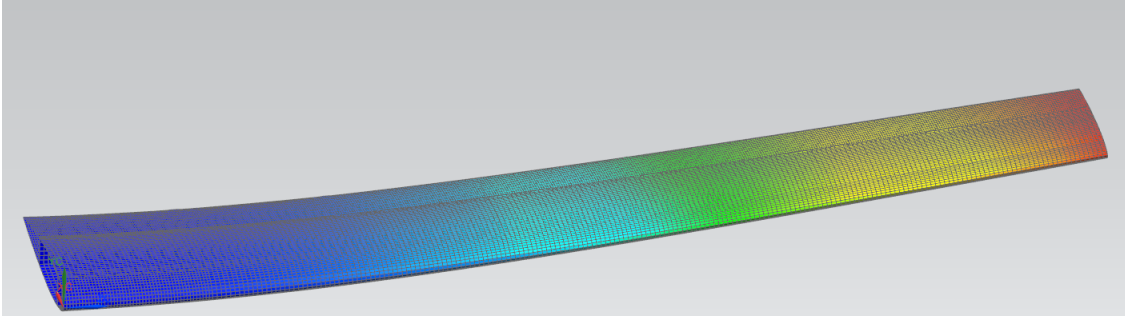
Figure IX.7: Wing FEA Displacement

Assuming the same elliptical load distribution, Euler-Bernoulli beam theory calculations predicted a displacement of 23.7 in at the wing tip. This calculation only involved a single spar and ignores the interaction of the skin and ribs. The FEA model found a tip displacement of 16.2 in and a deflection angle of 4°. These values are very reasonable for the maximum load case for the wing structure.
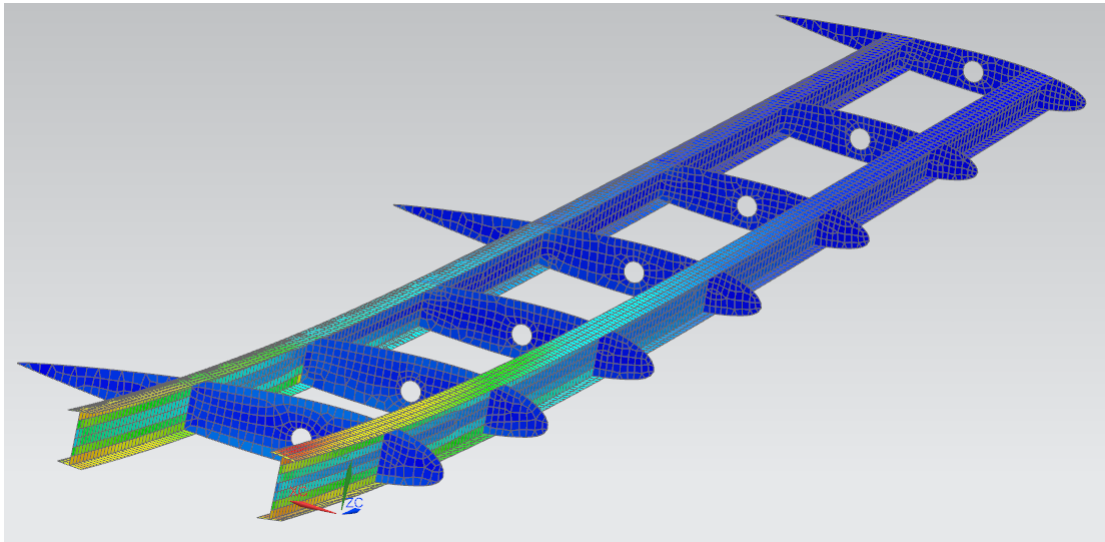
Figure IX.8: Wing FEA Internal Stresses

The stresses within the structural components were found using the FEA model. The maximum stress was found to be 21,490 psi which is well below the 63,000 psi yield limit for Al 7075-T6. Low stress regions can be seen on the ribs along the entire span of the wing. The rib holes are confirmed to be viable for the wing structure.

D. Fuselage Structure

The fuselage structure must be able to withstand various loads. These include loads due to maneuvering, turbulence, and gusts. Other loads to consider are those due to the weight of the propulsion system and landing gear impact loads. To withstand these loads, the SEAL was designed with a semi-monocoque fuselage. The fuselage structure was inspired by the designs of similar aircraft such as the Cessna 210 and Piper PA-46. The fuselage consists of a combination of longerons, frames, and bulkheads that support the skin of the aircraft. One bulkhead is located behind the baggage compartment, and the other bulkhead is located at the front of the cockpit. The front bulkhead also acts as a fire wall between the engine and the cabin in the event of a fire. These bulkheads also support the pressurization of the cabin during flight. The skin thickness was sized to withstand the cabin pressurization loads. Aircraft cabins are typically pressurized to be equal to an altitude of 8,000 feet. The skin was sized using pressure at 5,000 feet as a conservative measure. Cruising at 20,000 feet results in a pressure differential of 5.5 psi for the cabin. A hoop stress analysis was utilized to size the skin thickness necessary for safe cabin pressurization. The stress of 110 psi was calculated when sizing the skin thickness to be 0.05 in. This is far below the yield stress of Al 7075-T6 and thus is safe for cabin pressurization.
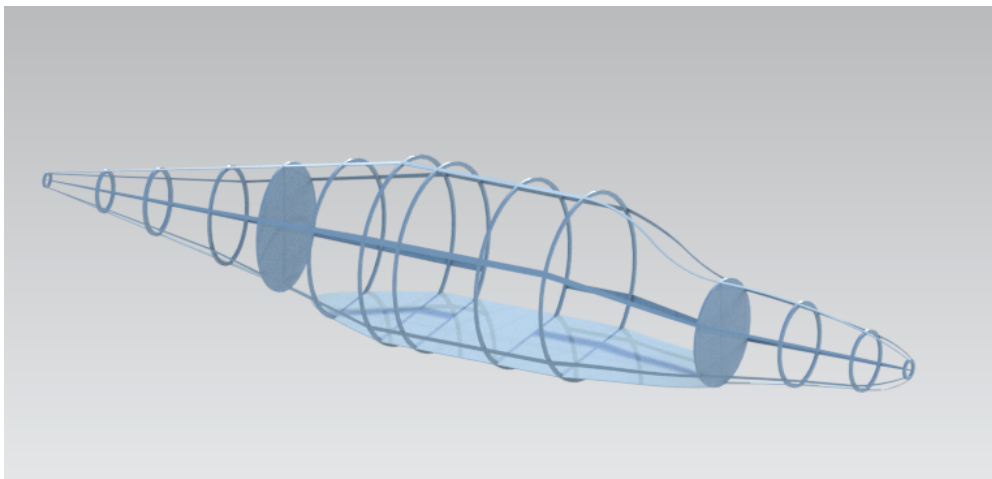
Figure IX.9: Internal Fuselage Structure

Roskam recommends a frame thickness of 1.5 in and a frame spacing of 24-30 in for light aircraft [3]. The frame thickness that is used for the SEAL is 1.5 in. There are fourteen frames on the aircraft, two of which are bulkheads, with an average spacing of 26.6 in. This spacing fits into the range that Roskam recommended. There are six longerons that are continuous lengthwise along the aircraft and equispaced $60°$ apart. The longerons help support the skin and transfer loads from the skin to the frames. To highlight the internal structural members, the fuselage structure without the skin is shown in Figure IX.9. The frames in the cabin are not all spaced equally to accommodate for the cabin passenger door.

E. Empennage Structure
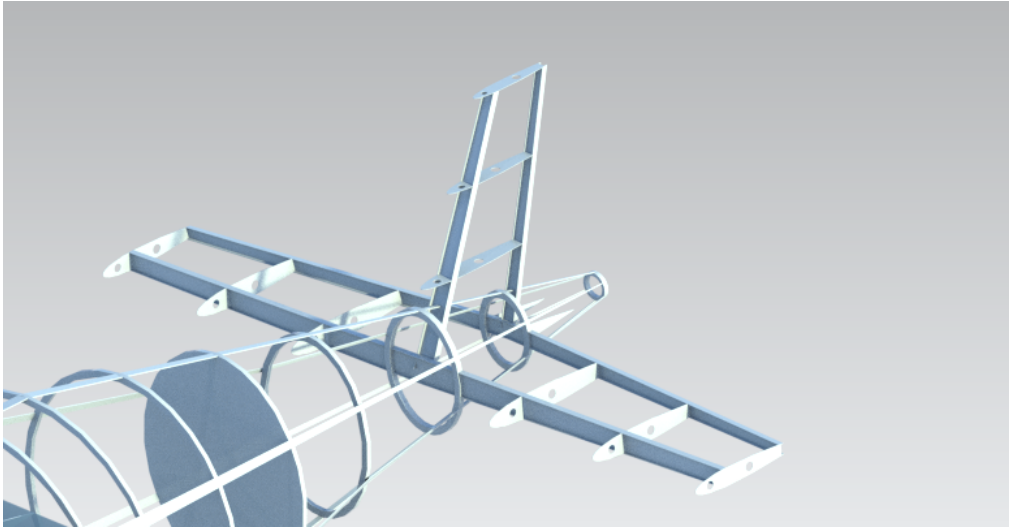
Figure IX.10: Empennage Structure

The empennage structure is shown above in IX.10. The empennage consists of the horizontal and vertical tail. Both of these have very similar structures to that of the wing. Roskam recommends the front spar to be located at 15-25% of chord for both the vertical and horizontal tail. Roskam also recommends that the rear spar is located at 70-75% of chord [3]. The horizontal tail has the front spar and rear spar located at 22% and 70%, respectively. The vertical tail has the front spar and rear spar located at 18% and 70%, respectively. The rear spar being located at 70% is to allow for sufficient area for the elevators and rudder control surfaces. The differing front spar locations was done to align the spars with the fuselage frames. This allows the empennage to be attached to the frames of the fuselage which allows loads from the empennage to be transfered into the fuselage. Roskam recommends the empennage rib spacing for light airplanes to be 15 to 30 inches [3]. The rib spacings for the horizontal tail and vertical tail are 27.6 in, and 17.4 in, respectively. Both of these rib spacings fall within Roskam's recommendation. The rib trailing edges were removed to accommodate for the rudder and elevators. Rib holes were made in both the horizontal and vertical tails to allow for control systems integration as well as reducing structural weight.

F. Landing Gear

The landing gear was chosen to be a three-wheel tricycle design that retracts into the fuselage to allow for better fuel efficiency. Three wheel landing gear is very common for historical aircraft of a similar size because the three wheels provide enough stability during take off and landing without adding unnecessary weight or drag. The tricycle undercarriage was chosen over the taildragger configuration because it provides improved stability when landing, better visibility over the nose while on the ground, and better steering while taxiing [3]. After comparing other aircraft designed for similar missions it was decided that fixed landing gear would provide a greater benefit than retractable landing gear,

if feasible. Fixed landing gear provides lower complexity and cost, lower weight, and insignificant maintenance cost when compared to retractable landing gear. After analyzing the performance of the aircraft with fixed landing gear, however, it was determined that retractable landing gear would be necessary to complete the required missions due to the extra drag caused by the landing gear. The nose and main landing gear were placed on the front bulkhead and a major cabin frame of the aircraft structure so as to direct the load paths through other major structural components, such as the longerons and other frames. The location of the nose and main gear from the nose of the plane are 6.65 and 14.375 feet respectively. With this landing gear placement, 13 percent of the aircraft weight during landing is carried by the nose gear with the other 87 percent of the load being carried by the main gear. This fits perfectly into the target of 5 percent-20 percent, which is the target load that the nose gear should carry so that the aircraft is able to lift its nose during takeoff as well as steer well, which requires a minimal normal force on the nose gear [3]. In IX.11 and IX.12 below, the nose and main landing gear of SEAL are pictured.

Figure IX.11: Nose landing gear of SEAL

Figure IX.12: Main landing gear of SEAL

For tire sizing of SEAL, the required missions were analyzed along with the different routes that SEAL will likely take and it was decided that type-III tires are desired – because they can land on wet grass and allow for more ambitious missions. With this in mind, a tire with a maximum pressure of 55 psi is desired so as to be able to safely land in these soft-ground conditions. Soft-ground landings are the most harmful to tires, and with this capability the aircraft is able to land on almost any other surface including dirt, gravel, asphalt, and concrete. Next, the maximum static and dynamic loads on each tire were calculated using the algorithm found in Roskam [3]. Roskam states that a gear load factor of 3.0 should be applied to the weights of the landing gear as well as a factor of 1.45 should be applied to the maximum static loads for type-III tires to account for the load transfer from the tires, to the landing gear struts, and up through the airframe. With the maximum dynamic and static loads calculated, the maximum tire operating speeds were also calculated per roskam. With a desired tire pressure, load rating, and tire type in mind, the tire data table in roskam was referenced to find a tire that fits SEAL's needs and requirements. The Goodyear Flight Special II 606C86-3 tire was chosen with a rated speed of 160mph, rated load of 2350 lbs, and outer diameter of 17.5 in. [3]. The main landing gear, shown below in Figure IX.12 in its extended position, consists of a steel telescoping rod that shrinks before retraction in order to properly fit inside the fuselage. During deployment, the main landing gear rotates a full 90 degrees downward as well as a full 90 outward in order to get in position for landing. A steel constraint holds the landing gear into position to allow for a safe landing. In the stowed positions, two steel pegs constrain the main gear into position in the fuselage for storage. The retracting system is powered by the hydraulic system aboard the SEAL.

X. Stability

A. Stabilizer Configuration

During preliminary market research, tails of many comparable planes were studied to weigh the pros and cons of each configuration. Amongst competing planes, the vast majority had one of three possible layouts: a T-tail, a cruciform tail, or a conventional tail. Each of these configurations have their own set of advantages and disadvantages.

Since the placement of the wing was one of the earliest decisions made in the design process of the SEAL, the development of the tail had to take into consideration the effects that the wing might have on it. In an ideal case, the tail of the plane will see "clean" air; in other words, it will not be in the wake of the wing. This avoids unpredictable tail behavior brought on by the turbulence of the wake and should provide reliable performance over a wide range of angles of attack. Due to the layout of the SEAL and its high wing design, the horizontal stabilizer of a reasonably sized T-tail would be thrown into the wake of the wing with an increase in the angle of attack of the plane. The same problem would occur with cruciform tails, but at slightly lower angles of attack. Planes within the SEAL's market tend to follow a trend of having a T-tail or cruciform tail coupled only with low wings. T-tail and cruciform configurations also have increased structural weight because of their need to support the horizontal tail further away from the main structure of the aircraft. With all of these considerations in mind, a conventional tail was chosen for its lightweight, easy construction and safety benefits over other configurations.

With the tail configuration decided, the next step in the design process was to size the area of both the horizontal and vertical stabilizers. Two methods were used so the calculations could be compared against each other. During market research, the tail sizes of comparable planes were measured and recorded. Averages of the tail sizes and plots of tail to wing area ratios vs tail lever arm were plotted to establish trends amongst general aviation airplanes. After analyzing this data, it was expected that the horizontal stabilizer size would be between 45 ft^2 and 55 ft^2, and the vertical stabilizer would be between 10 ft^2 and 20 ft^2.

Another common method for sizing aircraft tails is the tail volume ratio. A version of this equation can be found in Raymer and takes into account the size of the wing, tail, the tail's lever arm and historical data compiled from many different aircraft throughout history. [2]. The historical data compiled by Raymer provides a range of values that successful planes tend to fall within. Because of the SEAL's similar layout to other general aviation planes, the tail volume ratio equation would provide a range of values that will be perform well in this configuration.

Using the tail volume ratio equation, the horizontal tail area was found to be around 47.58ft^2 and the vertical tail area was 13.02ft^2. These values were found using an iterative method with initial tail chord and lever arm guesses and allowing results to converge to their final values. Both the horizontal and vertical tail fell within their expected range of 45 ft^2 - 55 ft^2 and 10ft^2 - 20ft^2 respectively. These values were checked against other aircraft within the same market and were found to be similar as was expected. With this last check, the tail areas for the SEAL were finalized.

B. Stabilizer Methodology and Performance

Airfoil, sweep, aspect ratio and other tail parameters needed to be calculated after the sizing of the tail was finished. Historical values for different types of planes were compiled in a document by E.G. Ulapurkara from the Indian Institute of Technology and were used as guidelines for the selection of these dimensions [26]. Each of these values fell within historical ranges. In past iterations of the tail, the vertical tail had no sweep, but the design was not as aesthetically pleasing. This form factor is not common on modern planes for this reason. In order to increase the sleekness of the plane and thus appeal to the potential ticket buyers, the addition of sweep and an increase in taper were considered. Though this change would result in a small reduction in effectiveness, the SEAL would remain acceptably stable and controllable, as will be shown in X.D. In steady level flight, the vertical tail ideally produces no lift, so its efficiency is not as important as the efficiencies of the wing and horizontal tail. With these considerations in mind, the changes for increased aesthetic appeal were implemented. The values chosen are shown below in Table X.1.

Table X.1: Key parameters of the vertical tail and horizontal stabilizer

Parameter	Horizontal Stabilizer	Vertical Tail
Airfoil	NACA0012	NACA0012
AR	4	1.45
Λ [°]	0	23.54°
λ	0.7	0.6
S [ft^2]	47.58	13.02
Lever Arm from CG to $\frac{1}{4}$ Chord [ft]	13.44	14.16
Distance from Nose to LE [ft]	25.69	26.75
C (volume coeff.)	0.7	0.04
Span [ft]	13.799	4.340
c$_{tip}$ [ft]	2.839	2.265
c$_{root}$ [ft]	4.056	3.75

It is important to note that the aspect ratio of the vertical tail as calculated in Ulapurkara's tail sizing lecture is defined as $A_{vt} = \frac{h_{vt}^2}{S_{vt}}$ with typical values falling between 1.0 and 2.0. This is different from how aspect ratios are typically calculated because a fin does not have two sides like a wing does.

Figure X.1 is a scissor plot for the SEAL, which show the various aerodynamic and stability limits that the aircraft has. A static margin above the acceptable range will cause the aircraft to lose its ability to effectively pitch. Static margins that are below the acceptable range or negative cause the plane to become underdamped or unstable. The minimum tail area ratio as determined by these limits is shown by the dash-dotted line, and the SEAL's chosen tail area ratio is shown by the dotted line. The higher range of acceptable CGs that the chosen area ratio works for allows for changes in the design and unforeseen loading cases to be handled without changes to the tail.
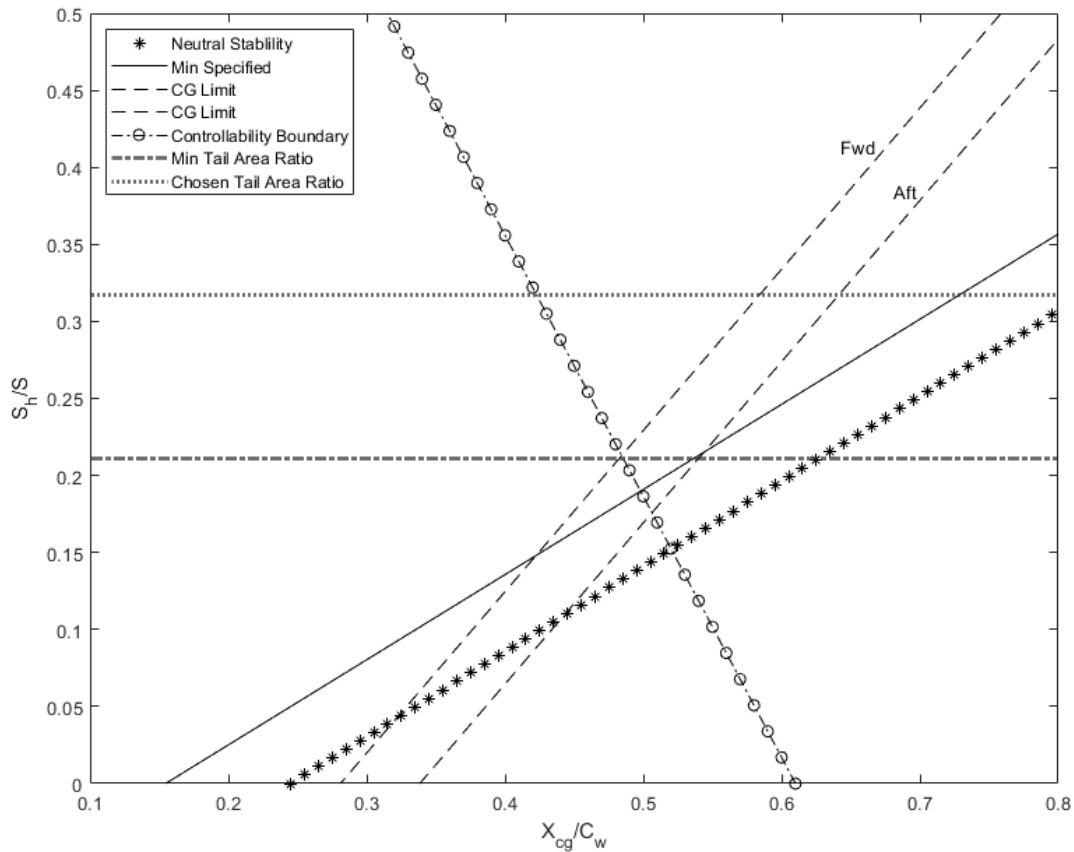
Figure X.1: Scissor Plot for the SEAL

Stability characteristics of the SEAL were analyzed to ensure acceptable performance. The distribution of the system's mass affects the static margin of an airplane, which is an important factor in the stability and controllability of an aircraft. Static margins for a given aircraft can be found by dividing the distance between the neutral point and center of gravity of the aircraft by the mean aerodynamic chord. A static margin greater than zero ensures a stable aircraft, but values of static margin beyond 30% tend to degrade the controllability of an aircraft by increasing pitch stiffness and can put the plane out of the realm of linear aerodynamics, making flight dynamics much harder to predict.

To accurately estimate the center of gravity, weight and location information of all major components on the SEAL were tabulated. Methods for estimating the weights and the placement of each component were discussed in Section VIII. From these values a range of centers of gravity were found. The forward and rearward centers of gravity were the most important values since they determined the range of static margins that the SEAL can see in flight.

With these restriction on the static margin of the SEAL in mind, the geometry of the wing and stabilizers were recreated in XFLR5, an analysis tool that uses vortex lattice and 3D panel methods to create polars and run stability analyses on a wing or plane. Stability analyses were run to ensure the aircraft was both stable and trimmable. Graph X.2 (a) shows the C_m vs α values for plane with the final tail design. The negative slope of the line shows that the plane will return to steady, level flight by pitching down when disturbed in a nose up manner, and pitching up when disturbed in a nose down manner. The positive y-intercept of the graph means that the design configuration can be trimmed to have no moment at a positive angle of attack where it can produce lift. These characteristics are essential to the stability of an aircraft. X.2 (b) shows the lack of stability of the SEAL with no tail by having a positive C_m vs α slope. Static margin will be discussed in further detail later in this section.

(a) C_m vs. α showing stability and trimmability for final horizontal tail size

(b) C_m vs. α for wing with no tail
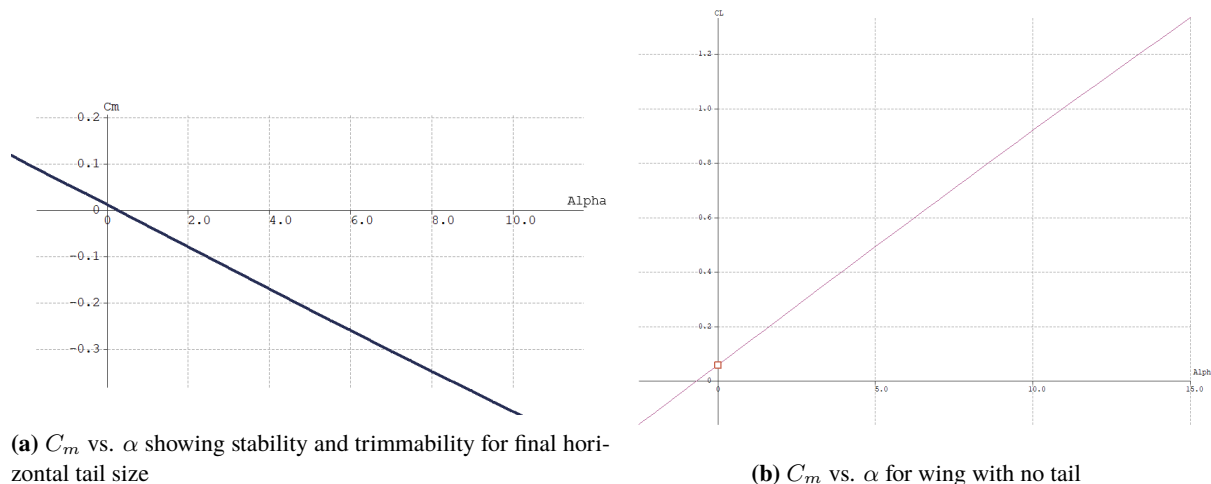
Figure X.2: C_m vs. α graphs for the SEAL with large and small horizontal stabilizer with no tail incidence

Selecting an airfoil for the tail sections presented a number of considerations before a final decision was made. Stall is not desirable on any lifting surface during regular flight, and this holds especially true for control surfaces. A trade study was conducted to choose the best airfoil possible for this application. Since both tail surfaces can be given incidence to improve stability or decrease the likelihood of stall, and the ideal airfoil would have a large range of operating angles of attack, a number of tests were run on four thin, symmetric airfoils to determine which one would perform best as a empennage airfoil. The NACA 0008, NACA 0010 and NACA 0012 were the chose airfoils for this trade study.
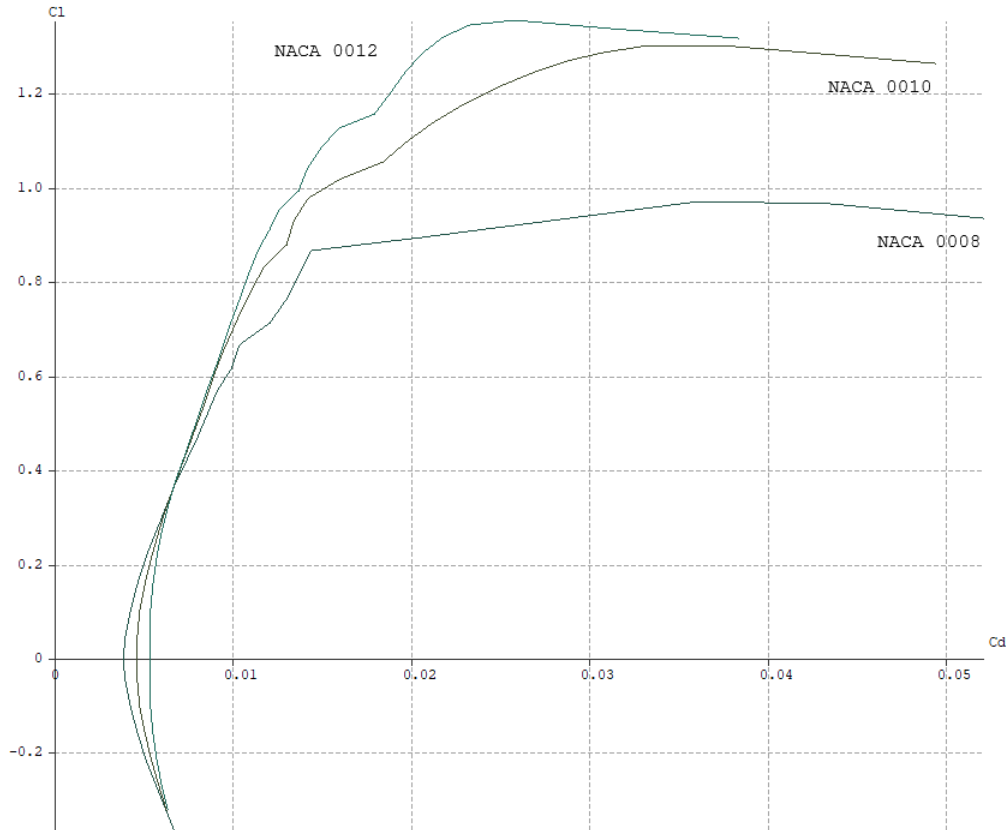
Figure X.3: Cl vs. Cd for NACA 0008, NACA 0010, NACA 0012

Shown in X.3 are the Cl vs Cd plots for the various airfoils in this trade study. For low to medium ranges of Cl, all three airfoils perform relatively similar. At higher Cl values, the NACA 0012 starts to distinguish itself from the others as having lower drag than the other airfoils. Increased performance at higher angles of attack can be seen in X.4.

The NACA 0012 has a smoother stall at a higher angle of attack than the other airfoils while still providing the best Cl vs Cd profile of the test airfoils. This makes it an ideal airfoil to use on an empennage and will work well in the SEAL's configuration. Under even irregular loading, the chances of stalling the tail is low, preventing loss of control and controlling the plane back to level flight.

As further justification for this airfoil on the SEAL, the NACA 0012 is a common airfoil on tail surfaces for other, comparable aircraft. The historical precedent for use of this airfoil on the empennage of the SEAL provided additional evidence to the validity of this study on tail airfoil selection. With the tail sizing completed and airfoil selected, the control surfaces and high lift devices for the SEAL had to be sized.
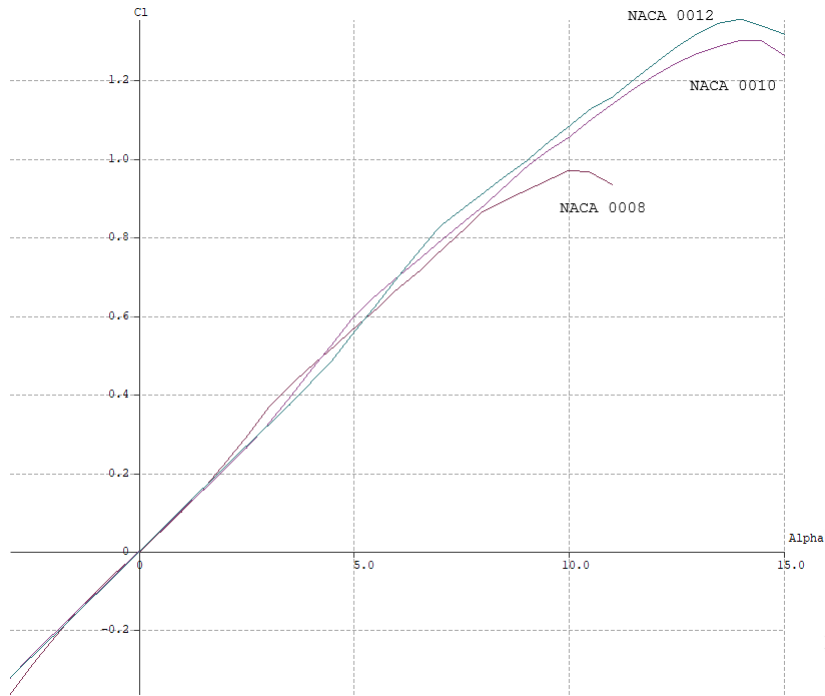
Figure X.4: Cl vs. α for NACA 0008, NACA 0010, NACA 0012

C. Control Surface Methodology and Sizing

To calculate the size of the flaps, ailerons, elevator, rudder, and maximum deflection angle, a number of comparable planes were studied to determine control surface sizing trends [2] [19]. The span and area of each control surface was compared to span and area of the body it was on. For clarity, the elevator's span and area would be compared to the horizontal stabilizer's span and area. The use of the mean aerodynamic chord as the "measuring stick" of each historical aircraft was avoided to minimize measurement errors that could occur when trying to estimate the MAC of a complex wing geometry. Averages were calculated from this data and the results are tabulated in Table X.2. Actual values for the SEAL's control surfaces are shown in TableX.3

Table X.2: Historical Averages for Control Surfaces

Parameter	Flaps	Ailerons	Elevator	Rudder
Span (% of body span)	25% - 30%	50% - 60%	90% - 100%	90% - 100%
Area (% of body area)	7% - 11%	3% - 9%	25% - 30%	30% - 35%
Chord (% of body chord)	20% - 30%	20% - 30%	20% - 30%	30% - 40%

Table X.3: Dimensions for the SEAL's control surfaces. (Note: % Measurements are relative to the body the control surface is on)

Parameter	Flaps	Flap %	Ailerons	Aileron %	Elevator	Elevator %	Rudder	Rudder %
Span [in]	83.56	36.0%	55.74	24.0%	78.6	95.0%	45.71	87.4%
Area [in^2]	971.0	9.0%	653.3	6.1%	940.8	27.5%	465.8	24.8%
Chord [in]	0.97	25%-23%	0.97	27%-30%	1.00	25%-35%	0.85	29%-37%
Max Deflection [°]	-30°		±25°		±25°		±25°	

CAD drawings were created to provide a clear picture of the layout of the horizontal and vertical stabilizers and wing and their respective control surfaces, and are shown in Figure X.5. Reasonable confidence can be placed in the sizing of these control surfaces since similar values have been used on aircraft in the same market as the SEAL. Actual analysis of the performance of these surfaces will be seen later in this section. During the design of the empennage and its control surfaces, care was taken to ensure that none of the control surfaces would interfere with each other during flight. The rudder was placed above the highest point that elevator can reach at its maximum $-25°$ deflection.
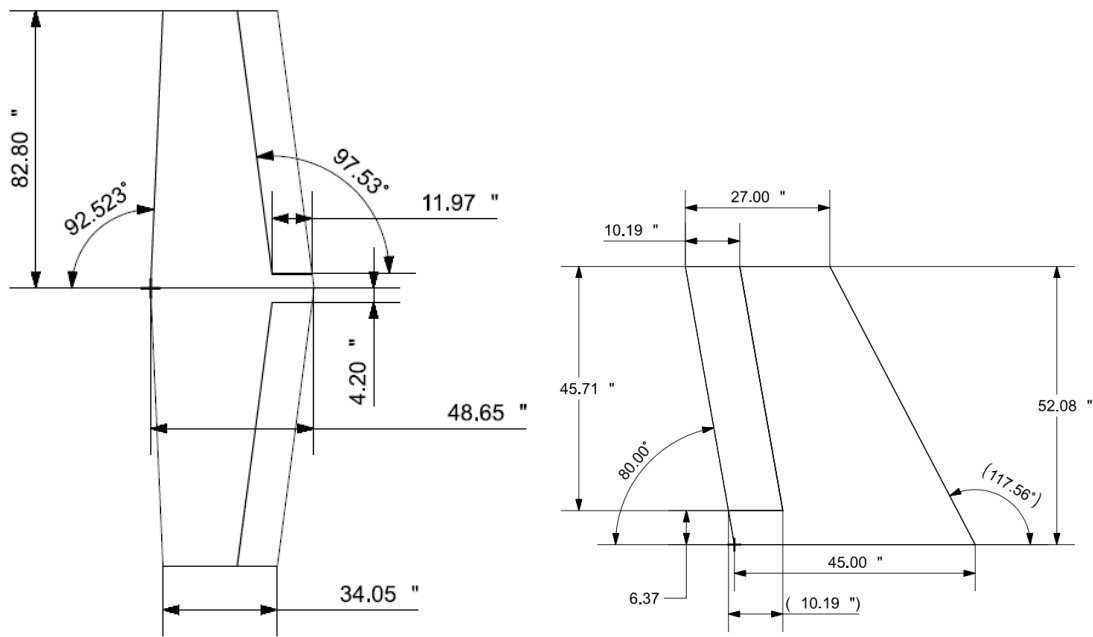
(a) Horiztonal tail configuration with elevator dimensions (left side faces forward) **(b)** Vertical tail configuration with rudder dimensions (right side faces forward)

Figure X.5: Final Stabilizer Dimensions
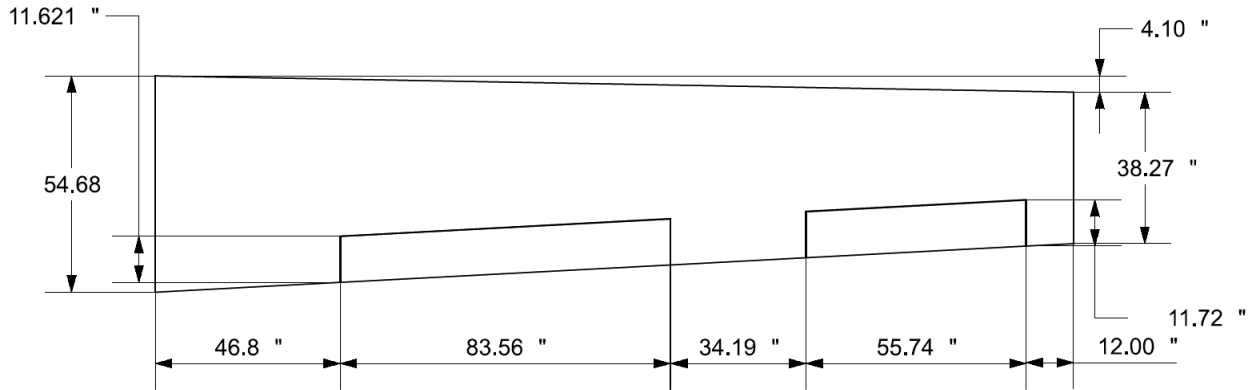
Figure X.6: Wing with flap and aileron dimensions (top side faces forward)

D. Longitudinal Stability

Longitudinal stability of an aircraft is comprised of two main sections. The static stability is the tendency of the aircraft to return to its equilibrium position in steady level flight. The dynamic stability takes into account the aircraft's response to disturbances over time. In this section, the static and lateral stability of the SEAL will be examined.

Static stability is a prerequisite for dynamic stability. In X.2 the longitudinal static stability and trimmability of the SEAL was demonstrated with the negative C_m vs α slope and positive y-intercept. The static margins of most general aviation aircraft fall between 5% and 30%. By using data from VIII, the minimum and maximum static margin for the SEAL could be calculated for all three phases of flight.

Table X.4: Fore and Aft CG Limits

Segment	X_{NP}	Fore X_{CG}	Aft X_{CG}	SM Lower	SM Upper
Takeoff	173.43 [in]	159.460 [in]	164.88 [in]	18.20%	27.4%
Cruise	172.47 [in]	159.60 [in]	164.88 [in]	16.15%	29.7%
Landing	173.54 [in]	159.60 [in]	164.88 [in]	18.45%	29.45%

As seen in Table X.4, the static margins for all phases of flight at the forward and aft loading conditions fall within the acceptable static margin range for general aviation, meaning the SEAL will be stable and have appropriate pitch stiffness.

After static stability was demonstrated given the loading conditions and the neutral points of the different phases of flight, dynamic stability could be could be tested. The goal of dynamic stability is to make sure that the plane returns to steady, level flight within a reasonable time after a disturbance. The first iteration of the SEAL's design was recreated

in XFLR5 and a stability analysis was run. It was found that with no incidence on the tail or the wing, the SEAL was found to have an equilibrium $\alpha = 0.234°$ with a cruise speed of 316 KTAS at the cruising altitude of 20,000 ft. This speed is not only above the desired cruise speed, but also above the limit allowed by 14 CFR Part 23. A change to the layout had to be made before dynamic stability testing could be continued. Ideally, the SEAL was to cruise at the desired speed of 225 KTAS and at an α of less than 3° (this 3° limit is a general rule that is followed in the industry to ensure passenger's comfort). A trade study was performed on tail incidence to determine what angle would trim the aircraft with little or no elevator deflection during cruise. A 1° angle of incidence was applied to the wing in order to prevent very high tail incidence and angle of attacks outside of the acceptable range. More incidence could be applied to the wing if the tail was unable to trim the aircraft within the requirements during the trade study.

Table X.5 tabulates values for α, cruise speed, and whether or not this configuration achieves the requirements laid out in the paragraph above. There was only one incidence angle that was tested that satisfied all of these. Tail incidence of -1.00° was chosen because it allowed the SEAL to cruise at the desired speed and within the α range designated for passenger comfort.

Table X.5: Horizontal Incidence Trade Study

Tail Incidence [°]	α [°]	Speed [KTAS]	Part 23 Speed Limit	Under 3° Limit	$\pm$5 KTAS of Cruise
0.00°	0.234°	316 KTAS	No	Yes	No
-0.25°	0.688°	283 KTAS	No	Yes	No
-0.50°	1.141°	259 KTAS	No	Yes	No
-0.75°	1.596°	239 KTAS	Yes	Yes	No
-1.00°	2.050°	225 KTAS	Yes	Yes	Yes
-1.25°	2.506°	211 KTAS	Yes	Yes	No

Several analyses for both longitudinal and lateral dynamic stability were performed in XFLR5 with our finalized wing and empennage configuration. The response to disturbances were plotted and convergence back to equilibrium was checked. The time requirement for convergence depends on the type of disturbance seen by the aircraft, and a time response graph for short period oscillation can be seen in Figure X.7. A short period oscillation occurs when the aircraft is pitched upwards or downwards quickly enough that the velocity can be assumed to be unchanged. These modes usually take place over a time period of a few seconds. In Figure X.7 θ represents the pitching angle of the SEAL, u and w represent the forward and downward velocity respectively, and q represents the time derivative of θ, or the longitudinal angular velocity. The q value comes out extremely large near the 0 seconds mark on the graph because

of the way XFLR5 takes the derivative of θ. This results in extremely large initial values before quickly still converging towards accurate results after the initial error. The graphs of each of these variables decay towards zero within the first two seconds of the SEAL feeling a disturbance. By examining all of these graphs qualitatively, it is found that the SEAL settles back into equilibrium within two seconds of a pitch disturbance. This time period is comparable to the performance of other general aviation aircraft.
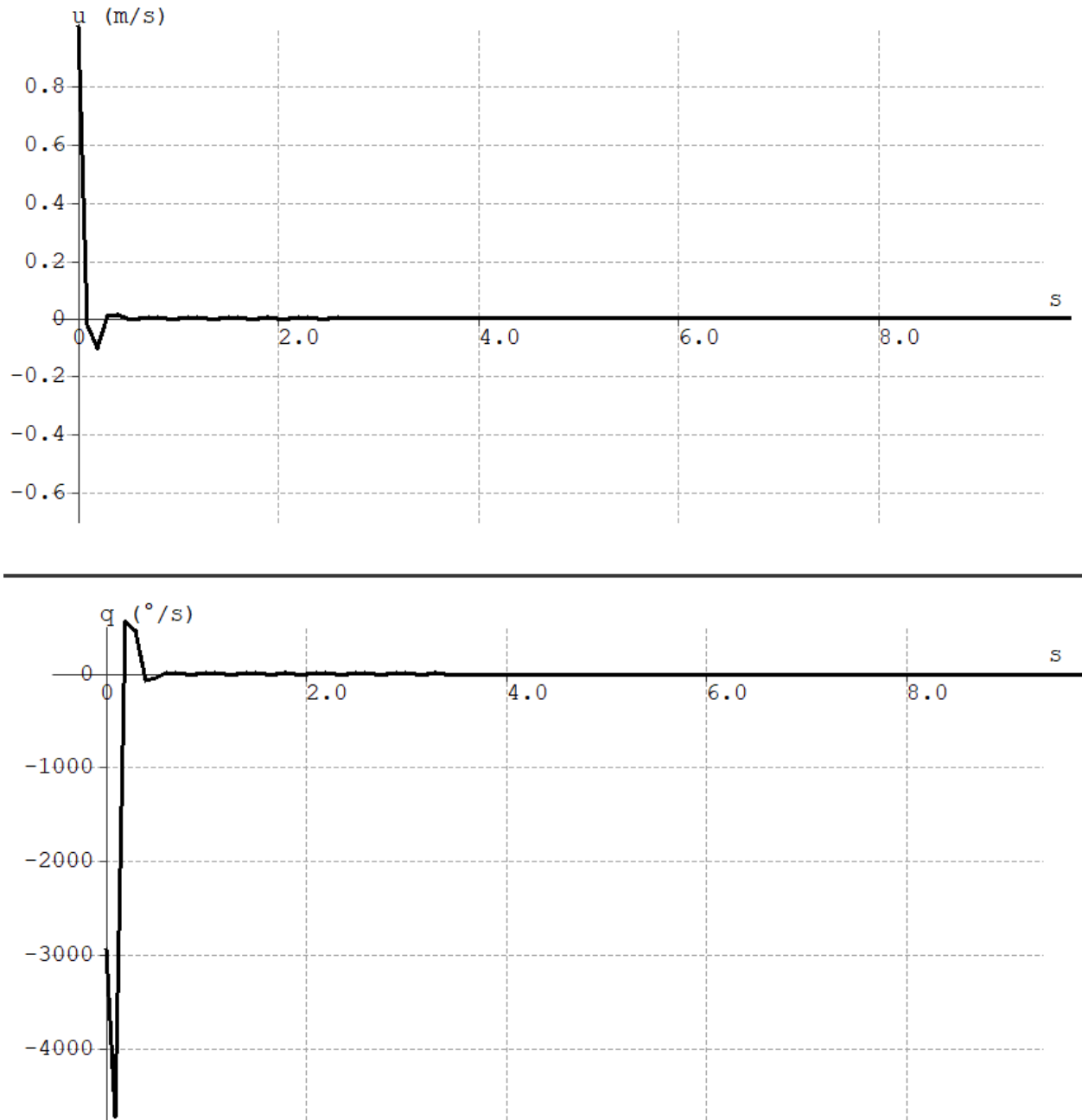
Figure X.7: Longitudinal Dynamic Stability

A more quantitative approach can be taken when examining disturbance response, and proves especially helpful when studying phugoid modes of aircraft. A phugoid mode is much longer than a short period mode. Often these disturbances occur over periods of time on the order of a hundreds of seconds. Phugoid modes are characterized by large changes in altitude and flight speed, but very small change in angle of attack. These modes can be plotted as well but offer less insight than the analysis of their eigenvalues. XFLR5 calculates the eigenvalues for each of these modes. Using equations from Peet [35] to calculate the natural frequencies, ω_n, damping periods, d, and half lives, γ for both short and phugoid modes, a comprehensive quantitative analysis of the SEAL's longitudinal dynamic stability performance could be carried out. The results are shown in Table X.6.

Table X.6: Longitudinal Stability Quantitative Analysis

Mode	λ	ω_n	d	γ
Short Period	-11.3646+16.4945i	3.188 [Hz]	-3.565	0.0610 [s]
Phugoid	-0.0033+0.0811i	0.013 [Hz]	-0.254	210.0 [s]

Table X.6 gives a few important facts about the longitudinal stability of the SEAL. Since both eigenvalues are negative, phugoid and short mode disturbances are stable and will return to equilibrium within a comparable amount of time to other aircraft in the SEAL's market. The half life of the short period mode is extremely small, meaning the SEAL will respond quickly to any pitch disturbance and adjust back to steady level flight in a short period of time. The long period mode, while stable, has an extremely long half life. Since the natural frequency of this mode is so small, pilots can easily input some control to bring the plane back to equilibrium. Both the short and phugoid modes behave as expected when compared to other aircraft of similar layout.

E. Lateral and Directional Stability

When designing an aircraft, lateral and directional stability are not as complex as longitudinal, but are just as important to the safety and performance of the plane. The SEAL has been created with stability along these axes in mind. The vertical tail has been designed to provide enough correcting moment when the plane is disturbed in the yaw direction to bring it back to equilibrium in a timely manner. As was discussed previously in this section, the tail volume ratio equations were used with historical data to provide tail sizing for the SEAL that has been proven to work on similar aircraft. The high wing layout of the SEAL combined with the tendency of a wing to correct itself back to level flight should make the SEAL stable along roll axis. As a note: wings tend to correct back to level flight because the side-slip caused from banked flight increases the angle of attack, and thus the lift, of the lower wing.

XFLR5 is able to run stability analyses along these axes to predict a plane's response to roll and yaw disturbances as well as Dutch roll and spiral dynamic modes. Shown in Figure X.8 are the roll and yaw time responses.
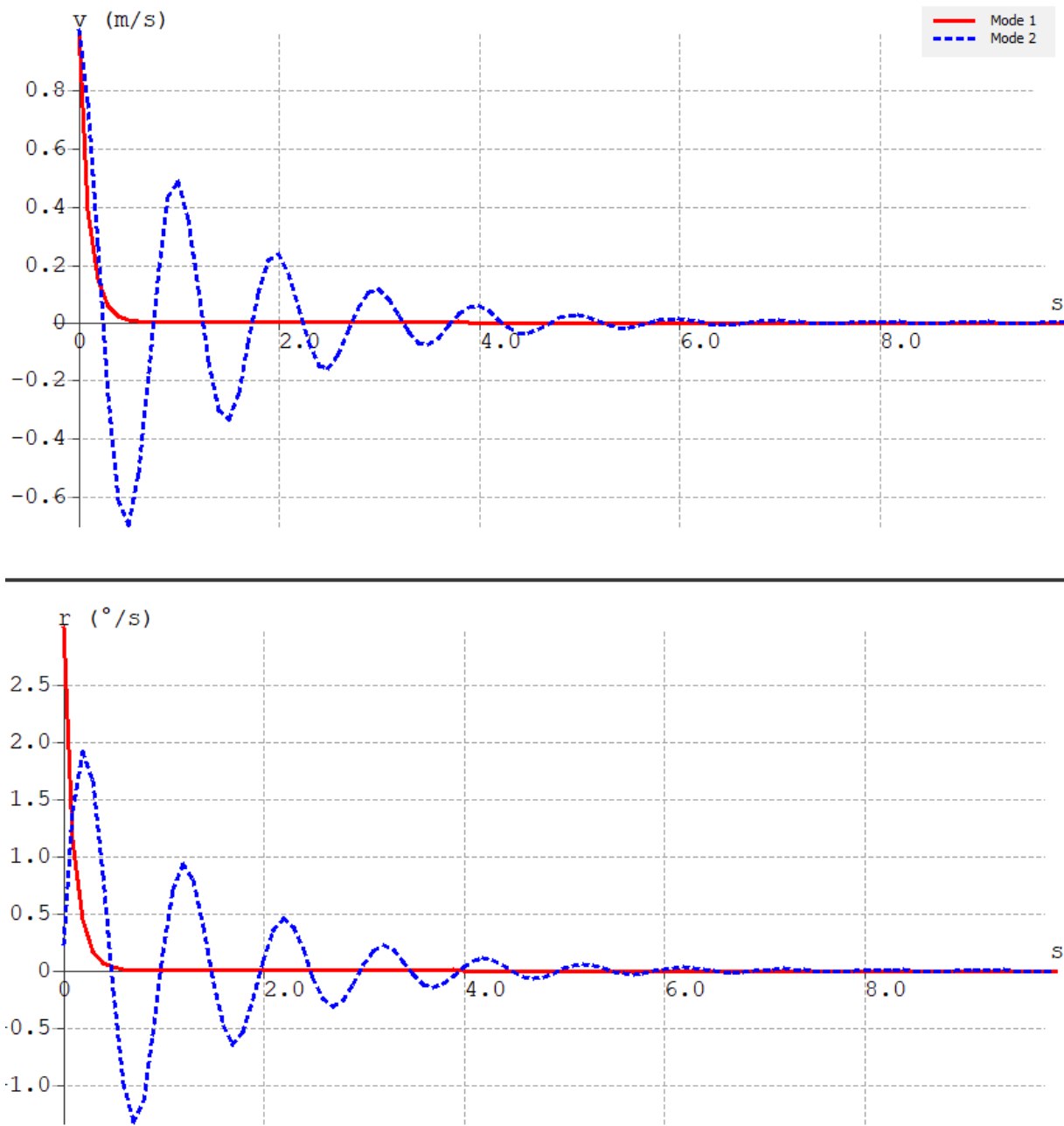
Figure X.8: Lateral Stability Phase Diagram

These graphs show similar state variables for the SEAL as the longitudinal dynamic stability graph in Figure X.7. v stands for the side-to-side component of velocity, p stands for the roll rate, r stands for the yaw rate and phi stands for roll angle. Similarly to longitudinal stability, the disturbances in these graphs converge to zero. The roll disturbance

(mode 1), shown by the solid line, is corrected much faster than the yaw disturbance(mode 2), which is the dotted line. At first glance yaw disturbance might not seem stable enough when compared to roll, but with most of the amplitude damped out by the four second mark, yaw dynamic stability is sufficient from a qualitative standpoint.

Similar to the phugoid mode in longitudinal stability, dutch roll and spiral dynamic modes are better analyzed quantitatively. XFLR5 is able to calculate the eigenvalues of these modes and Peet [35] again gives equations for calculating the natural frequency, damping ratio, and half lives for these modes. A time constant can also be found for roll. These values are recorded in Table X.7 The negative real parts of the eigenvalues for roll and dutch roll imply that these modes are stable and will converge to zero over time. The spiral mode is unstable as it has a positive real eigenvalue, but has a long doubling time allowing the pilot a large window to correct for this mode.

Table X.7: Lateral Stability Quantitative Analysis

Mode	λ	ω_n	d	γ	Doubling Time	τ
Roll	-9.6449	–	–	0.07185 [s]	–	0.07488
Dutch Roll	-0.7160+6.3165i	1.012 [Hz]	0.0610	0.9679 [s]	–	–
Spiral	0.0040	–	–	–	175.08 [s]	–

Two other considerations for the lateral and directional stability of the SEAL are the cross wind performance during takeoff and landing and the roll time through a specified range of angles. 14 CFR 23.157 mandates that a roll time from $-30°$ to $+30°$ in landing configuration with gear retracted for aircraft weighing less than 6,000 lbs must be less than 5 seconds. In addition to this regulation, a standard that was set for the SEAL was the ability to handle crosswinds of at least 20% of the takeoff and landing speed. The SEAL was tested to make sure it complied with both of these benchmarks.

Many of the variables used in the equations to check the SEAL's adherence to these standards were stability derivatives. These measure changes in flight conditions relative to changes in other parameters. For example, the derivative $C_{L_{\delta_e}}$ is the change in the coefficient of lift with respect to the change in elevator deflection. AVL, another vortex lattice software, was used to find stability derivatives for the SEAL. When possible, values from both programs were compared to add redundancy to the analysis. Some values, such as ϵ_α and C_{l_p} were calculated by hand using equations found in [37]. Some of these derivatives can imply stability based on their sign. Shown in Table X.9 are the derivatives that can imply stability, their values and whether or not they satisfy the stability criterion. All of the SEAL's applicable derivatives met their criterion.

Table X.8: Stability Derivatives used in Calculations

Derivative	Value	Derivative	Value
C_{L_α}	5.772	C_{l_r}	0.0005157
C_{m_α}	-1.547	$C_{n_{\delta_r}}$	0.05546
$C_{m_{\delta_e}}$	-2.629	$C_{y_{\delta_a}}$	0.001031
ϵ_α	0.317	$C_{l_{\delta_r}}$	-0.1337
C_l	-0.01289	$C_{l_{\delta_a}}$	-0.2184
C_{l_p}	-0.571	$C_{n_{\delta_a}}$	-0.0004011
C_{l_r}	0.03022	C_y	-0.2142
C_{m_p}	-0.0021	C_y	-0.2142
C_{n_r}	-0.07187	–	–

Table X.9: Stability Derivatives used in Calculations

Derivative	Value	Stability Criterion	Stable
C_{l_β}	-0.0129	$C_{l_\beta} < 0$	Yes
C_{m_α}	-1.547	$C_{m_\alpha} < 0$	Yes
$C_{l_{\delta_a}}$	-0.2184	$C_{l_{\delta_a}} < 0$	Yes
$C_{n_{\delta_a}}$	-0.00040	$C_{n_{\delta_a}} < 0$	Yes
C_{n_β}	0.0826	$C_{n_\beta} > 0$	Yes

To check that the SEAL meets the crosswind requirements, it had to be shown that the required rudder angle to hold the plane straight was within the $\pm 25°$ deflection range. Using equations from *Dynamics of Flight: Stablity and Control* by Bernard Etkin were used to find rudder deflection as a function of sideslip angle [36]. Rudder deflection was tested for both takeoff and landings and the results are shown below in Table X.10.

Table X.10: Takeoff and Landing Rudder Deflectiom

Phase	Crosswind Speed	Rudder Deflection	Within $\pm 25°$ Limit
Takeoff	27 [ft/sec]	18.56°	Yes
Landing	23.6 [ft/sec]	17.12°	Yes

Using equations for roll rate from [36], roll rates could be calculated for takeoff and approach. With a takeoff roll rate of $14.00 (°/sec)$ and $15.17 (°/sec)$ for approach, the SEAL satisfies the FAA requirements in CFR Part 23.157 with $60°$ roll times of 4.29 seconds at takeoff and 3.96 seconds at approach. In addition to satisfying FAA regulations, these roll times will provide the SEAL safe handling characteristics at takeoff and approach.

F. Trim Analysis

Another important characteristic of a plane in flight are the trim points that much be reached to keep the plane in steady level flight, as well as the elevator deflections that hold the plane there. Use of the elevator allows a plane to be trimmed to different angles of attack through all phases of flight depending on the required speed and the amount of lift that needs to be generated. The SEAL was designed to need as close to $0°$ of elevator deflection during flight at cruise speed to avoid constant input from the pilot. During takeoff and landing, a moment must be generated from the elevator to hold the SEAL at the required angle to provide the lift needed to keep the plane flying at its desired speed. Shown in Figures X.9a, X.9b, and X.9c are the trim diagrams for all three phases of flight.

The trim diagrams plot the coefficient of moment about the SEAL's center of gravity vs the angle of attack for three different elevator deflections. When the coefficient of moment is 0, the plane is no longer pitching. By using three different elevator deflections, it is possible to interpolate between the points of no moment to find elevator deflection for any angle of attack. The most significant angle of attack is the desired angle for each phase of flight. A point is plotted at this location with the interpolated elevator deflection value listed. There are only three points in Figure X.9b because the $\delta_e = 0$ line crosses at the cruise angle of attack, meaning less than $1°$ of elevator deflection is required to trim the aircraft at cruise.
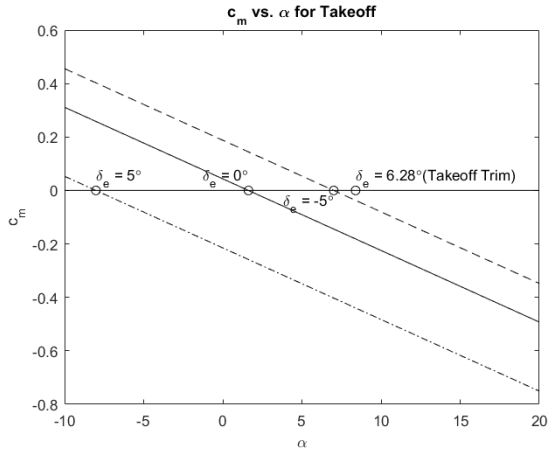
(a) Trim diagram during takeoff with 15° of flap
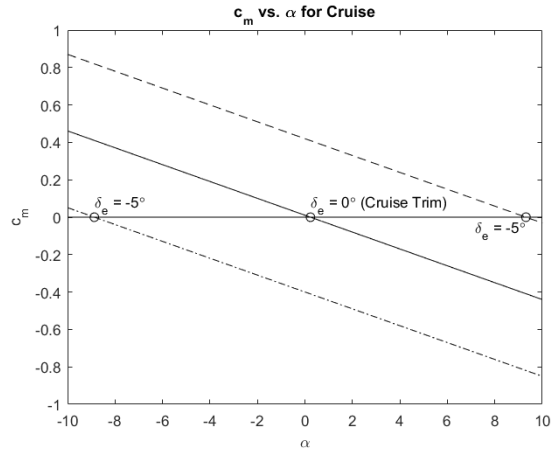
(b) Trim diagram during cruise with 0° of flap
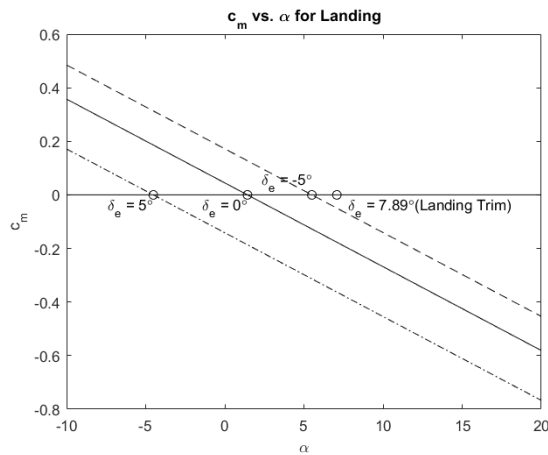
(c) Trim diagram during landing with 30° of flap

Figure X.9: Trim diagrams at different flap deflections.

XI. Auxiliary Systems

The primary systems of SEAL consist of a fuel system, engine control system, flight control system, hydraulic system, electric system, environmental control system, and avionics. These systems all work together seamlessly to provide a safe and comfortable flight for all passengers and crew onboard. The interdepency between each subsystem allows for more advanced and safe flying practices that are not found in older aircraft. Additionally, the systems include many redundancies which allow for control of the aircraft even case of emergencies and potential malfunctions.
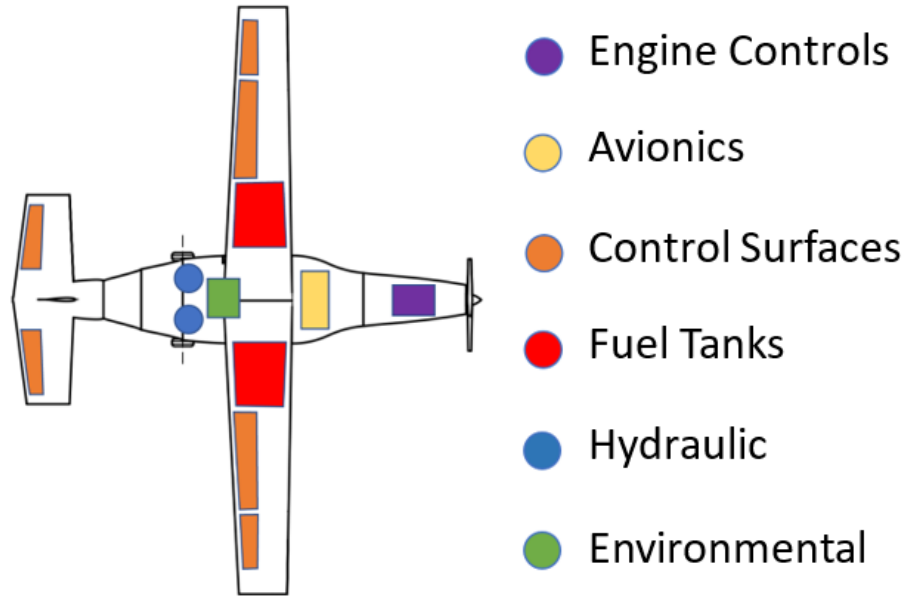
Figure XI.1: Schematic showing placement of large systems within SEAL

Figure XI.1 above shows a high level schematic of all the major subsystems onboard the SEAL. This layout was carefully configured to ensure both efficient and safe flying practices.

A. Fuel Systems
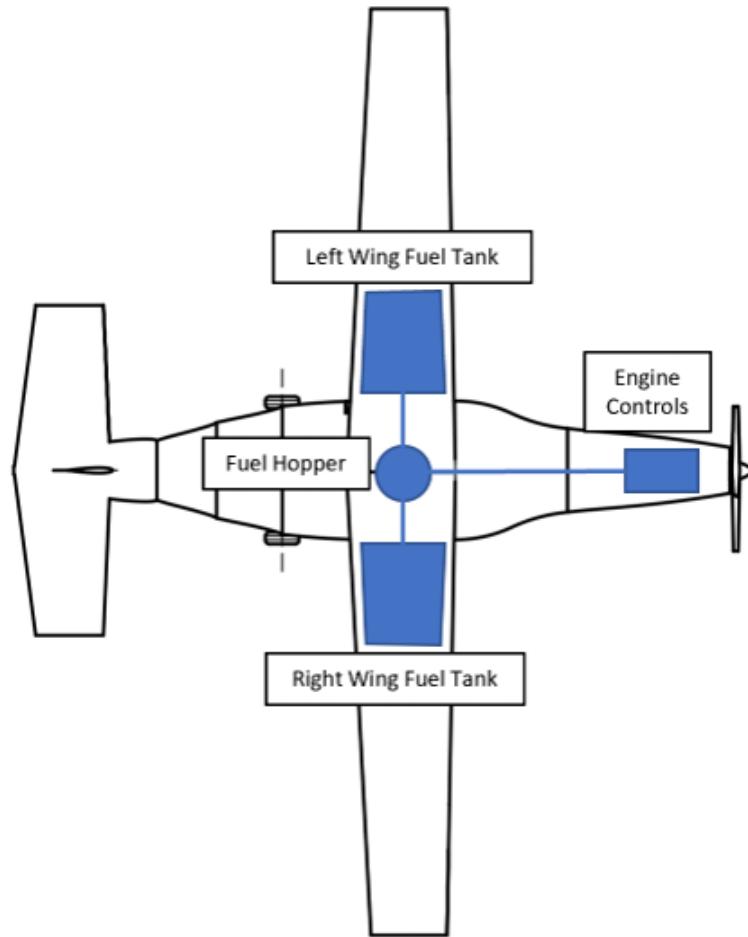
Figure XI.2: Fuel system schematic

SEAL's fuel system serves to safely store and feed fuel to the engine when needed. Two main fuel tanks located in each side of the wing store all of SEAL's fuel. The fuel in these two tanks are constantly kept at equal volumes to maintain the balance of the aircraft. When fuel is required by the fuel control unit in the engine, it is collected by the fuel hopper which then pumps the fuel to the engine. One major reason for choosing a high-wing aircraft vs. a low-wing aircraft is to ensure the fuel can be gravity-fed to the engine in case of pump malfunction [13]. Additionally, valves, probes, and level sensors located in the fuel tanks and fuel lines help ensure proper fuel management.

For the more demanding mission required of SEAL - the sizing mission - 375 lbs of fuel is required. Jet A-1 fuel was chosen which has a density of 6.71 lbs/gal, meaning SEAL 55.89 gallons of fuel to complete this mission. This fuel estimate was used to size the two main fuel tanks which will each hold 30 gallons of fuel to account for 5 percent fuel that will be trapped in the tanks. This gives surplus of approximately 2 gallons of fuel in each tank.

B. Engine Controls
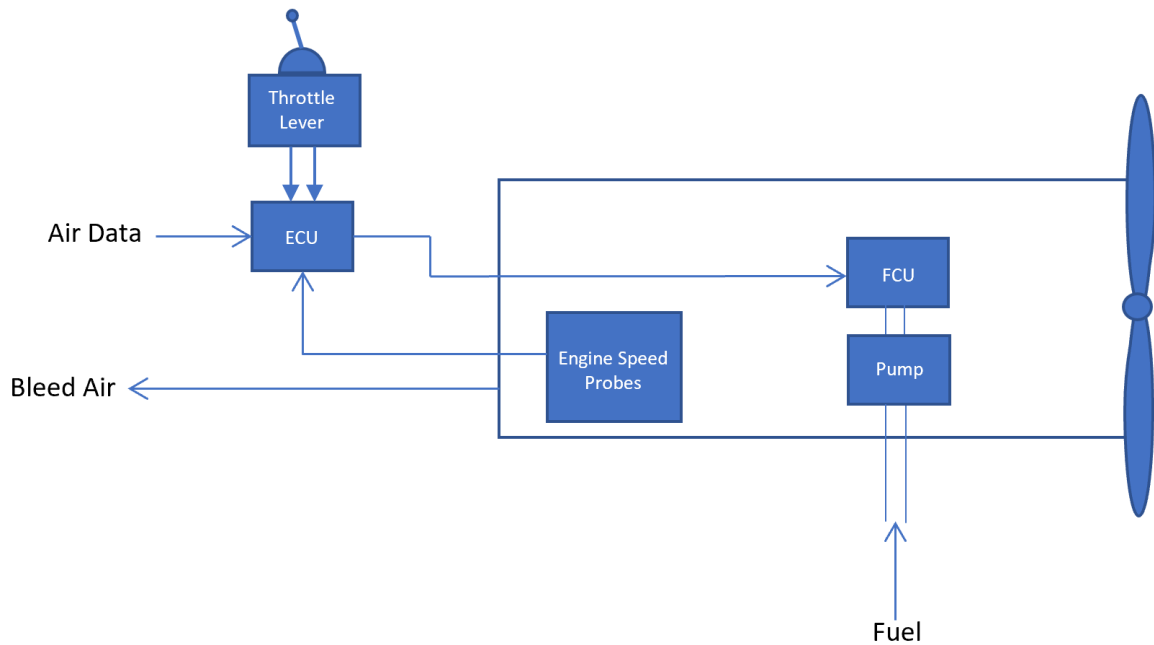
Figure XI.3: Engine control system schematic

SEAL's engine control system serves to control the flow of fuel and air into the engine in order to operate at optimal efficiency at all times. Figure XI.3 above shows a high level break down of how the system works. The pilot handles the throttle in order to increase and decrease thrust in times such as takeoff and landing. The engine control unit (ECU) receives inputs from the throttle lever as well as air data from exterior sensors which are analyzed 70 times per second [13]. The ECU then computes and applies parameters for fuel flow and sends that information to the fuel control unit (FCU),which operates with two important safety precautions. The first safety measure prevents the pilot from making any moves that could compromise the aircraft. This reduces the potential effect of human error when calculating fuel needed for a given required thrust. Secondly, there are two separate digital channels that send information to the ECU and between the ECU and FCU. This reduntant electrical wiring ensures that the engine will still be operable in the case of electrical malfunction. After the FCU receives digital information from the ECU, it sends the corresponding signals to the fuel pump to supply the engine with power. Finally, gearbox mounted speed probes send engine rotation speed information back to the ECU completing a closed loop feedback system. The schematic above shows bleed air running off the engine which will supply power to various other systems of the aircraft discussed in further sections below.

C. Flight Controls

The SEAL's primary flight controls consists of one aileron on each side of the wing, one elevator on each side of the horizontal stabilizer of the tail, and a rudder on the vertical stabilizer of the tail. The pilot will control the ailerons and the elevator by a control column in the cockpit and the rudder with pedals. The SEAL's secondary flight controls consists of trim on both the elevators and the rudder, and plain flaps on the wings to increase lift during landing and take off in order to meet the respective runway requirements. Plain flaps were chosen over slotted flaps or fowler flaps because they provide enough lift while also being the simplest to install and more cost efficient to manufacture [13]. The trim on the elevators and rudder can be manually controlled by the pilot or by the autopilot system. These flight controls are hydraulically actuated through a system of two pumps that can control each flight control surface independently. This hydraulic system is discussed more in Section XI.E.

Although movement of the flight controls is powered by hydraulics, it is the SEAL's fly-by-wire system that sends the necessary signals to the hydraulic pumps. The main flight control computer located in the cockpit receives signals from the pilot's controls and then calculates how much the respective flight control surface needs to be moved and how much hydraulic fluid is needed for actuation. This information is sent by electrical signal to the hydraulic pumps which then actuate the control surface. Sensors on each control surface allow for a feedback signal back to the flight control computer to ensure that the surface is being properly actuated. There is a secondary backup computer also located in the cockpit which is capable of sending the same signals to the hydraulic system in case of failure of the main flight control computer. This fly-by-wire system is superior to the tradition manual (cable and pulley) system which tends to lack safety features and weigh much more [13]. Finally, the main flight control computer allows for autopilot during cruise by adjusting the elevator and rudder trim to maintain steady-level flight.

D. Hydraulics Systems
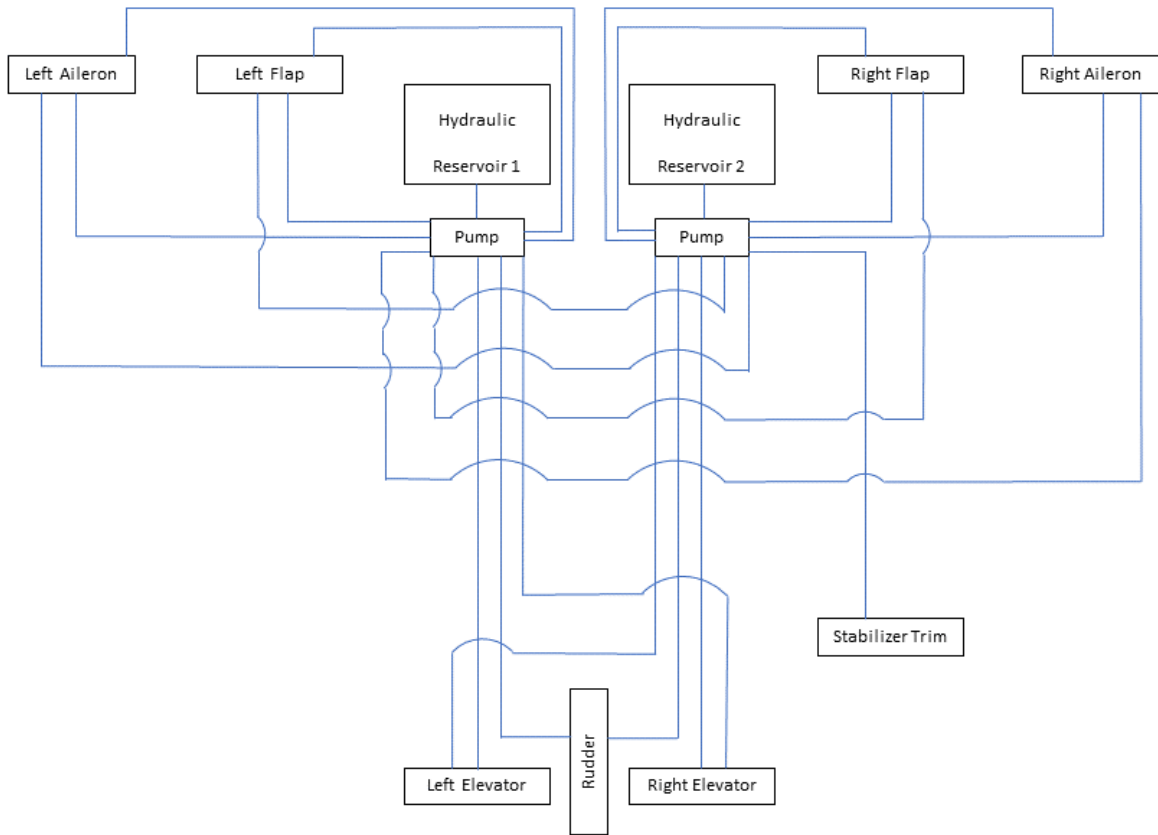
Figure XI.4: Hydraulics and flight controls system schematic

Figure XI.4 is a high-level break down of the hydraulics system of SEAL. Pictured are two separate hydraulic reservoirs which store the system's hydraulic fluid. In addition to each reservoir is an engine-driven pump which supplies pressure to the system and allows the transfer of hydraulic fluid to each flight control surface. The engine drive pumps are mounted on an engine-drive gear box which use shaft work to power the pumps. Secondary air driven pumps are also connected to each hydraulic reservoir in case of failure of both engine driven pumps. The air driven pumps are powered by bleed air from the engine. SEAL's hydraulic system is operated at a pressure of 4000 psi in order to reduce unnecessary weight addition that would be caused by pumps of a bigger size [13]. The use of two separate hydraulic reservoirs and pumps is for safety; therefore, each flight control surface has two actuators - one from each pump that can move each respective control surface when signals are sent from the primary flight control computer. In the case that there is a failure of one of the two pumps or one of the many hydraulic lines, SEAL's control surfaces will still be controllable due to this redundancy. In this case, controllability will be reduced due to less actuation on

each control surface and therefore slower moving control surfaces, but the aircraft will still be flyable. Further, the hydraulic lines from each pump run in separate areas of the aircraft so that a possible emergency that causes failure in one hydraulic line will be less likely to affect the other hydraulic line that leads to each respective control surface.

E. Electric System
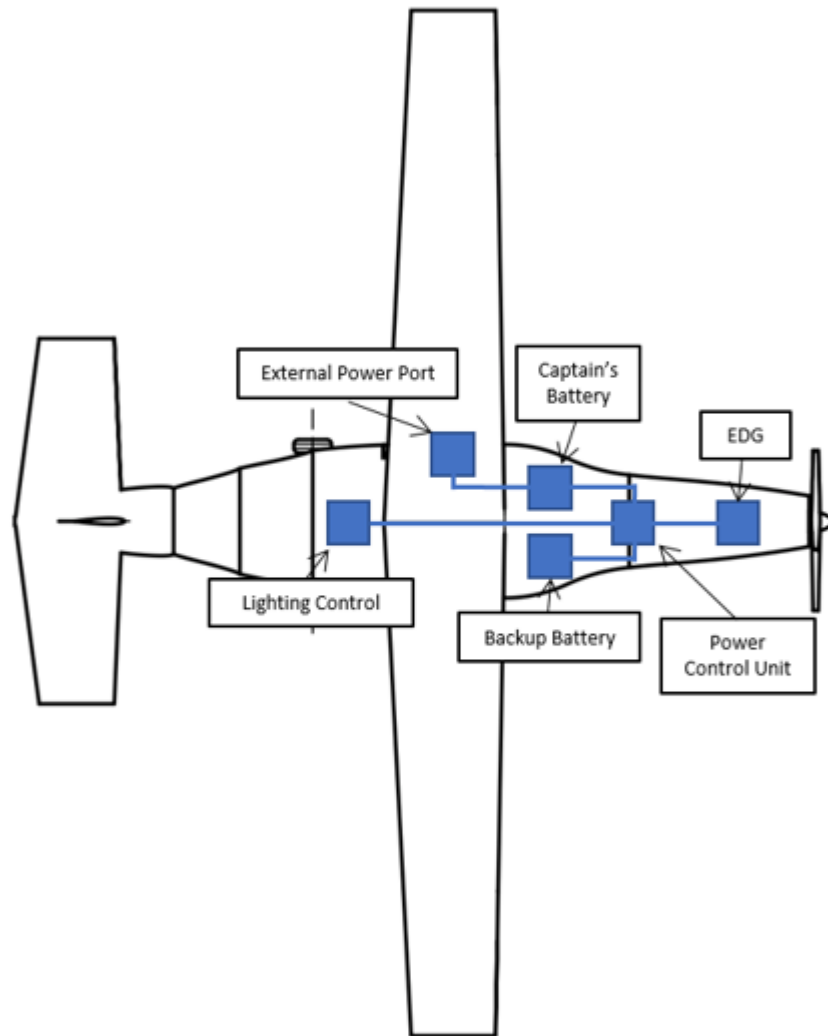
Figure XI.5: Electric system schematic

The SEAL's power generation system consists of one engine driven generator (EDG) which uses a gearbox attached to the engine to convert mechanical energy to electrical electrical. This power is sent to the power control unit which serves to frequency-convert the power for passenger use in the cabin as well as to convert AC power to DC power for the two batteries on board. The main battery on board is the captain's battery which is located in the cockpit and supplies power for the avionics. This battery is held at a full charge during flight in case of failure of the EDG. The EDG also

supplies power for a second battery located in the front of the aircraft which is also used for backup power. Further, SEAL has one external power connection that is used for startup as well as for servicing and ground maintenance. Finally, the EDG supplies power for both the external and internal lighting systems on SEAL. This lighting is supplied by 28 VDC converted by the power control unit and is used for navigation lights, taxi lights, emergency lights, and flight deck and cabin lighting. Lighting is achieved with conventional filament lightbulbs ranging from 3 watts internal illumination to 600 watts for landing lights [13]. A high level schematic of this system can be seen in figure XI.5. It is important to note that an auxiliary power unit (APU) is not necessary to provide SEAL's needed electric power and would only add unnecessary weight and cost.

F. Pneumatics and Environmental Control System
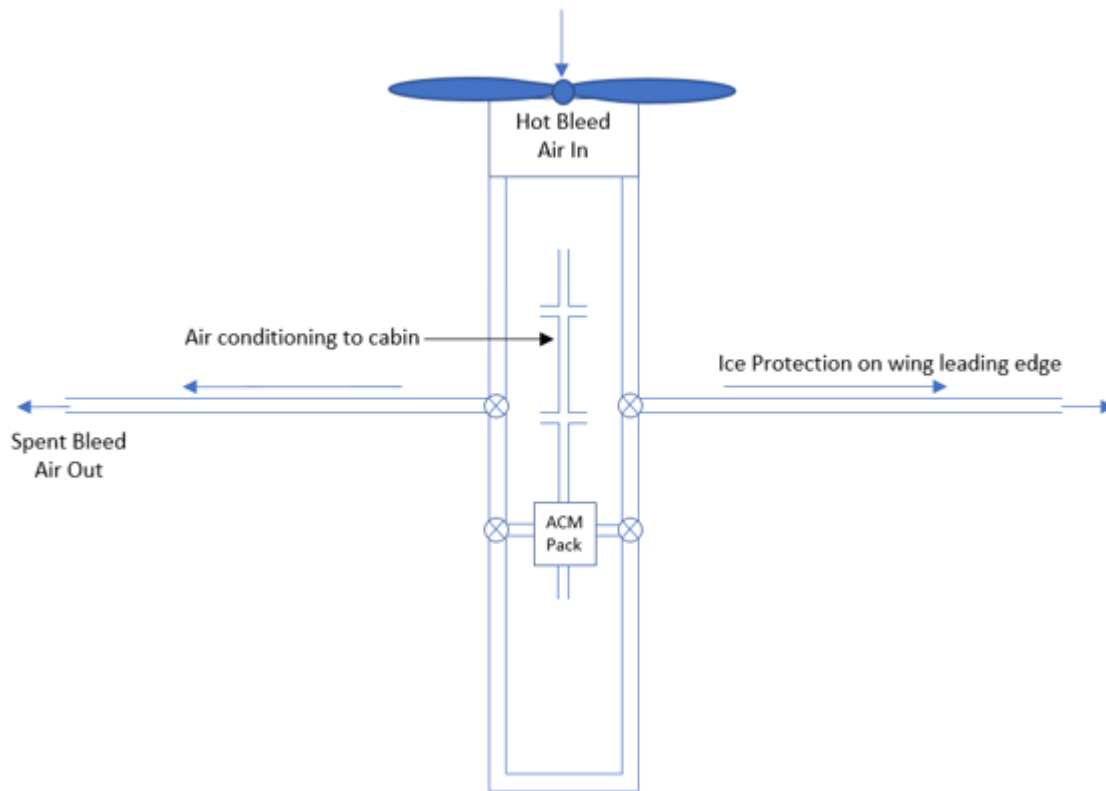
Figure XI.6: Environmental control systems schematic

SEAL's environmental control system will ensure that all passenger's fly in suitable and breathable conditions. SEAL is equipped with an air conditioning system that allows for comfortable cabin temperatures and regulates breathable air. Because SEAL will cruise at 12,000 feet, the need for cabin pressurization is not necessary. FAA regulations state that pressurization is only required at an altitude above 12,000 feet, and due to the short-haul nature of SEAL's mission, passengers will feel comfortable throughout their time on the flight. Adding pressurization would provide

unnecessary expenses and weight and would drive up ticket costs. Although cabin pressurization will not be a feature of SEAL, oxygen masks are provided at every seat in case of emergency. Bleed air from the engine allows this system to achieve these conditions in conjunction with transferring heat to the wings and tail to provide suitable flying conditions in several types of weather. Figure XI.6 above shows a schematic of how this system operates. Bleed air comes in the front of the aircraft from the engine and is sent to the wings and the air cycle machine which refrigerates the air. The amount of air sent to each respective area is controlled by valves denoted by the crossed circles in the figure. The system is open-looped which means that air is continually bled from the engine, which cools the cabin and equipment, and is then ejected at the rear. An open loop system was chosen over a closed loop system due to its significantly reduced cost and weight [13]. Closed loop systems allow for more efficient engine use but are unnecessary for short haul missions such as SEAL's. The other primary use of the aircraft pneumatic system is to protect the wings from icing during flight. Icing can happen due to the build up of precipitation, typically on the leading edges of the wings or the tail. Just like with the open loop air conditioning system, air is continuously bled off the engine to transfer heat to the interior of the wings and tail leading edges. This anti-ice system prevents the freezing of water onto the exterior of the wing and reduces the need for a de-icing system.

G. Avionics

The aircraft is equipped with modern navigation and communication system. The Garmin G1000 avionics package was chosen for SEAL. It has a glass flight deck which presents flight information, navigation , weather, terrain and traffic on high resolution displays. It has GRS77 Attitude and Heading Reference System (AHRS) which provides accurate and digital output as compared to the traditional mechanical gyroscopic instruments. It is also capable of restarting and repositioning it accurately while in flight. G1000 provides enhanced situational awareness, fully-integrated autopilot system and the ability to see clearly in IMC conditions. By presenting key aircraft performance, navigation and terrain and traffic information on its large high-resolution displays with audio warnings, it boosts the confidence of the pilot and also reduces the pilot workload. Garmin G1000 is one of the most advanced packages available for short-haul aircraft. It has a high-performance graphics accelerator which speeds up the display of images making it possible to achieve 3d effects which were otherwise not possible. It is also equipped with an infrared port which helps to accomodate data entries via a handheld Garmin digital assistant without connecting a cable. There is a choice of display formats available to the pilots which allow them to select the attitude/heading presentation which they prefer. There are two formats available : Standard 360 ° HSI and 140 ° HSI. The main benefit of Garmin G1000 is that it is a fully integrated system. The package includes display of attitude, air data, engine and airframe status, position derived by GPS. Complete VHF comm, VOR/ILS and transponder functions controlled by knobs and selector keys located on Primary and Multi-Function Display bezels are also included.

Trade studies were carried out between different Garmin avionics packages and others like Avidyne and Honeywell

Primus Apex. Garmin products were chosen over others mainly because they are integrated. The two packages considered finally were Garmin G1000 and G500. They have a lot of similarity with each other but there is a huge difference in their prices. Also, G1000 is more advanced and houses certain features which G500 does not. Table shows the comparison between G1000 and G500 packages.

Table XI.1: Comparison of Garmin G1000 and G500

	G1000	G500
Cost	26,700 US dollars	15,995 US dollars
Integrated avionics package	Yes	Yes
Option of 12" and 15" displays in addition to the standard 10" displays	Yes	No
GRS 77 AHRS system	Yes	Yes
SafeTaxi supported	Yes	Yes
Terrain and Warning system included	Yes	No (optional)
Integrated with the engine	Yes	No
Optional display formats	Yes	No
GFC 700 digital autopilot integration	Yes	Yes
Choice of a 3-display system	Yes	No
Linked to Iridium satellite network	Yes	Yes
Jeppeson navigation database	Yes	Yes

Table XI.1 shows that there are many similarities in the two avionics packages. While a lower price of G500 is more economical, G1000 was chosen for SEAL because of its additional safety features like the link with engine. This important feature is not available in G500 and hence the pilot won't be as aware as with G1000.

The G1000 avionics package used in SEAL provides semi-autonomy.It is integrated with the GFC 700 autopilot system which uses the flight data to navigate and maintain airspeed references and optimize performance over the entire flight envelope. G1000's Envelope and Protection system can be easily disabled when the pilot wants to fly the aircraft manually and is automatically disabled below 200 ft. The ESP kicks in when the aircraft is about to leave the flight envelope and the pilot takes no action. GFC 700 autopilots also allow automated go-arounds.The autopilot installed in G1000 does not require flight director to be on to take over when the aircraft is leaving its envelope. However, Avidyne's

Figure XI.7: Primary Flight Display of G1000

envelope protection requires flight director to be on to control the aircraft. A semi-autonomous package was chosen because the RFP requires the aircraft to enter into service by 2025. An autonomous flight is not a much developed subject yet and it may not be possible to develop the required technology by 2025.

Figure XI.8: Multi-Function Display of G1000 with audio panel

XII. Acoustics

As outlined in the RFP [1], the aircraft must meet the single-engine noise limits described in Part 36 Sec. G36.301(c). The requirements state that the acceptable amount of noise created by the aircraft is determined by the MTOW, beginning at a noise level of 70 dB(A) for all aircraft with a MTOW at or below 1,257 lb. The limit increases logarithmically by 10.75 dB(A) per doubling of MTOW. This logarithmic increase continues until the upper limit of 85 dB(A) is reached [27]. Using the logarithmic curve fit function, the equation for the logarithmic growth was solved for. The equation was used to determine that any aircraft within this classification and that has a MTOW at or above 3,307 lb would have a noise limit of 85 dB(A). The MTOW of the SEAL is 4,535 lb, therefore the noise limit of the aircraft will be 85 dB(A). The same aircraft examined during the initial sizing similarity analysis, shown in Table III.3, were examined for the noise produced by the engine. Using the certification databases provided by the FAA [28] and the EASA [29] [30], the noise data was gathered from each of these aircraft engines. Then, after finding the noise output from the engine that was chosen for the SEAL, all of the data was plotted. That plot is shown in XII.1.
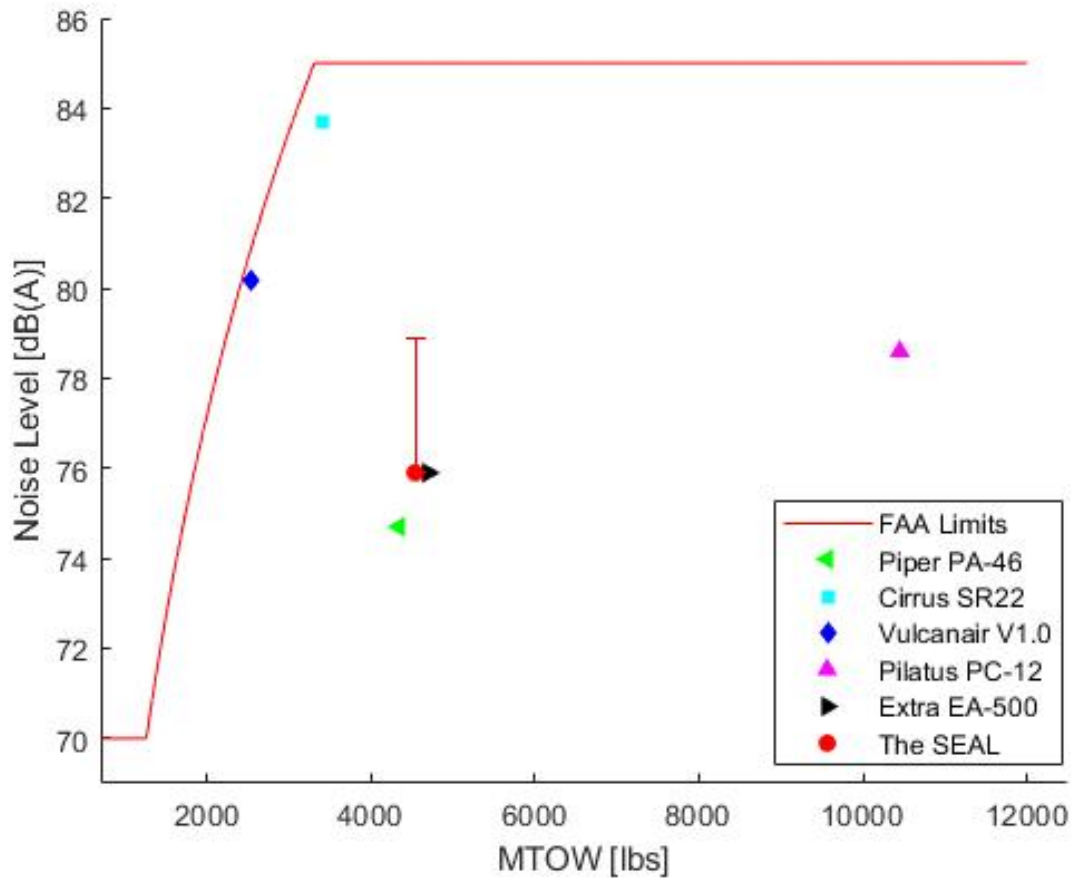
Figure XII.1: Noise Level vs. MTOW Similarity Analysis

As the plot illustrates, the aircraft most similar to the SEAL are the Piper PA-46 and the Extra EA-500. These two aircraft, as well as the SEAL, are over 9 dB(A) below the 85 dB(A) limit at their respective MTOWs. In the absence of empirical tools for noise, the acoustic analysis would take into consideration the engine noise and the noise produced by the airframe. The noise of the airframe would not exceed the noise produced by a second engine. If the SEAL would have two engines, and therefore double the power available, the noise level would increase nominally by 3 dB(A). The error bar shown in XII.1 shows the range of potential noise values for the SEAL up to 3 dB(A) more than the engine certification. Even with this increased noise level, the SEAL falls well within the acoustic limits outlined in Part 36 Sec. G36.301(c). While this estimate predicts that the SEAL will be well withing the limits, it is important to note that this is not a guarantee of proper acoustic performance. There are many characteristics of an aircraft that affect the noise produced by the aircraft. One large factor is the fuel-air mixture exhausted by the engine. Typically this data is provided by the engine manufacturer. This data would allow for a more accurate estimate of the noise levels produced by the aircraft.

XIII. Cost

For the SEAL to be a success, it must make financial sense to the companies that will be buying it. A cost analysis was done to ensure that the SEAL would compete with other aircraft in the same market.

The cost model that was used came from Gudmundsson [37] and has been tailored specifically towards the development and operation of general aviation aircraft. By focusing on general aviation aircraft, results from this method came much closer to other airplanes in the SEAL's market. On top of being purpose made to estimate general aviation costs, this model was created in 2012, which makes it more reliable than other cost estimation methods that were designed decade ago.

Table XIII.1: Cost per Unit for Different Production Levels and Runs

Unit Cost [$/Unit]

Units	1 Year Production Run	2 Year Production Run	5 Year Production Run	10 Year Production Run
1	44,307,000	43,938,200	43,475,900	43,144,300
10	9,539,600	9,475,000	9,393,900	9,335,700
50	3,645,100	3,625,900	3,601,900	3,584,700
100	2,489,400	2,478,100	2,463,900	2,453,700
500	1,116,700	1,113,300	1,109,100	1,106,100
1000	821,100	819,100	816,600	814,800
2000	618,000	616,800	615,400	614,300

Table XIII.2: Sale Price Per Plane

Unit Price [$/Unit]

Units	1 Year Production Run	2 Year Production Run	5 Year Production Run	10 Year Production Run
1	47,389,200	46,994,800	46,500,300	46,145,700
10	10,203,300	10,134,100	10,047,400	9,985,200
50	3,898,700	3,878,200	3,852,500	3,834,100
100	2,662,600	2,650,500	2,635,300	2,624,400
500	1,194,400	1,190,800	1,186,300	1,183,100
1000	878,200	876,100	873,400	871,500
2000	661,000	659,700	658,200	657,000
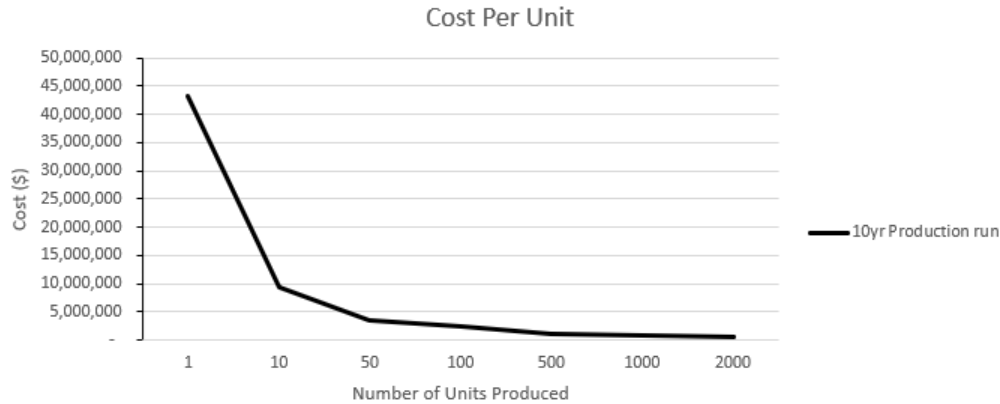
Figure XIII.1: SEAL Cost vs Quantity Produced (2yr and 10yr Runs)

Shown in Table XIII.1 are the prices to produce a quantity of SEALs at differing production run lengths. Figure XIII.1 demonstrates the drops in price as more units are produced. In order to make the SEAL as competitive in the market as possible, more units should be produced. Table XIII.2 shows the sale price per unit. This takes into account the costs to develop and produce the SEAL and provide the manufacturer with an industry comparable 8% profit margin [37]. The SEAL's price is competitive within its industry starting around 500 produced units, and moves into the inexpensive segment of the market between 1000 and 2000 units.

Operating costs take into account all expenses that occur after the purchase of the plane. Shown in Figure **??** are the inputs used by this model and the total costs over the course of a year associated with each, as well as the yearly and hourly rates these break down into.

Table XIII.3: Total Operating Costs for 1000 Flights Hours per Year

Sector	Cost [$]
Maintenance	160,800
Storage	3,000
Fuel	170,269
Insurance	10,355
Inspection	500
Overhaul	5,000
Monthly Loan Payment	26,520
Crew	70,000
Total Yearly Cost	376,440
Cost per Flight Hour	380

These prices vary with the number of hours that the SEAL is flown per year, so multiple potential operating cases were analyzed to provide the best information possible to potential buyers. This is shown below in Table XIII.4.

Table XIII.4: Yearly and Hourly rates for various operating cases

Units Produced	2,000	1,000	500	100
Total Yearly Cost [$]	712,510	376,440	208,410	73,980
Cost per Flight Hour [&]	356	376	417	740

In order to estimate the cost for the price of a single reference mission as defined by the RFP [1], a typical use case for a SEAL is defined and was chosen as 1000 hours of flight time per year. At $376/hour, a 45 minute mission should cost $282. With 5 passengers, tickets prices for the reference mission come out to $62 per seat including a 10% profit margin. This seems to be a reasonable price for the speed, convenience, and comfort that the SEAL provides. With a break-even price per ticket of $56, the SEAL will also provide the operators the ability to sell their tickets at a range of prices without being too expensive for the typical buyer.

Since the goal of any business is to make money, the cheaper the SEAL can be produced the better. Several ideas have been proposed to reduce the cost of the SEAL and increase profits. Avionics packages can vary dramatically in price and choosing a cheaper model could lower the price of the SEAL. Use of drag reduction devices could increase fuel efficiency of the SEAL which can add up to large savings over the course of its lifetime. Higher fuel efficiency could also bring up the selling price of the aircraft to increase profit margins. The engine on the SEAL is an older engine that has already been certified. In the long term, a newer engine could be picked that is more efficient. While this engine could cost more, it may save money over the lifetime of the SEAL in the same way that drag reduction devices can.

Given the complexity and length of an aircraft development program, many assumptions had to be made which results in inaccuracies. When calculating the yearly and hourly operating costs, it was assumed that a company financed 100% of the cost of the plane for 10 years with an interest rate of 4%. Given today's 10 year treasury rate of around 2.5%, a company with good credit should be able to borrow with a 4% interest rate, but this can change quickly if the economy changes. The economy also plays a roll in the price of labor which will change the rates at which engineers and manufacturers are paid. Global events have had major impacts on the cost of fuel in the past and could happen again. This can dramatically increase the operating costs of the SEAL.

XIV. Conclusions

Team Eta has design an aircraft which fits emerging thin-haul transport market space. This design is powered by a single turboprop engine, has a range of 270 nmi at 225 ktas while carrying five passengers, and is capable of taking off over a 50 ft obstacle within 1,064 ft, satisfying the requirements laid out by the AIAA RFP. This design is able to stay competitive in the market space by offering faster speeds and increased passenger capacity and comfort compared to similar aircraft such as the Cirrus SR22. The SEAL will be able to provide cost-effective service to operators and an excellent passenger experience in the emerging thin-haul and air taxi markets.

The team was able to use sizing methods from aircraft design textbooks in initial sizing to obtain parameters that satisfied the design requirements. Next, empirical methods and first order tools such as AVL and OpenVSP were used to validate these designs to obtained more detailed calculations in aerodynamics, performance, stability and control, structures, and mass properties. After verifying the design, the team performed a detailed analysis with computations in aerodynamics and stability and control completed in AVL and Finite Element Analysis for structural components. To obtained a fully detailed design, a detailed Computational Fluid Dynamics analysis will need to be performed and exact systems and parts will need to be sized to obtain the exact locations of systems and mass properties.

As the demand for air travel begins to move towards on-demand service, the SEAL will be able to meet the demands of operators and customers. We hope that our comfort will be well-received by passengers and our low cost of purchase and operations while carrying higher payloads will be beneficial operators. As technologies such in areas such as composite manufacturing and hydrid-electric engine technology advance, future revisions to the SEAL can take advantage of them to offer increased

References

[1] "Request for Proposal, 2018-2019 Undergraduate Team Aircraft", AIAA, 2018.

[2] Raymer, D. P., "Aicraft Design: A Conceptual Approach", 5th ed., AIAA, Reston, Virginia, 2012, Chaps. 4, 6, 11 - 16, 18.

[3] Roskam, J., "Airplane Design, Parts I-VIII", 2nd Edition, DAR Corporation, Lawrence, KS, 2003, Parts 5, 6.

[4] Kroo, I.L., "Aircraft Design: Synthesis and Analysis", Ver. 0.99, Desktop Aeronautics, In.c, January 2001, Chap. 10.

[5] "Malibu Mirage PA-46-350P SN 4636196 and Up Pilot's Operating Handbook", The New Piper Aircraft, Inc., VB-1710, Verona Beach, Florida, February 1999.

[6] "Airplane Information Manual for the Cirrus Design SR22", Cirrus Aircraft Corporation, P/N 20880-002, Duluth, Minnesota, September, 2011.

[7] "Vulcanair V1.0", *Vulcan Air Aircarft*, http://www.vulcanair.com/vulcanair-v1-0 [retrieved 29 January 2019].

[8] "Pilot's Informaion Manual, PC-12 Series 10 and 10A", Pilatus Aircraft Ltd, 02211, Stans, Switzerland, September, 1984.

[9] "Information Manual EA 400-500 (Extra 500)", EXTRA Flugzeugproduktions- und Vertriebs- GmbH,Flugplatz Dinslaken, Republic of Germany, 2013.

[10] "Aircraft Performance Data." RisingUp Aviation - Everything Aviation, Generally Speaking, www.risingup.com/planespecs/info/airplane423.shtml.

[11] Vink, Peter. Aircraft Interior Comfort and Design. Taylor amp; Francis Inc., 2011.

[12] Soban, D., "Some Propulsion Characteristics," AE 3310 Performance, Mar. 2019.

[13] Moir, Ian. Aircraft Systems Mechanical, Electrical, and Avionics Subsystems Integration. Wiley, 2010.

[14] Lednicer, David, "Airfoils of US and Canadian Aircraft", *Aerofiles.com*, http://www.aerofiles.com/airfoils.html [Retrieved 3 March 2019].

[15] Abbott, Ira H., Albert E. von Doenhoff, and Louis S. Stivers, Jr, "Summary of Airfoil Data", https://ntrs.nasa.gov/archive/nasa/casi.ntrs.nasa.gov/19930090976.pdf [Retrieved 3 March 2019].

[16] Sheldahl, R E, and Klimas, P C., "Aerodynamic characteristics of seven symmetrical airfoil sections through 180-degree angle of attack for use in aerodynamic analysis of vertical axis wind turbines", USDOE, 1981.

[17] "In-Flight Icing Encounter and Uncontrolled Collision with Terrain Comair Flight 3272", National Transportation Safety Board, https://www.ntsb.gov/investigations/AccidentReports/Reports/AAR9804_body.pdf [Retrieved 19 April 2019].

[18] MIT, "Wing Taper Considerations", https://ocw.mit.edu/courses/aeronautics-and-astronautics/16-01-unified-engineering-i-ii-iii-iv-fall-2005-spring-2006/systems-labs-06/spl8a.pdf [Retrieved 3 March 2019].

[19] Extra Aircraft Company, "Information Manual, EA 400-500", https://www.extraaircraft.com/docs/service/POH_500_20130522_CUS.pdf [retrieved 25 February 2019].

[20] Anderson, J., "Aircraft Performance and Design", Tata McGraw Hill Edition 2010.

[21] Federal Aviation Administration, "TYPE CERTIFICATE DATA SHEET NO. E10CE",

[22] McCormick, B.W., "Aerodynamics, Aeronautics, and Flight Mechanics", John Wiley & Sons. Inc., 1979, Chap. 6,

[23] Canaday, Henry. "COMPOSITES VS. METALS." Techdirections December 2017, Prakken Publications, Inc, May 2015, www.omagdigital.com/article/COMPOSITES+VS.+METALS/1986792/254792/article.html.

[24] Bruhn, E. F. Analysis and Design of Flight Vehicle Structures. Tri-State Offset, 1973.

[25] Schrenk, Oskar. A Simple Approximation Method for Obtaining the Spanwise Lift Distribution. National Advisory Commitee for Aeronautics, 1940, pp. 1–16, A Simple Approximation Method for Obtaining the Spanwise Lift Distribution.

[26] Tulapurkara, E.G., "Airplane Design (Aerodynamic)", https://nptel.ac.in/courses/101106035/039_Chapter%206_L30%20_(04-10-2013).pdf [retrieved 25 February 2019].

[27] "14 CFR Appendix G to part 36 - Takeoff Noise Requirements for Propeller-Driven Small Airplane and Propeller-Driven, Commuter Category Airplane Certification Tests on or After December 22, 1988", *Cornell Law School*, https://www.law.cornell.edu/cfr/text/14/appendix-G_to_part_36 [Retrieved 3 February 2019].

[28] FAA, "Noise Levels for U.S. Certified and Foreign Aircraft", https://www.faa.gov/about/office_org/headquarters_offices/apl/noise_emissions/aircraft_noise_levels/ [Retrieved 17 February 2019].

[29] EASA, "Type-Certificate Data Sheet for Noise: No. EASA.A.613 for Vulcanair P.64, P.66, V1 Series", https://www.easa.europa.eu/sites/default/files/dfu/TCDSN%20EASA.A.613%20Issue%202.pdf [Retrieved 21 February 2019].

[30] EASA, "Type-Certificate Data Sheet for Noise: No. EASA.A.089 for PC-12", https://www.easa.europa.eu/sites/default/files/dfu/TCDSN%20EASA.A.089%20Issue%207.pdf [Retrieved 21 February 2019].

[31] AVCO Lycoming, TYPE CERTIFICATE DATA SHEET NO. E10EA, 1986.

[32] Meier, N., "Nate Meier's jet-engine.net," Civil Turbojet/Turbofan Specifications Available: http://jet-engine.net/.

[33] Broomfield Designers, "All Aircraft Battery Specifications From Concorde Battery Corporation," Concorde Aircraft Battery, http://www.concordebattery.com/allaircraftbatteries.php [Retrieved]

[34] Roskam, J.,"Airplane Aerodynamics and Performance", DAR Corporation, Lawrence, KS, 1997.

[35] Peet, Matthew M., "Spacecraft and Aircraft Dynamics Lecture 12", Illinois Institute of Technology. http://control.asu.edu/Classes/MMAE441/Aircraft/441Lecture12.pdf [Retrieved 4/16/2019].

[36] Bernard Etkin, Lloyd D. Reid, Dynamics of Flight: Stability and Control, 3rd Edition, Wiley, 1995.

[37] Gudmundsson, S., General aviation aircraft design: applied methods and procedures, Amsterdam: Butterworth-Heinemann, 2016.